UNIVERSIDAD DE GRANADA

FACULTAD DE FARMACIA

Departamento de Farmacología

Programa de Doctorado en Medicina Clínica y Salud Pública

MICROBIOTA Y COMPLICACIONES CARDIOVASCULARES ASOCIADAS AL LUPUS ERITEMATOSO SISTÉMICO

Tesis Doctoral para aspirar al Grado de Doctor presentada por

Néstor de la Visitación Pastor

Bajo la dirección de las Doctoras:

Rosario Jiménez Moleón

Marta Toral Jiménez

Granada, 2020

Editor: Universidad de Granada. Tesis Doctorales
Autor: Néstor de la Visitación Pastor
ISBN: 978-84-1306-608-0
URI: http://hdl.handle.net/10481/63682

INDEX

INDEX

ABBREVIATIONS **XIII**

ABSTRACT **XVII**

INTRODUCTION **3**

1. Systemic Lupus erythematosus **3**

1.1. Definition 3
1.2. Pathogenesis 3
1.3. Features of SLE 6
1.4. SLE and Cardiovascular disorders 8
1.5. SLE and microbiota 11
1.5.1. Dysbiosis in SLE patients 12
1.5.2. Dysbiosis in SLE mice 16
1.5.3. Gut barrier and immune activation 18
1.6. SLE and probiotics 21

2. Murine models of SLE **25**

JUSTIFICATION AND OBJECTIVES **31**

MATERIALS AND METHODS **37**

1. Animals and experimental groups **37**

1.1. Role of Gut microbiota in the development of hypertension in a genetic mouse model of SLE 37
1.1.1. Experiment 1 37
1.1.2. Experiment 2 38
1.2. Effects of probiotic supplementation on cardiovascular and renal complications in SLE 39
1.3. TLR-7-driven lupus autoimmunity induces hypertension and vascular alterations in mice. 39
1.3.1. Experiment 1 39
1.3.2. Experiment 2 40
1.3.3. Experiment 3 40
1.4. Effects of probiotic supplementation on cardiovascular and renal complications in an inducible model of SLE. 40

2. Blood pressure (BP) measurements 41

3. Plasma and urine determinations 41

4. Morphological variables 42

5. Vascular reactivity 42

6. Histopathological analysis 43

7. In-situ detection of vascular reactive oxygen species levels 43

8. NAPDH oxidase activity 44

9. Quantitative polymerase chain reaction 45

10. Western blotting analysis 47

11. Flow cytometry 48

12. DNA extraction, 16s rRNA gene amplification and bioinformatics 50

13. Reagents 51

14. Statistical analysis 52

RESULTS 55

1. Gut microbiota is involved in the development of hypertension in a mouse model of systemic lupus erythematosus 55

1.1. Changes in microbiota composition with the development of hypertension in SLE mice 55

1.2. Antibiotic treatments induced changes in gut microbiota, and inhibited the increment of blood pressure, target organ hypertrophy, and disease activity in lupus-prone mice 61

1.3. Antibiotic treatments induced changes in intestinal integrity and permeability. 65

1.4. Antibiotic treatments attenuate T cells imbalance 66

1.5. Antibiotic treatments prevent endothelial dysfunction, vascular oxidative stress and Th17 infiltration in aorta 69

1.6. Gut microbiota from NZBW/F1 mice increased blood pressure and impaired endothelial function in mice without lupus genetic background 71

2. Lactobacillus fermentum CECT5716 is a novel alternative for the prevention of vascular disorders in a genetic mouse model of systemic lupus erythematosus 73

2.1. LC40 treatment prevents gut dysbiosis in SLE mice 74
2.2. LC40 treatment improves intestinal integrity, inflammation and endotoxemia 80
2.3. LC40 treatment improves morphological variables, plasma parameters, and blood pressure 81
2.4. LC40 treatment attenuates SLE disease activity and T cells imbalance 84
2.5. LC40 treatment prevents endothelial dysfunction and vascular oxidative stress 86
2.6. LC40 treatment reduces IL17/ROCK/eNOS pathway and vascular inflammation 89

3. Lactobacillus fermentum CECT5716 prevents renal damage in the NZBW/F1 mice model of systemic lupus erythematosus 92

3.1. LC40 treatment prevents renal damage 92
3.2. LC40 treatment prevents renal oxidative stress and inflammation 95

4. Toll-like receptor 7-driven lupus autoimmunity induces hypertension and vascular alterations in mice. 98

4.1. Blood pressure, target organs damage and systemic inflammation are increased in SLE induced by TLR-7 activation 98
4.2. TLR-7 activation-induced SLE promotes vascular remodelling and endothelial dysfunction 104
4.3. Vascular oxidative stress and inflammation are increased in SLE induced by TLR-7 activation. 109
4.4. Role of ROS in cardiovascular alterations induced by TLR-7 activation 113
4.5. Involvement of IL-17 in hypertension and vascular dysfunction induced by TLR-7 activation 115

5. Probiotics prevent hypertension in a murine model of SLE induced by TLR-7 activation 116

5.1. Probiotics improve intestinal integrity without preventing gut dysbiosis in SLE mice 116

5.2. Probiotics attenuate lupus disease activity and modulate the immune response 121
5.3. Probiotics prevent endothelial dysfunction, oxidative stress and hypertension 125

DISCUSSION 133

1. Gut microbiota is involved in the development of hypertension in a mouse model of systemic lupus erythematosus 133

2. *Lactobacillus fermentum* CECT5716 is a novel alternative for the prevention of vascular disorders in a genetic mouse model of systemic lupus erythematosus 138

3. Lactobacillus fermentum CECT5716 prevents renal damage in the NZBW/F1 mice model of systemic lupus erythematosus 142

4. Toll-like receptor 7-driven lupus autoimmunity induces hypertension and vascular alterations in mice. 145

5. Probiotics prevent hypertension in a murine model of SLE induced by TLR-7 activation 149

CONCLUSIONS 157

BIBLIOGRAPHY 161

FIGURE INDEX

Figure 1. *Production of anti-dsDNA antibodies after stimulation by abnormal macrophages.* 4

Figure 2. *Autoantibody production through Toll Like Receptors (TLR) activation.* 5

Figure 3. *Anomalous activation of B and T cells.* 6

Figure 4. *Common steps for all panels studied. Specific gating from CD45+ cells for panel I* 49

Figure 5. *Specific gatings from CD45+ cells for panels II, III and IV.* 50

Figure 6. *Analysis of gut microbiota composition in control (CTR) and systemic lupus erythematosus (SLE) mice at 26 weeks of age.* 56

Figure 7. *Composition and evolution of gut microbiota in control (CTR) and systemic lupus erythematosus (SLE) mice.* 57

Figure 8. *Phyla changes in the microecological parameters and gut microbiota composition in control (CTR) and hypertensive 32-week-old systemic lupus erythematosus (SLE).* 58

Figure 9. *Family changes in the gut microbiota composition in control (CTR) and hypertensive 32-week-old systemic lupus erythematosus (SLE).* 59

Figure 10. *Genera changes in the gut microbiota composition in control (CTR) and hypertensive 32-week-old systemic lupus erythematosus (SLE).* 60

Figure 11*. Z-score for predictive functional profiling for microbial communities.* 61

Figure 12. *Antibiotic treatments inhibited the increase of blood pressure, target organ hypertrophy and disease activity in systemic lupus erythematosus (SLE) mice.* 64

Figure 13. *Effects of antibiotic treatments on splenomegaly in activity in systemic lupus erythematosus (SLE) mice.* 64

Figure 14*. Effects of antibiotic treatments on epithelial integrity markers and permeability in systemic lupus erythematosus (SLE) mice.* 66

Figure 15. *Effects of antibiotic treatments on lymphocytes populations. in systemic lupus erythematosus (SLE) mice.* 67

Figure 16. *Effects of antibiotic treatments on splenocytic populations in systemic lupus erythematosus (SLE) mice.* 68

Figure 17. *Effects of antibiotic treatments on blood lymphocyte population in systemic lupus erythematosus (SLE) mice.* 69

Figure 18*. Effects of antibiotic treatments on endothelial function, NADPH oxidase activity and aortic infiltration of immune cells in systemic lupus erythematosus (SLE) mice.* 70

Figure 19. *Effects of faecal microbiota transplantation (FMT) on evolution of systolic blood pressure (SBP), disease activity and lymphocytes populations in mesenteric lymph nodes.* 72

Figure 20. *Effects of vancomycin (VANCO) and antibiotic mix (MIX) treatments on the vascular nitric oxide pathway and the role of Th17.* 73

Figure 21. *Effects of Lactobacillus fermentum CECT5716 (LC40) treatment on phyla changes in the microecological parameters and gut microbiota composition.* 75

Figure 22. *Effects of Lactobacillus fermentum CECT5716 (LC40) treatment on changes in the gut microbiota composition.* 78

Figure 23. *Effects of Lactobacillus fermentum CECT5716 (LC40) treatment on genera changes in the gut microbiota composition.* 79

Figure 24. *Effects of Lactobacillus fermentum CECT5716 (LC40) treatment on proinflammatory and epithelial integrity markers.* 81

Figure 25. *Effects of Lactobacillus fermentum CECT5716 (LC40) treatment on both blood pressure (BP) and lymphocytes populations in mesenteric lymph nodes and spleen.* 82
Figure 26. *Effects of Lactobacillus fermentum CECT5716 (LC40) treatment on systemic lupus erythematosus (SLE) activity.* 84
Figure 27. *Effects of Lactobacillus fermentum CECT5716 (LC40) treatment on T-cell polarization in spleen.* 85
Figure 28. *Effects of Lactobacillus fermentum CECT5716 (LC40) treatment on plasma cytokines.* 86
Figure 29. *Effects of Lactobacillus fermentum CECT5716 (LC40) treatment on endothelial function, vascular oxidative stress, and NOX pathway.* 87
Figure 30. *Effects of Lactobacillus fermentum CECT5716 (LC40) treatment on vascular nitric oxide pathway.* 88
Figure 31. *Effects of Lactobacillus fermentum CECT5716 (LC40) treatment on aortic T cells infiltration.* 90
Figure 32. *Effects of Lactobacillus fermentum CECT5716 (LC40) treatment on vascular inflammation.* 91
Figure 33. *Effects of Lactobacillus fermentum CECT5716 (LC40) treatment on urinary parameters.* 93
Figure 34. *Effects of the Lactobacillus fermentum CECT5716 (LC40) treatment on morphological renal cortex features.* 94
Figure 35. *Effects of Lactobacillus fermentum CECT5716 (LC40) treatment on oxidative and inflammatory parameters in renal cortex.* 96
Figure 36. *Effects of Lactobacillus fermentum CECT5716 (LC40) treatment on T-cells infiltration in renal cortex.* 97
Figure 37. *TLR-7 activation promotes blood pressure increase in imiquimod (IMQ)-induced autoimmunity.* 99
Figure 38. *TLR-7 activation leads to higher levels of serum anti-double-stranded DNA (anti-dsDNA) autoantibodies, marked splenomegaly and altered clearance of apoptotic cells in imiquimod (IMQ)-treated mice.* 101
Figure 39. *TLR-7 activation by topical application of imiquimod (IMQ) promotes renal injury.* 102
Figure 40. *TLR-7 activation induces an increase in splenic B cells and T cells and promotes T cell polarization to proinflammatory phenotype.* 103
Figure 41*. TLR-7 activation by topical application of imiquimod (IMQ) raises plasma levels of proinflammatory cytokines.* 104
Figure 42. *TLR-7 activation promotes vascular remodelling in imiquimod (IMQ)-treated mice. Effects of TLR-7 activation on structural modifications induced in superior mesenteric arteries from IMQ-treated mice.* 105
Figure 43. *TLR-7 activation leads to marked impairment of endothelium-dependent vasorelaxation in imiquimod (IMQ)-treated mice.* 107
Figure 44. *Increases in vascular TLR-7 mRNA expression were found after TLR-7 activation by topical application of imiquimod (IMQ).* 109
Figure 45. *TLR-7 activation promotes a significant increase in vascular reactive oxygen species and NADPH oxidase activity in aorta from imiquimod (IMQ)-treated mice.* 110
Figure 46. *TLR-7 activation promotes a significant increase in NADPH oxidase activity in mesenteric arteries from imiquimod (IMQ)-treated mice.* 111
Figure 47. *TLR-7 activation promotes a higher gene expression of vascular adhesion molecules and proinflammatory cytokines in aorta from imiquimod (IMQ)-treated mice.* 112

Figure 48. *Antioxidant treatment prevents hypertension, vascular remodelling, endothelial dysfunction and increased NADPH oxidase activity induced by TLR-7 activation in imiquimod (IMQ)-treated mice.* 114
Figure 49. *Role of IL-17a in hypertension, endothelial dysfunction and increased NADPH oxidase activity induced by TLR-7 activation in imiquimod (IMQ)-treated mice.* 115
Figure 50. *Effects of probiotic treatments on phyla changes in the microecological parameters and gut microbiota composition.* 117
Figure 51. *Effects of probiotic treatments on changes in the gut microbiota composition.* 119
Figure 52. *Effects of probiotic treatments on epithelial integrity markers.* 120
Figure 53. *Effects of probiotic treatments on systemic lupus erythematosus activity.* 123
Figure 54. *Effects of probiotic treatments on percentage of B and Tcells in spleen and mesenteric lymph nodes.* 124
Figure 55. *Effects of probiotic treatments on T-cell polarization in mesenteric lymph nodes.* 124
Figure 56. *Effects of probiotic treatments on T cell polarization in spleens.* 125
Figure 57. *Effects of probiotic treatments on endothelial function and vascular oxidative stress-inflammation.* 126
Figure 58. *Effects of probiotic treatments on vascular nitric oxide pathway.* 127
Figure 59. *Effects of the probiotics on the evolution of blood pressure.* 129

TABLE INDEX

Table 1. Gut microbiota shifts in SLE patients. 15
Table 2. Gut microbiota shifts in different lupus animal models. 18
Table 3. Probiotic effects in different lupus animal models. 25
Table 4. Oligonucleotides for qPCR. 46
Table 5. Antibodies used for cytometry. 48
Table 6. Effects of *Lactobacillus fermentum* CECT5716 (LC40) treatment on phyla changes in the gut microbiota. 77
Table 7. Morphological and plasma parameters of all experimental groups. 83
Table 8. Effects of *Lactobacillus fermentum* CECT5716 (LC40) on renal damage. 95
Table 9. Morphological parameters. 100
Table 10. Maximal contractile response to U46619 in intact aortic rings in the presence of physiological salt solution (PSS). 108
Table 11. Phylum breakdown of the 6 most abundant bacterial communities in the fecal samples from all experimental groups. 118
Table 12. Morphological parameters of all experimental groups. 122

ABBREVIATIONS

ABBREVIATIONS

ACh, acetylcholine; anti-dsDNA, Anti-double-stranded DNA; Antiox, antioxidant cocktail; Apo, apocynin; C1qa, Complement C1q subcomponent subunit a; C1qb, Complement C1q subcomponent subunit b; CFU, Colony forming units; DAPI, 4,6-diamidino-2-phenylindoledichlorohydrate; DHE, Dihydroethidium; DTPA, Diethylene-triamine-pentaacetic acid; eNOS, endothelial NO synthase; F/B, *Firmicutes*/*Bacteroidetes*; ESRD, End-stage renal disease; FoxP3, Forkhead Box P3; GAPDH, Glyceraldehyde-3-phosphate dehydrogenase; H&E, Hematoxylin-eosin; HEPES, 4-(2-hydroxyethyl)-1-piperazineethanesulfonic acid; HR, heart rate; IAP, intestinal alkaline phosphatase; IFN, Interferon; IL, Interleukin; IMQ, imiquimod; LC40, *Lactobacillus fermentum* CECT5716; LN, Lupus nephritis; L-NAME, N(v)-nitro-L-arginine methyl ester; LD, lumen diameter; LDA, linear discriminant analysis; lpr, Lupus-prone MRL/Mp-Fas; LPS, Lipopolysaccharide; M/L, media–lumen ratio; MABP, mean arterial blood pressure; MCSA, media cross-sectional area; MIX, antibiotic mix; Mfge-8, Milk fat globule-EGF factor 8 protein; MT, media thickness; MUC, mucin; NADPH, Nicotinamide adenine dinucleotide phosphate; nIL-17, IL17-neutralizing antibody; NO, nitric oxide; NOX, NADPH oxidase; NZBW/F1, New Zealand Black/White; O_2^-, superoxide anions; OTU, operational taxonomy unit; Phe, phenylephrine; QIIME, Quantitative Insights Into Microbial Ecology; qPCR, quantitative polymerase chain reaction; RhoA, Ras homolog gene family, member A; RLU, relative luminescence units; RORγ, RAR-related orphan receptor gamma; ROS, Reactive oxygen species; RPL13, Ribosomal protein L13; RT-PCR, Reverse transcriptase-polymerase chain reaction; SBP, Systolic blood pressure; SLE, Systemic lupus erythematosus; SNP, sodium nitroprusside; T-bet, T-box expressed in T cells; TGF-β, Transforming growth factor beta; Th, T helper; TLR, Toll-like receptor; TNF, Tumour necrosis factor; Treg, T regulatory; Tsp-1, Thrombospondin-1; VANCO, vancomycin; VCAM-1, vascular cell adhesion molecule-1; ZO-1, Zonula occludens-1.

.

ABSTRACT

ABSTRACT

El lupus eritematoso sistémico (LES) es una patología inflamatoria crónica y multisistémica caracterizada por el anormal funcionamiento de linfocitos B, los cuales producen autoanticuerpos que, al formar inmunocomplejos que se depositan en el sistema vascular, causan daños en diversos órganos, como la piel, los riñones o el propio sistema vascular, produciendo una serie de complicaciones. Por ello, las complicaciones cardiovasculares asociadas al lupus son la principal causa de mortalidad en esta enfermedad, y la mayoría de los pacientes las presentan, aunque puede que de forma subclínica, incluyendo la disfunción endotelial. Según los conocimientos con los que se contaba hasta ahora, el desarrollo de estas complicaciones vasculares va asociado a un ciclo capaz de autoperpetuarse que involucra la inflamación, la respuesta celular inmune y el estrés oxidativo.

Así, la modulación de los elementos que conforman este ciclo es de gran interés para el desarrollo de nuevas estrategias terapéuticas en esta patología. Un aspecto prometedor es el vínculo descubierto entre los cambios en la composición de la microbiota intestinal (o disbiosis) y la respuesta inmune en las enfermedades autoinmunes. Esta disbiosis va asociada a cambios en las poblaciones de linfocitos, que pueden tener un efecto sobre la pared vascular, al causar inflamación y un aumento de especies reactivas de oxígeno (ROS), disminuyendo la biodisponibilidad de óxido nítrico (NO), importante agente vasodilatador, y por tanto empeorando la función endotelial. Por otra parte, la modificación dirigida de la microbiota intestinal podría ser un potencial elemento en un nuevo arsenal terapéutico al revertir o prevenir estos efectos. Así, siguiendo estas hipótesis, los objetivos desarrollados en la tesis fueron los siguientes:

I) Analizar el papel de la microbiota intestinal en el desarrollo y mantenimiento del LES en un modelo genético murino de la enfermedad (NZBW/F1), centrándonos en las alteraciones renales y vasculares.

Hemos podido demostrar que la microbiota intestinal es capaz de modular la función endotelial y la presión arterial en este modelo murino de LES. Al tartar a ratones

hembra de este modelo con vancomicina o un cóctel de antibióticos, pudimos observar cómo mejoran la función endotelial, la presión arterial, el estrés oxidativo, asociado a la reducción masiva en la biomasa fecal en ambos tratamientos. Teniendo en cuenta que ambos tratamientos hicieron efecto al mismo nivel, puede deducirse que algunas bacterias sensibles a vancomicina poseen un papel fundamental en el desarrollo de las complicaciones cardiovasculares ya mencionadas, esto se ve apoyado por el incremento en bacterias sensibles a vancomicina en ratones NZBW/F1 no tratados con antibióticos, como *Parabacteroides*, *Pedobacter*, *Olivibacter* y *Clostridium*. Por otro lado, el trasplante fecal de donantes NZBW/F1 a ratones control sanos resultó en un aumento de la presión arterial en estos ratones antes normotensos. Posiblemente por haber inducido un aumento en la concentración de bacterias nocivas con efectos prohipertensores, lo cual refuerza la importancia de la composición de la microbiota intestinal en el desarrollo de hipertensión asociada al LES.

La activación de linfocitos B, productores de autoanticuerpos, no se vio afectada por los tratamientos con antibióticos. Así mismo, el trasplante fecal tampoco modificó la activación de linfocitos B. Sin embargo, sí se apreciaron cambios en las poblaciones de linfocitos T helper (h)17, los cuales, mediante la producción de interleucina (IL)-17, se sabe que son capaces de inducir un mayor estrés oxidativo por activación de la NADPH oxidasa, principal productora de ROS a nivel vascular, lo cual va asociado a una disminución en la biodisponibilidad del NO y a disfunción endotelial. El trasplante fecal de NZBW/F1 a animales control logró cambiar estas poblaciones linfocitarias, afectando a la actividad de la NADPH oxidasa, incrementándola, produciendo disfunción endotelial.

II) Establecer el posible papel protector como suplemento dietético del microorganismo *Lactobacillus fermentum* CECT5716 (LC40) sobre las complicaciones vasculares y renales del LES.

Administrando el LC40 a nuestro modelo genético murino hemos podido constatar que es capaz de atenuar la progresión de la enfermedad, disminuyendo la

proliferación de linfocitos B y la subsiguiente producción de autoanticuerpos. También observamos una disminución de Th17 infiltrados a nivel renal y vascular, así como de Th1 especialmente a nivel renal (población que puede tener mayores efectos sobre este órgano por su producción de interferón gamma, el cuál va asociado a la enfermedad renal en lupus), con los ya mencionados efectos sobre la producción de ROS y los niveles de NO, además de una mejora en la función de barrera intestinal por restauración de la mucosa y un descenso en los niveles de endotoxemia, así como un menor daño renal por depósito de inmunocomplejos e inflamación. Todo ello se encuentra asociado a una mejora en la función renal y endotelial, acompañada por la prevención del desarrollo de hipertensión.

III) Caracterizar las posibles complicaciones cardiovasculares en un modelo inducible de LES mediante administración de un agonista de TLR-7.

El tratamiento con imiquimod (IMQ) resulta en un incremento gradual de la presión arterial, acompañado de la polarización de linfocitos esplénicos hacia un fenotipo proinflamatorio (aumento de Th17 y Th1 frente a una disminución en T reguladores). Adicionalmente, la activación de TLR7 con su agonista indujo el remodelado vascular de vasos de resistencia y disfunción endotelial en la aorta. Dichas alteraciones vasculares están posiblemente relacionadas con los cambios en la biodisponibilidad del NO por la también observada producción aumentada de ROS por la NADPH oxidasa, desencadenados por la inflamación local. Así mismo, a partir de las 4 semanas de edad, los ratones mostraron albuminuria alteraciones morfológicas renales, acompañadas de un aumento en la producción de autoanticuerpos. También se observó un aumento en citocinas típicamente proinflamatorias como IFNα, IFNγ, IL-6, IL-1β e IL-17a, las cuales se sabe también incrementan la actividad de la NADPH oxidasa, así como una disminución de IL-10 y TFG-β, los cuales inhiben la actividad de esta enzima. Posiblemente, este desequilibrio humoral en el estado inflamatorio sea responsable de las alteraciones vasculares observadas. Esto fue corroborado al realizar

tratamientos concomitantes primero con un cóctel de antioxidantes utilizado para eliminar los efectos de la NADPH oxidasa, y segundo con un anticuerpo neutralizante de IL-17a, eliminando así la actividad de esta citocina proinflamatoria. Ambos tratamientos dieron como resultado la mejora en la función endotelial y por ende en la presión arterial.

IV) Determinar si *Lactobacillus fermentum* CECT5716 (LC40) y/o *Bifidobacterium breve* CECT7263 (BFM) pueden prevenir disbiosis intestinal la disfunción endotelial y la hipertensión en nuestro modelo inducible.

Ambos tratamientos consiguieron prevenir el desarrollo de hipertensión y disfunción endotelial unido a la modulación exitosa del estrés oxidativo vascular, disminuyendo además los niveles de autoanticuerpos, y los porcentajes de Th17 en nódulos mesentéricos, además de mejorar la función de barrera intestinal. Mientras que los ratones tratados con IMQ presentaban una disbiosis consistente con lo ya publicado hasta la fecha, caracterizada por una reducción en la ratio Firmicutes/Bacteroidetes, y un menor número de especies entre otros parámetros, ambos probióticos fueron incapaces de modular la disbiosis descrita, aunque sí fueron capaces de colonizar la microbiota intestinal de forma exitosa. Posiblemente, la producción de metabolitos característicos de estos microorganismos esté detrás de su efecto a nivel fisiológico.

INTRODUCTION

INTRODUCTION

1. Systemic lupus erythematosus

1.1. Definition

Systemic lupus erythematosus (SLE) is a multisystemic chronic inflammatory autoimmune disorder, characterized by abnormally functioning B lymphocytes (Johnson *et al.,* 2015), which produce a high number of autoantibodies that, forming immunocomplexes, deposit along the vascular system, causing damage to several tissues and organs such as the kidneys, the skin or the vascular system itself (Sanz and Lee, 2010). This may generate a series of complications characteristic of this pathology, like renal injury or hypertension (Frostegård, 2008) depending on the patient, since SLE is a highly heterogenous disease, although some complications, like atherosclerosis, are extremely frequent.

The prevalence of SLE is significantly higher in women than in men, usually referred to as a 9:1 ratio (Tucker *et al*., 1995), the ratios actually range from 1.2:1 to 15:1, depending on the geographical location of the study, which already points to a complex amalgamate of root causes for the development of the disease. The peak age for the development of SLE being for women between 45 and 69 years of age and for men between 40 and 89 (Rees *et al*., 2017).

Even though SLE has, up until now, an unknown aetiology, it is believed to be triggered by a complex interaction of hormonal, genetic and environmental factors, that provoke the loss of tolerance against nucleic acids and their associated proteins.

1.2. Pathogenesis

As an autoimmune disease, the involvement of the immune system in SLE is crucial in the development of the pathology. Although SLE is mainly characterized by the proliferation of active B cells and the subsequent production of autoantibodies, other immune elements are present in the pathological process. Up until now, three

major immune pathways have been identified to be involved in the development of SLE:

I) The aberrant elimination of cell debris and immune complexes; macrophages and monocytes from lupus patients present a significantly reduced phagocytic capabilities, which results in an accumulation of non-digested cell debris that can act as a source of auto-antigens, promoting the occurrence of auto-antibodies. The swift elimination of apoptotic cells by macrophages is essential for the prevention of autoimmune diseases. Although the factors that partake in the processes of recognition and phagocytosis of apoptotic cells have been identified, the transcriptional basis for the detection and elimination of these cells is unknown (Liu and Davidson, 2012) (**Figure 1**).

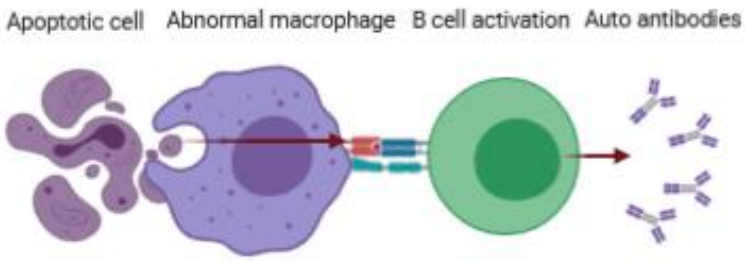

Figure 1. *Production of anti-dsDNA antibodies after stimulation by abnormal macrophages.*

II) The excessive activation of the innate immune system through Toll Like Receptors (TLR) and type I interferons (IFN)-α and IFN-β. These receptors, specially the endosomal variants, through the activation of the myeloid differentiation primary response 88 (MYD88) protein signalling pathway, have been shown to be involved in the development of SLE in general and its associated nephritis in particular (Christensen and Schlomchik, 2007),

including the necessary change in antibody isotype to IgG experienced commonly in SLE (Ehlers *et al*., 2006) (**Figure 2**).

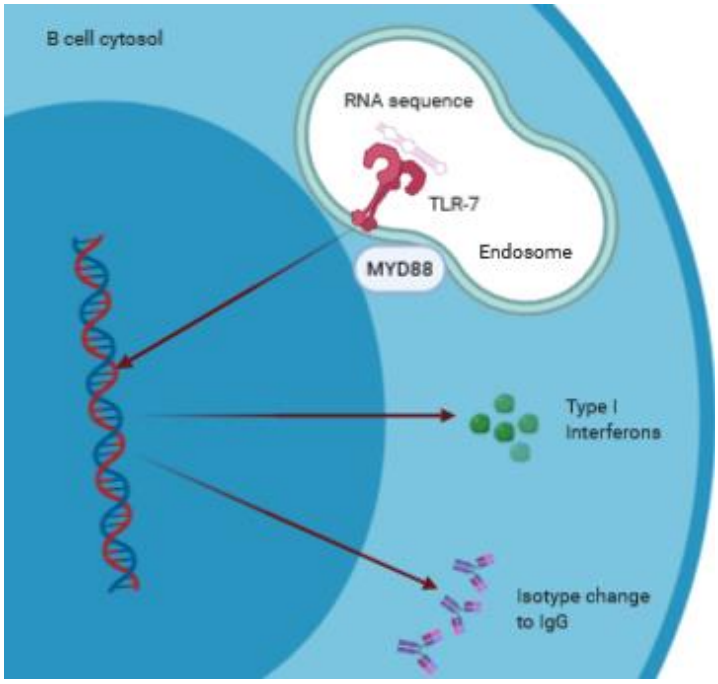

Figure 2. *Autoantibody production through Toll Like Receptors (TLR) activation. Abbreviations: MYD88, myeloid differentiation primary response 88.*

III) The abnormal activation of T and B lymphocytes; changes in T, B, Natural Killer and dendritic cells in the spleen of lupus-like murine models had been recently shown. Typically, aberrant B lymphocytes may present on their surface autoantibodies attached to autoantigens, which can be recognised by T cell receptors (TCR), and subsequently produce the maturation of the naïve T cell, this can create a non-stop feedback loop of stimulation between the two mentioned cells (De Groof *et al*., 2017) (**Figure 3**).

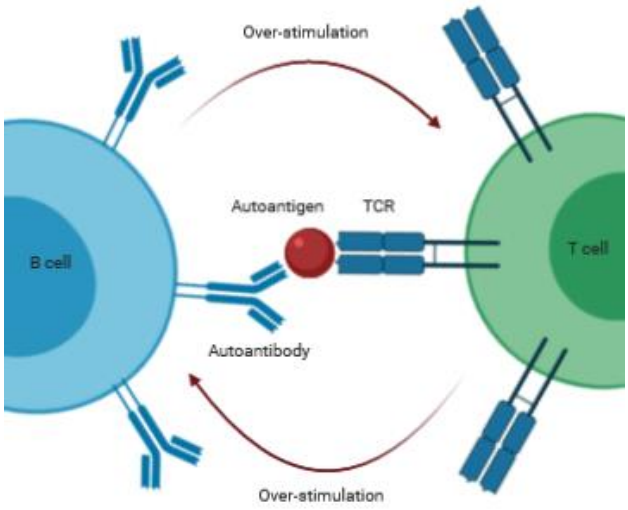

Figure 3. *Anomalous activation of B and T cells. Abbreviations: TCR, T cell receptor.*

Despite the diversity of these pathways, all the processes mentioned above culminate in the same fashion: the development of auto-antibodies, and their subsequent accumulation and deposit in the target organs. As already explained, the derived complications are the main symptoms of this pathology. Furthermore, these complications form a feed-back loop that increases inflammation, and the loss of function of the affected tissues or organs.

1.3. Features of SLE

Gender differences in SLE cases go further than just its incidence (Yacoub Wasef, 2004). Female cohorts of patients tend to present higher prevalence of such phenomena as the Raynaud syndrome, in which a reduced blood flow is caused due to a spasm in arteries, especially visible in hands; arthritis; low blood cell counts; psychiatric symptoms and a significant greater incidence of relapses. On the other

hand, male patients experiment more frequently renal disease, serositis (pleuritis and/or pericarditis), skin manifestations, peripheral neuropathy and seizures.

Still, several symptoms and signs are considered as markers of the pathology. A common phenomenon in SLE is the development of skin lesions, which can be divided into acute, subacute and chronic cutaneous lupus. Around 30% of European patients develop a recognizable malar rash, covering the cheeks and the nasal bridge according to a study by Cervera *et al.* (Cervera *et al*., 2003). In that same study, it was shown that up to 48% of patients manifested one or more episodes of arthritis, which led to the proposal of a possible link between SLE and rheumatoid arthritis by Heminki *et al.* (Heminki *et al.,* 2009). This number combined with the sufferers of arthralgias puts the percentage of patients at 95% for this kind of musculoskeletal manifestations according to other studies (Nzeusseu Toukap *et al*., 2007). Also, 28% displayed active nephropathy, although other studies point out that almost every single case of SLE presents deposit of autoantibodies at kidney level, placing the incidence for clinical nephritis around the 50% of patients (Ben-Menachem, 2010). On the latter, the deposition of immune complexes along the glomerular membrane, triggering a phenomenon called membranous glomerulonephritis, which may in turn provoke the apparition of proteinuria and/or hematuria, and even chronic renal impairment, possibly leading to acute or end-stage renal failure (Plantinga *et al.,* 2015). Thus, the presence of lupus nephritis (LN) in any of its forms is relatively common in SLE.

An assortment of cardiovascular signs can be observed in SLE patients. An increased incidence of risk factors for atherosclerosis has been found in this pathology. Autoimmune vascular injury in SLE may predispose to the development of an atherosclerotic plaque, which can be found in around a 30% of SLE patients (Asanuma *et al*., 2003). At heart level, pericarditis and myocarditis can affect these patients as well as accelerated ischemic coronary artery disease (Hahn, 2003). Of these cardiovascular complications we will proceed now to talk more extensively.

1.4. SLE and Cardiovascular disorders

Cardiovascular diseases as associated complications in SLE not only are common, but also are the main mortality cause among SLE patients. Furthermore, hypertension is the principal risk factor for the progression of renal and cardiovascular diseases. Fatal myocardial infarction has been reported to be 3 times higher in patients with SLE than in age- and gender -matched control subjects (Esdaile *et al*., 2001). A high number of studies show an elevated prevalence of hypertension in SLE patients, in fact, numbers ranging from 33% to 74% of these subjects have been described to present hypertension (Giannelou and Magravani, 2017) although mechanistic studies for hypertension in SLE are rare (Ryan, 2009).

Hypertension is usually present together with endothelial dysfunction. This dysfunction manifests itself as the inability of endothelial cells to induce vasodilation through the activation of the endothelial nitric oxide synthase enzyme (eNOS) and the release of its product, nitric oxide (NO). Although endothelial dysfunction is a common occurrence in hypertension, the physiopathological mechanisms involved can vary depending on the kind of hypertension and vessel, or vascular bed studied. A high number of SLE patients present a subclinical level of cardiovascular disease, which precedes the development of atherosclerosis. These subclinical abnormalities include endothelial dysfunction (with an intact muscular smooth muscle function) (Rajagopalan *et al.,* 2004), thickening of the arterial wall and abnormalities in coronary perfusion (Bruce *et al.,* 2003). Several studies suggest that the endothelium is prominently and severely affected in SLE, by the increase in auto-antibodies and proinflammatory cytokines. It seems that an imbalance between atheroprotective mechanisms and endothelial damage as a result of a high variety of factors, such as autoantibody activity, oxidized low-density lipoprotein (oxLDL) deposits, type I IFN or neutrophil extracellular traps, is an essential step in the development of atherosclerosis in lupus (Giannelou and Magravani, 2017). Some authors have been able to identify anti-endothelial cell antibodies in SLE, targeting a wide range of surface proteins on this cell type (Narshi *et al*., 2011), although the determination of their role and importance in the development of endothelial dysfunction in this autoimmune disease is still unclear.

High levels of type I IFN have been associated with endothelial dysfunction in SLE patients whereas others that would seem to display an obvious link, like lupus disease activity, strikingly lack this correlation (Somers*et al.,* 2012), which would position interferons as a very influential marker of endothelial dysfunction in this pathology. Specifically, IFN-α is able to block eNOS mRNA and protein expression and inhibit NO production through insulin stimulation (Buie *et al*., 2017).

Certain neutrophils characterized as low-density granulocytes have been identified as elements responsible for the development of endothelial dysfunction through the formation of neutrophil extracellular traps (NETs) (Knight and Kaplan, 2012). These NETs can provoke the transition from an endothelial to a mesenchymal phenotype in the vascular wall, with the subsequent loss of function, by degrading the vascular endothelial cadherin and activating the Wnt/β-catenin signalling pathway (Pieterse *et al*., 2017).

On the other hand, a raise in endothelin-1 (ET-1) might trigger an increment in water and sodium retention and renal vasoconstriction (Kuryliszyn-Moskal *et al*., 2008). This molecule and the renin-angiotensin-aldosterone system (RAAS) are capable of increasing reactive oxygen species (ROS) and, by extension, oxidative stress, being both key elements in the onset of SLE as well as hypertension (Alves and Grima, 2003). The RAAS modulates blood pressure (BP) through the angiotensin-converting enzyme (ACE), which has a fundamental role in blood volume homeostasis and might cause inflammatory tissue injury, commonly via the angiotensin II receptor type 1. Several authors have demonstrated how the RAAS is elevated in SLE patients (Wüthrich, 2009). In some ethnic populations, nephritis, hypertension or cardiovascular diseases can be influenced by an insertion/deletion polymorphism in intron 16 of the ACE gene (Rigat *et al.,* 1990). Nonetheless, there is not a clear link between the described allele and hypertension in asian SLE patients (Negi *et al*., 2015). The level of 24-h urinary potassium in SLE patients has been found decreased. Contrarily, sodium was found elevated when compared to healthy subjects. This was also linked to BP in this pathology, which points to a possible role of this ions in the regulation of hypertension in SLE patients. (Chae *et al*., 2001; Barnado *et al*., 2016).

In addition, numerous studies conducted on female subjects from a genetic murine model of SLE known as NZBW/F1, which is also characterized by the development of hypertension, have shown that several factors contribute to the pathogenesis of hypertension in SLE, including tumour necrosis factor (TNF)-α, an inflammatory cytokine, and oxidative stress. These local mediators of inflammation and the subsequent vascular dysfunction (Guzik. *et al*., 2003; Wu *et al.,* 2016; Small *et al*., 2018) are likely downstream of the initial immune system dysregulation (Taylor and Ryan, 2016) causing the main pathology.

TNF-α has been shown to act as a signal for total eNOS activity reduction. By bonding to its receptor, the TNFR (TNF-α Receptor), the cytokine is able to decrease protein transcription by a) supressing the enzyme's promoter activity, b) destabilizing its mRNA and c) inhibiting the degradation of the asymmetric dimethylarginine (ADMA), endogenous inhibitor of the enzyme (Neumann *et al*., 2004; Kleinbongard *et al*., 2010). Additionally, the administration of the cytokine in both rodents and humans has been shown to impair the endothelial function (Wang *et al.,* 1994; Chia *et al*., 2003).

Gómez-Guzmán *et al.* (Gómez-Guzmán *et al*., 2014) by treating the aforementioned NZBW/F1 mice with either hydroxychloroquine or an antioxidant cocktail, were able to inhibit superoxide anion (O_2^-) production from the NADPH oxidase, main source of vascular ROS, which reduced the oxidative stress characteristic of SLE, and, in turn, reduced hypertension and endothelial dysfunction in this model. ROS, especially O_2^-, are extremely reactive and deplete NO bioavailability by reacting with it, and producing peroxynitrites (Vanhoutte, 1989), which provoke a high number of negative effects on the structure and function of the vascular wall (Szabo. *et al*., 2007) playing a key role in the development of endothelial dysfunction. Plus, some of the pro-inflammatory cytokines typically present in SLE, such as TNF-α, IFN-γ or interleukin (IL)-17a are able to induce an increase in the activity of the NADPH oxidase (Huang *et al*., 2012; Nosalski and Guzik, 2017).

These three elements, autoantibodies, TNF-α and high levels of oxidative stress are able to induce the expression of cell adhesion molecules (vascular cell adhesion

molecule (VCAM) and intercellular adhesion molecule (ICAM) through the activation of nuclear factor-κB (NF-κB) (Cieślik *et al.,* 2008; Kleinbongard *et al.,* 2010; Kundu *et al*., 2012), facilitating leucocyte migration to the vascular wall. Hypertension is generally linked to immune cell infiltration into the adventitia and periadventitial fat, as well as to the activation of T cells, which produce proinflammatory cytokines like the already mentioned IL-17a, IFN-γ, and TNF-α (Guzik *et al*., 2007; Madhur. *et al*., 2010). In the NZBW/F1 model, hypertension is not sensitive to salt and is associated with low levels of renin in plasma. Also, it has been reported that treatment with anti-CD20 not only reduced splenic B cell populations and plasma levels of anti-double-stranded DNA (anti-dsDNA) antibodies, but also prevented hypertension (Mathis *et al.,* 2014), marking the relevance of B cell activation in the development of hypertension in this pathology, even though the precise effects of B and T cells activation, which constitutes a central event in all autoimmune diseases, in the development of hypertension is not clear.

Recent studies show, as exemplified above, that vascular disease is significantly affected by an apparent self-perpetuating cycle involving inflammation, immune cells and oxidative stress in this pathology (Wu *et al*., 2016). In this sense, cellular modulation of the autoimmune response is an area of great interest in lupus research, and one of the most promising perspectives for its study is the recently found link between the gut microbiome and the immune system. According to an ever-increasing number of studies, gut microbiota goes under a shift in composition in autoimmune diseases like inflammatory bowel disease, multiple sclerosis, type 1 diabetes and rheumatoid arthritis. These changes in the microbiota, usually associated with pathological states, is referred to as dysbiosis. Nonetheless, the role of this phenomenon in SLE and in its animal models is still unclear (Hevia *et al*., 2014; Mu et al. 2017; Li et al. 2018).

1.5. SLE and microbiota

A unique set of microorganisms (viruses, archaea, bacteria and fungi) that find their niches in and on the body compose the mammalian microbiome. One of those

niches is located in the gut, and it is particularly dominated by *Firmicutes* and *Bacteroidetes*, and in lower quantities by *Actinobacteria*, *Proteobacteria*, *Synergistetes*, *Verrucomicrobia* and *Fusobacteria*. Nonetheless, the prevalence of these bacteria can be altered due to changes in environmental factors such as hormones, diet or exercise, the microbiota is constantly adapting to the physiopathological state of the host (Gentile and Weir, 2018). Recently, there has been found a link between dysbiotic states in the human gut microbiome and several parameters of health and disease.

1.5.1. Dysbiosis in SLE patients

The human gut microbiome is highly variable at an interindividual basis (**Table 1**), which makes it extremely difficult to define and determine. That is the reason why certain ecological parameters of microbial stability like diversity or richness are frequently used as biomarkers for gut health instead of examining individual populations, also, they are extremely convenient due to their inverse correlation to the presence of chronic diseases (Cotillard *et al*., 2013), although the study of certain specific populations of bacteria can also be fundamental to discern the key mechanisms of dysbiosis and its link to the pathological state. Some changes in gut microbiota can be linked to SLE, however, these association is still not well characterized and understood, due to the above-mentioned variability, which is present in SLE, not only among human patients from different countries, but also in lupus animal models (He. *et al*., 2016). Different values for the already mentioned ecological parameters have been found. For instance, on one hand, He *et al*. (He *et al*., 2016) found no differences in ecological parameters that define alpha diversity like Simpson or Shannon indices in human patients, but he did in others like observed species and the Phylogenetic Diversity whole tree; on the other hand, Li *et al.* (Li *et al*., 2019) showed a decrease in observed species and another parameter called Chao index. Furthermore, Hevia *et al.* (Hevia *et al*., 2014) could not find significant changes in any of these metrics whatsoever. While the reason for these differences is unknown, it could be speculated that, since these studies were conducted in heterogenous

populations, the observed discrepancies may be linked to genetical, environmental and physiological factors from each individual, as well as to the progression of the disease itself.

Once the microbiota is studied in depth, disregarding these previous results on the alpha diversity level, and properly focusing in the microbial populations that reside in the gut, some evidence for the role of the gut microbiota in SLE are suggested. Even across different countries, at phylum level in SLE patients occurs an increase in *Bacteroidetes*, *Actinobacteria* and *Proteobacteria*, and a decrease in *Firmicutes* (He *et al*., 2016). It has also been reported that other phyla experiment changes, specifically, a decrease in *Tenericutes* and an increase in *Fusobatecteria* (Li *et al*., 2019). Generally, these shifts in bacterial populations could be described as a dysbiotic process associated with a disbalance in the *Firmicutes*/*Bacteroidetes* (F/B) ratio, even though some exceptions to this phenomenon have been found were the reduction of *Firmicutes* and expansion of *Bacteroidetes* is not observed (Luo *et al*., 2018).

At family level, depending on the study, SLE patients display more varying results that in the previous case, Spanish patients have shown a depletion of *Ruminococcaceae* and *Lachnospiraceae*, as well as an expansion of *Prevotellaceae* and *Bacteroidaceae*, being found only the increase in *Prevotellaceae* also in Chinese patients. Other expansions of bacterial families were found in different cohorts of patients, like *Megasphaera*, *Streptococcaceae*, *Rikenellaceae* and *Lactobacillaceae* (He *et al.,* 2016).

At genera level, in SLE patients *Roseburia*, *Faecalobacterium*, *Mollicutes*, *Bifidobacterium*, *Dialister*, *Pseudobutyrivibrio*, *Lactobacillus*, *Cryptophyta* and RF39 are depleted; while *Blautia*, *Eubacterium*, *Klebsiella*, *Rhodococcus*, *Eggerthella*, *Prevotella* and *Flavonifractor* are increased (He *et al*., 2016; Luo *et al*., 2018; Li *et al*., 2019). Interestingly, when studying the gut microbiota of patients in remission, an increase in *Bifidobacterium* was found, as opposed to the depletion showed during the active stage of the pathology (Li *et al*., 2019).

Finally, at species level, *Streptococcus anginosus*, *Lactobacillus mucosae*, *Veinella dispar* appeared increased (Li *et al*., 2019). Conversely, a decrease in *Ruminococcus gnavus* and *Bifidobacterium uniformis* has been described (Azzouz *et al*., 2019). Also, there is a positive correlation between the changes in the populations of *Campylobacter* and *Streptococcus*, specially *Streptococcus anginosus* present in stool samples and the Systemic Lupus Erythematosus Disease Activity Index (SLEDAI) registered by patients (Li *et al*., 2019). This could suppose a great step in the understanding of the subject.

Table 1. Gut microbiota shifts in SLE patients.

Patients	F/B	α- diversity	Phylum	Family	Genus	Species	Ref.
Women C 49.2 ± 10.7 yrs 20 patients	↓ F/B	No change	↓ *Firmicutes* ↓ Tenericutes ↑*Bacteroidetes*	↓*Lachnospiraceae* ↓ *Ruminococcaceae*			Hevia *et al.*, 2014
Women A 46.0 ± 1.8 yrs 35 patients	↓ F/B	↓PD_whole_tree ↓Observed species	↓ *Firmicutes* ↑*Bacteroidetes* ↑*Actinobacteria* ↑*Proteobacteria* ↑Fusobacteria	↑*Bacteroidaceae* ↑*Prevotellaceae* ↑ *Rikenellaceae*	↓ *Pseudobutyvibrio* ↓ *Dialister* ↓ *Bifidobacterium* ↑*Rhodococcus* ↑*Eggerthella* ↑*Klebsiella* ↑*Prevotella* ↑*Flavonifractor* ↑*Eubacterium*		He *et al.*, 2016
Women A 37.46 ± 14.17 yrs 40 patients	↓ F/B	↓Chao Richness ↓PD_whole_tree ↓Observed species	↓ Tenericutes	↑*Streptococcaceae*, ↑*Lactobacillaceae* ↑*Megasphaera*	↓*Mollicutes* ↓ *RF39* ↓*Faecalobacterium*, ↓*Cryptophyta* ↓*Roseburia*	↑*Streptococcus anginosus* ↑*Lactobacillus mucosae* ↑*Veinella dispar*	Lind *et al.*, 2019
Women 3AA (42.33 ± 13.39 yrs), 7 C (49.42 ± 8.51 yrs) Men 3 C (33 ± 6.57 yrs) 1 AA (29) 14 patients	Not change		↑*Proteobacteria*		↑*Blautia*		Luo *et al.*, 2018
Women 10 C (38.3 ± 4.32 yrs) 13A (38.3 ± 4.32 yrs) 16 AA (46.69 ± 4.33 yrs) 19 WH (44.84 ± 3.5 yrs) 3 BH (43 ± 9.57 yrs) 61 patients		↓Chao Richness		↓ *Ruminococcaceae*	↑*Blautia*	↓*Ruminococcus gnavus* ↓*Bacteroides uniformis*	Azzouz et al. 2019

Abbreviations: A, Asian; AA, Afro-American; BH, Black Hispanic; C, Caucasian WH, White Hispanic; Age (means ± SD); F/B, Firmicutes/Bacteroidetes.

1.5.2. Dysbiosis in SLE mice

Comparing murine with human microbiota when focusing on animal models of SLE points out several interesting differences, between humans and mice, but also among models. Studying genetic models, certain changes in composition have been observed in the Murphy Roths Large lymphoproliferative model (MRL/Mp-Fas^{lpr}, or simply lpr), the New Zealand black white model (NZWxNZB/F1, or NZBW/F1), TLR-7. 1 and the SNF1 model (SWRxNZB/F1); all these models present, regarding ecological parameters, an increased diversity both in early and advanced stages of SLE (Zhang *et al*., 2014; Luo *et al*., 2018). When examining another important parameter such as the F/B ratio, some authors were not able to see any differences at all in NZBW/F1 mice (Luo *et al*., 2018).

Meanwhile, at phylum level, lpr, NZBW/F1, TLR-7.1 and SNF1 models display several similarities with humans, like a raise in *Bacteroidetes* and a reduction in *Firmicutes*. The main differences between human patients and the murine models mainly occur at inferior taxonomic levels. At family level, the microbiota from the lpr model experiments a reduction in *Lactobacillaceae* and an expansion of *Rikenellaceae Desulfovibrionaceae*, *Ruminococcaceae*, *Lachnospiraceae*, or *Streptococcaceae* (Zhang *et al*., 2014; Mu. *et al*., 2017). Concurrently, at genera level, there has been demonstrated an increase in *Mollicutes*, *Roseburia, Butyrivibrio*, *Tenericutes*. Contrarily, *Bifidobacterium* and *Lactobacillus* were found decreased (Zhang, H. et al. 2014). In addition to this, the genus *Anaerostipes* has been found to be decreased in SLE, this is suspected to be highly relevant because of its capacity to synthesise butyrate (Luo *et al*., 2018).

Accordingly, similar changes in composition have been observed in the SNF1 model, such as the expansion of *Rikenellaceae* and *Lachnospiraceae* (Johnson *et al*., 2015). Still, some authors showed changes between the pre-disease and disease stages, and also, found a high level of *Lactobacillus*, opposing the results obtained from the lpr model. Plus, the genera *Dehalobacterium*, *Bilophila*, *Dorea*, *Oscillospira* and *Clostridium* might be increased (Luo *et al*., 2018).

In a similar fashion, the NZBW/F1 model of SLE experiments the alterations observed at phylum, family and genus levels in lpr and humans. Nonetheless, as in the SNF1 model, there is an increase in Lactobacillus, which can be linked to renal function impairment, systemic autoimmunity and other severe clinical signs (Luo *et al.*, 2018).

Recently, there has been developed a new model of SLE, the TLR-7.1. Its microbiota has already been characterised (Zegarra-Ruiz *et al.,* 2019), and the results are similar to the ones from previous models. The families *Rikenellaceae* and *Coriobacteriaceae* suffer an expansion, and *Clostridaceae* is decreased. Among the different genera present, *Prevotella* and *Desulfovibrio* are increased, and *Bifidobacterium*, *Anaerostipes*, *Coprobacillus*, *Turicibacter* are decreased. At species level, *Lactobacillus reuteri* was found increased, and also, it is translocated to mesenteric lymph nodes (MLN), spleen and liver, being this event linked to the evolution of SLE (**Table 2**).

Table 2. Gut microbiota shifts in different lupus animal models.

Model	F/B	α- diversity	Phylum	Family	Genus	Species	Ref.
NZBW/F1	↓ F/B or no change	↑α-diversity or no change	↓ *Firmicutes* ↑*Bacteroidetes*		<u>Pre-SLE</u> ↓*Bifidobacterium* ↑*Lactobacillus* ↓*Lactobacillus* <u>High severity</u> ↓*Anerostipes*		Luo *et al.*, 2018; Zhang *et al.*, 2014; Zegarra-Ruiz *et al.*, 2019
lpr	↓ F/B or no change	↑α-diversity or no change	↓*Firmicutes* ↑*Bacteroidetes*	↓*Lactobacillaceae* ↑*Rikenellaceae* ↑*Desulfovibrionacea* ↑*Ruminococcaceae* ↑*Lachnospiraceae* ↑*Streptococcaceae*	↓*Lactobacillus* ↓*Bifidobacterium* ↑*Tenericutes* ↑*Mollicutes* ↑*Butyrivibrio* ↑*Roseburia*		Mu *et al.*, 2017; Luo *et al.*, 2018; Zhang *et al.*, 2014; Zegarra-Ruiz *et al.* 2019
SNF1	↓ F/B or no change	↑α-diversity	↓*Firmicutes* ↑*Bacteroidetes*	↑*Rikenellaceae* ↑*Lachnospiraceae*	<u>Pre-SLE</u> ↓*Lactobacillus* <u>SLE</u> ↑*Lactobacillus* ↑*Clostridium* ↑*Dehalobacterium* ↑*Oscillospira* ↑*Dorea* ↑*Bilophila*		Johnson *et al.* 2015; Luo *et al.* 2018
TLR-7.1	↓ F/B	↑α-diversity	↓*Firmicutes* ↑*Bacteroidetes*	↓*Clostridaceae* ↑*Coriobacteriaceae* ↑*Rikenallecea*	↓*Turicibacter* ↓*Bifidobacterium* ↓*Coprobacillus* ↓*Anaerostipes* ↑*Prevotella* ↑*Desulfovibrio*	↑*Lactobacillus reuteri*	Manfredo Vieira *et al.* 2018

Abbreviations: F/B, Firmicutes/Bacteroidetes; SLE, systemic lupus erythematosus.

1.5.3. Gut barrier and immune activation

All the alterations of the microbiota, in human patients and animal models, mentioned above are associated with changes in the epithelium of the intestinal barrier, which can be described as an impairment in junction proteins such as claudin, zonulin

(ZO)-1 or occludin; and thus, increasing intestinal permeability, characterized using the fluorescein isothiocyanate (FITC)-dextran test (Mu *et al*., 2017). This impairment of the intestinal barrier functions might be a key component for the modulation of SLE and its cardiovascular complications, since some bacteria or their metabolic products and structural components would be able to cross the intestinal epithelium and through the bloodstream gain access to different tissues.

For instance, *Enterococcus gallinarum* has been proved to be able to translocate from its usual niche in the gut microbiota to the liver, this phenomenon is thought to cause the production of anti-dsDNA antibodies by the activation of TLR-7/8 in genetically predisposed hosts such as genetic murine models like the (NZW x BXSB)F1 hybrid or human patients (Manfredo-Viera *et al*., 2018). Interestingly, once the depletion of *E. gallinarum* from liver is achieved with an adequate antibiotic treatment, pathogenic autoantibodies and T cells are successfully eliminated. Similarly, there seems to be a negative correlation between *Synergistetes* gut levels and anti-dsDNA antibody titers and IL-6 levels in plasma (Katz-Agranov and Zandman-Goddard, 2017). This interleukin is able to promote and increase the differentiation of T helper (Th)17 and the production of IL-17a, which is a proven key driver of autoimmunity in SLE (Chen *et al*., 2010; Kimura and Kishimoto, 2010). Furthermore, the microbiota from SLE patients stool samples is able to induce the differentiation of Th17 on its own in *in vitro* studies.

Some bacteria are able to modulate the immune response, that could be either beneficial or detrimental, besides regulating anti-dsDNA antibody levels. Among this alternative pathways which modify the immune system is the activation of TLR-4 through the presence of bacterial components such as lipopolysaccharides (LPS) deriving from the wall from Gram negative bacteria, like *Bacteroidete*s, which is increased in SLE mice, inducing the proinflammatory cytokines (IL-6, type I IFN and TNF-α), typically found elevated both in human patients and murine models (Yu *et al*., 2018). TLR-7 can also induce the production of IFN-α, which is able to induce endothelial disfunction in SLE patients (Buie *et al*., 2017), this specific TLR dedicated to RNA-sensing has been found overexpressed in lupus (Manfredo-Viera *et al.,* 2018).

Furthermore, several bacteria are capable of producing short chain fatty acids (SCFA), which activate free fatty acid receptors with deleterious of beneficial effects on SLE (Arpaia *et al*., 2013). Both *Lachnospiraceae* and *Clostridium* are able to synthesise butyrate, which can activate the G-protein-coupled receptor (GPR)-109a, promoting the differentiation and maturation of regulatory T cells (Treg) in MLN, colon and spleen; butyrate can also increase IL-18 production, thus, promoting an anti-inflammatory response (Singh *et al*., 2014). Contrarily, propionate and acetate are found in higher concentrations in faecal samples from SLE patients when compared with healthy subjects, and there are no significative differences in butyrate levels (Rodríguez-Carrio *et al*., 2017). Shifts in specific bacterial metabolic pathways might be the reason for these changes in the synthesis of bacterial by-products. In fact, probably because of the raise in *Bacteroidetes* in SLE human subjects, the glycan degradation pathways are overrepresented in the SLE microbiome (Martens *et al*., 2011). Plus, the downregulation of LPS biosynthesis was achieved with a vancomycin treatment (Mu *et al*., 2017).

Hence, in order to improve the prognosis of SLE, the modulation of the microbiota is a very attractive perspective for the treatment of this pathology. Plus, several bacteria can be linked to remission stages in SLE or modifications characteristic from other innovative or more traditional treatments. *Rikenellaceae* and *Lachnospiraceae* were found increased and *Erysipelotrichaceae* decreased, and some changes observed in lupus were restored when treating SLE with retinol (Katz-Agranov and Zandman-Goddard, 2017). Glucocorticoids (prednisone and dexamethasone are typically used in SLE patients) increase markers of alpha diversity like the Shannon index, which might translate into a more balanced microbiome (Luo et al. 2018; He *et al.,* 2019). Prednisone reduced *Deferribacteres* and *Proteobacteria* at phylum level. At the genus level, *Anaerostipes* and *Prevotella* are expanded, while *Bilophila*, *Mucispirillum*, *Rikenella* and *Bilophila* are decreased (He *et al*., 2019). Besides, the antibiotic vancomycin increased *Lactobacilli* like *L. reuteri* and *L. rhamnosus* and depleted *Bacteroidales* and *Clostridiales* (Mu *et al*., 2017).

To summarise, there is evidence for cardiovascular and renal complications in SLE as a consequence of the pathological immune response, which is worsened by several antigen-presenting bacteria like *Bacteroidetes* and *Lachnospiraceae*, altogether with the depletion of *Firmicutes*, which translates into decreased levels of butyrate, T cell dysfunction and the onset of chronic inflammation and, subsequently, cardiovascular risk (Kasselman *et al*., 2018). Nonetheless, whether intestinal dysbiosis is cause or consequence in SLE remains unknown (Lopez *et al*., 2016). All evidence points to the capability of certain microorganisms to modulate the initiation and development of autoimmune diseases like lupus. In spite of the advances in understanding the role of bacteria in the pathophysiology of SLE, the number of studies published on the subject is still scant. To further emphasise the systemic effect of gut microbiota in SLE, there has been stablished a link between microbiota, SCFA levels in serum and biomarkers of endothelial activation (Rodriguez-Carrio *et al*., 2017). Still, there has not been found any direct association between endothelial dysfunction in SLE and gut dysbiosis yet. Several possibilities for the prevention of cardiovascular complications have risen; it may be possible by decreasing Th17 polarization through the expansion of butyrate-producing bacteria or reducing endotoxemia levels via the improvement of the intestinal barrier integrity. It also might be possible through the reduction in autoantibody production by decreasing levels of microorganisms capable of producing RNA-binding autoantigens, Ro60 structural homologs (Greiling *et al*., 2018), or preventing the translocation to secondary lymph organs and to the liver of crucial bacteria like *Lactobacillus reuteri* (Zegarra-Ruiz *et al*., 2019) or *Enterococcus gallinarum* (Manfredo-Vieira *et al*., 2018).

1.6. SLE and probiotics

Since shifts in gut microbiome composition are linked to the development of lupus, the induction of changes in gut microbiota can lead to an improvement in this pathology, which makes the microbiota an interesting therapeutic target. The current strategy for treating SLE patients is focused on non-steroidal anti-inflammatory drugs,

hydroxychloroquine, glucocorticoids and immunosuppressive agents (Chan *et al*., 2013), which is considered a partial success, since treatment results in an improvement in prognosis, although it is still a challenging matter due to the adverse effects characteristic from these therapies and the possibility of refractory disease. As a matter of fact, azathioprine and corticosteroid therapies are linked to a higher risk of cardiovascular disease in SLE patients. Thus, there is a need for new therapeutic strategies that will improve the renal and cardiovascular complications associated to SLE.

One promising approach to the modulation of the gut microbiota to improve these associated complications is the supplementation with specific bacterial strains. This same strategy, especially when using *Lactobacilli*, has shown very positive results in other autoimmune diseases (Schiffer *et al*., 2011; Zamani *et al*., 2016), ameliorating the pathology symptoms. Furthermore, it has been proven that *Lactobacillus spp.* when supplemented to the lpr murine model prolongs survival and mitigates nephritis, both effects linked to the capacity of this therapeutic approach to decrease anti-ds-DNA antibody levels in plasma (Mu *et al*., 2017).

On this subject, according to the International Scientific Association for Probiotics and Prebiotics (ISAPP), the microorganisms that “in adequate amounts can provide a health benefit on the treated host”, as the ones described above, can be gathered under the name of probiotics. With the caveat that these probiotics must be “live microorganisms with a suitable viable count of well-defined strains with a reasonable expectation of delivering benefits for the wellbeing of the host” (Hill *et al*., 2014). When evaluating the effectiveness of these microorganisms in the treatment of cardiovascular diseases, probiotics have been shown to be a valid alternative for obese postmenopausal women. The use of Ecologic® Barrier, a multispecies probiotic, is able to modulate biochemical and functional markers of vascular dysfunction, improving cardiometabolic parameters, and, even reducing BP (Szulińska. *et al*., 2018a and 2018b). Women supplemented with this probiotic, present lower levels of LPS in plasma, which may be the reason behind the other observed effects. Still, whether the

probiotic is able to improve or prevent endothelial dysfunction or not is yet to be dilucidated in SLE.

Probiotics have a wide range of physiological responses, although the main pattern of action shown by a majority of them usually consists of changes in the immune system, decreasing the proinflammatory tendency, and so, the complications of autoimmune diseases are ameliorated. Frequently, the mechanisms involved in this anti-inflammatory effect of probiotics are related to the modulation of Treg and Th17 populations (Mardani *et al.,* 2018), but alternative less known pathophysiologic mechanisms might take a part in the observed effects.

For instance, when the probiotic *Lactobacillus delbrueckii subsp. Lactis* PTCC1743 is administered to a SLE murine of model induced by pristane (Mardani *et al*., 2018), mice experimented a symptomatologic improvement, and also a decrease in Th17 lymphocytes and, also, one of the possible components in the triggering and development of the inflammatory process, plus an important cytokine produced by Th17: IL-17a. Also, the probiotic *Lactobacillus rhamnosus* ATCC9595 is able to modulate the retinoic acid receptor-related orphan receptor gamma (RORγ), which is a Th17 maturation transcription factor. Furthermore, both *Lactobacillus delbrueckii subsp. Lactis* PTCC1743 and *Lactobacillus rhamnosus* ATCC9595 are capable of reducing Th1 and one of its related cytokines, IFN-γ, another molecule that can be responsible for the inflammatory state in SLE.

Meanwhile, a different strain of *Lactobacillus*, *Lactobacillus reuteri* GMNL263, was able to modulate SLE activity through the other mechanism mentioned above, it increases Treg populations in the NZBW/F1 model (Tzang *et al*., 2017), similarly to *Lactobacillus rhamnosus* ATCC9595, it regulates the expression of a transcription factor that promotes the maturation of Treg, the forkhead box P3 (FoxP3). Treg modulate the activity of other components of the immune system (Th17 among them), and are traditionally seen as anti-inflammatory. The probiotic is also capable of reducing levels in liver of TLR-4, TLR-5, TLR-7 and TLR-9, which mediate in the

development of inflammation, and increasing the antioxidant activity in this same organ.

These changes experimented with *Lactobacillus reuteri* GMNL263, on the expression levels of TLR and on the oxidative stress status, are also present in the treatment with *Lactobacillus paracasei* GMNL32 and *Lactobacillus reuteri* GMNL89, while the effects on Treg populations are not observed. Interestingly, these three treatments have also in common a reduction in liver pro-inflammatory cytokines such as IL-6, IL-1β and TNF-α, via the suppression of the mitogen-activated protein kinase and NF-κB signalling pathways, decreasing even the occurrence of apoptosis (Hsu *et al*., 2017). On the subject of cardiovascular complications, *Lactobacillus paracasei* GMNL32 has been shown to display similar effects on cardiac tissue, reducing left ventricular hypertrophy (Hu. *et al.,* 2017).

There have been also some attempts to study directly the interactions between the probiotics and the immune system. In *in vitro* studies (Lopez. *et al*., 2016), the incubation of dendritic cells with different probiotic-enriched SLE microbiota , and the subsequent co-incubation of these dendritic cells with naïve T cells rendered some interesting results: when incubating with *Bifidobacterium bifidum* LMG13195, the level of activation of T cells was decrease; meanwhile, when the probiotics employed were *Blautia coccoides* DSM935 and *Ruminococcus obeum* DSM25238, the resulting Th17/Th1 ratio from the activation of T cells was in both cases decreased, although IL-17a and IFN-γ levels remained unchanged.

To summarise, examining the mentioned evidence, we can conclude that there is a lack of publications centred on the cardiovascular complications of SLE. Although we are starting to cast some light on the role of the immune system, specially Th17 and Treg, in the development of lupus and its modulation by the gut microbiota. Nonetheless, even though probiotics have been proven to be able to improve the condition of the pathology, and thus, could become an attractive alternative approach to the treatment of SLE, more experiments are needed to better understand the

implication of the microbiome and its modulation in the evolution of SLE, exemplified by the lack of human trials in Clinicaltrials.gov (**Table 3**).

Table 3. Probiotic effects in different lupus animal models.

Probiotic	Model	Observed effects	Ref.
Lactobacillus delbrueckii subsp. lactis PTCC 1743	Pristane-induced murine model	↓Th17 ↓IL-17a ↓Th1 ↓IFN-γ	Mardani *et al.*, 2018
Lactobacillus rhamnosus ATCC 9595	Pristane-induced murine model	↓RORγ ↓Th17 ↓Th1 ↓IFN-γ	Mardani *et al.*, 2018
Ruminococcus obeum DSM25238	*In vitro*	↓Th17/Th1 ratio	López *et al.*, 2016
Blautia coccoides DSM935	*In vitro*	↓Th17/Th1 ratio	López *et a*l., 2016
Lactobacillus reuteri GMNL 263	NZBW/ F1	↑FoxP3 ↑Treg ↓TLR-4 ↓TLR-5 ↓TLR-7 ↓TLR-9	Tzang *et al.*, 2017
		↓IL-1β ↓TNF-α ↓IL-6	Hsu *et al.*, 2017
Bifidobacterium bifidum LMG13195	*In vitro*	↓T lymphocytes activation	López *et al.*, 2016
Lactobacillus reuteri GMNL 89	NZBW/ F1	↓TLR-4 ↓TLR-5 ↓TLR-7 ↓TLR-9	Tzang *et al.*, 2017
		↓IL-1β ↓TNF-α ↓IL-6	Arpaia *et al.*, 2013
Lactobacillus paracasei GMNL 32	NZBW/ F1	↓TLR-4 ↓TLR-5 ↓TLR-7 ↓TLR-9	Tzang *et al.*, 2017
		↓IL-1β ↓TNF-α ↓IL-6	Hsu *et al.*, 2017

Abbreviations: FoxP3, forkhead box P3; IFN, interferon; IL, interleukin; RORγ, RAR-related orphan receptor gamma; Th, T-helper; TLR, toll-like receptor; TNF-α, tumor necrosis factor alpha; Treg, T regulatory.

2. Murine models of SLE

As seen above, a broad spectrum of murine models is used in lupus research, each model presenting its own specifications which may explain the observed differences in gut microbiota composition and evolution during the development of the pathology. As a consequence of the variety of approaches to simulating SLE in rodent subjects, the

degree of similarity to the real human lupus changes depending on the model used and the affected organs examined, although most of them concur in the production of autoantibodies, and a subsequent development of glomerulonephritis (Du *et al.*, 2015), but in essence, none of the known murine models can present a total holistic approach to SLE, due to the heterogeneity of this disease (Nadeau, 1989).

Generally speaking, SLE murine models can be divided into two groups, neatly compartmentalizing the two moieties of the nature vs nurture debate:

I) Spontaneous models. Which depend on the genotype of the mice employed. In this group we can find models such as the cross between the New Zealand Black and the New Zealand White mouse, the NZBW/F1 mouse, which is probably one of the most extended models in the market (Jacob *et al.*, 1987), it develops autoantibodies (mainly anti-dsDNA) splenomegaly, glomerulonephritis, hypertension and, in some occasions, vasculitis, although they do not present the characteristic rash or arthritis (Dixon, 1978). Derived from this murine strain, more than 20 other models where obtained catalogued under the collective name of NZM (New Zealand mix), which display altered levels of the symptoms already expressed in the NZBW/F1 (Rudofsky and Lawrence, 1999). More recently, parting from crossings between C57BL6 mice and one of the NZM strains, congenic mice with 3 altered loci affecting their susceptibility to SLE were developed, the sle1,2,3 model (Morel *et al.*, 2000). Aside from these models, all derived from the original NZBW/F1 strain, other models can be found, such as the lpr strain, the result of the cross between LG, B6, AKR and C3H mice. This model differs from the previous ones in that it more frequently displays vasculitis, and develops other SLE signature symptoms such as arthritis or the rash and a more complete and diverse panel of autoantibodies although it does not present hypertension (Ruch *et al.*, 1982). At a different approach, it has been also developed another model where the pathology is only present in the male individuals, the BXSB model, which focus in an alteration in the Y chromosome, a loci resulting

from the translocation from the X chromosome containing the TLR7 gene, producing an overexpression of this receptor. Also, the new gene-editing techniques have allowed for a broad range of knock-out and transgenic models like the introduction of sequences coding for autoantibody chains in the genome or the knock out models for TLR genes (William *et al*., 2006; Nickerson, 2013).

II) Induced models. Which are obtained by finding appropriate molecular triggers for the onset of SLE or SLE-like pathologies. One of the most used methods of SLE induction is the intraperitoneal injection of the mineral oil pristane in BALB/c mice to provoke a proinflammatory reaction which in months will produce autoantibodies not dissimilar to those found in SLE, arthritis and glomerulonephritis (Satoh, 1995). Similarly, to the BXSB spontaneous model, several agonists of TLR-7 like resiquimod or imiquimod (IMQ) (Yokogawa, 2014) have been proven to enable SLE symptoms through an increased TLR7 activity and its associated type I IFN production, although contrarily to its spontaneous counterpart, this model does develop endothelial dysfunction. Other less utilized models also exist like the graft-versus-host models, which requires the transplant of bone marrow from an SLE mouse to F1 cross subjects (Eisenberg and Via, 2012).

JUSTIFICATION AND OBJECTIVES

JUSTIFICATION AND OBJECTIVES

Several recent studies reported that intestinal microbiota is involved in the pathogenesis of SLE. Gut microbiota might trigger symptoms and progression of this autoimmune disease in both humans and mouse models of SLE (Hevia *et al.,* 2014; Zhang *et al.,* 2014; López *et al.,* 2016 Katz-Agranov *et al.,* 2017; Mu *et al.,* 2017a, b; Luo *et al.,* 2018; Manfredo Vieira *et al.,* 2018; Li *et al.,* 2019, Ma et al., 2019; Zegarra-Ruiz *et al.,* 2019). Despite this strong information linking gut disbiosis and autoimmunity in SLE, scarce investigations are available focused on the role of microbiota in the development of SLE hypertension (Small *et al.,* 2018). On the other hand, T cell activation has been involved in the increase of blood pressure induced by dysbiotic microbiota from spontaneously hypertensive rats, increasing Th17 infiltration, which leads to inflammation and oxidative stress in the vascular wall (Toral et al., 2019). This led to our first objective:

I) To analyse whether intestinal microbiota can increase the susceptibility to disease activity and T-cell activation in secondary lymph organs in the gut, leading to endothelial dysfunction and hypertension in female NZBWF1 mice.

Nowadays, the treatment and management of SLE is primarily based on non-steroidal anti-inflammatory drugs, glucocorticoids, hydroxychloroquine, and immunosuppressive agents (Chan *et al.,* 2013). Progress in the treatment of SLE has resulted in a significant improvement in prognosis. Nonetheless, SLE management is challenging because of the adverse effects of conventional therapies and the occurrence of refractory disease. In fact, corticosteroids and azathioprine therapies have been associated with an increased rate of cardiovascular disease in lupus patients. Therefore, there is an imperative need for new treatment strategies that would allow us to treat renal and cardiovascular disorders in lupus patients without compromising their health state. In this

sense, manipulation of the gut microbiota may lead to the development of novel therapies in SLE patients. This possibility was the basis for our second objective:

II) To stablish the possible protective role as dietary supplementation with the probiotic microorganism *Lactobacillus fermentum* CECT5716 (LC40) on SLE disease activity, hypertension and renal disease.

Recently, a lupus model induced by epicutaneous application of the TLR7 agonist IMQ has been described in several genetic backgrounds, including BALB/c mice (Yokogawa *et al.,* 2014). TLR7 activation leads to several phenotypic and functional changes characteristic of human SLE, including elevated levels of autoantibodies and multiple organ involvement (Yokogawa *et al.,* 2014). Although several studies have used TLR7 transgenic (TLR7tg) lupus-prone mice to elucidate the pathogenesis of SLE (Bolland et al., 2002; Deane *et al.,* 2007), these genetically modified lupus models have disadvantages because of their polygenic [disease is driven by multiple alleles, such as B6.RIIB(-/-)/yaa mice] or monoallelic nature (disease is driven by single alleles, such as B6. Yaa), thereby adding additional confounding factors to the effect of TLR7 activation alone. To date, no previous studies have evaluated changes in blood pressure in murine lupus induced by TLR7 activation. In addition, no studies have directly assessed whether alterations in vascular structure and function may contribute to raise blood pressure during lupus disease progression in this model. Therefore, our next objective was:

III) To characterise whether chronic topical application of IMQ in wild-type female BALB/c mice would induce an increase in blood pressure, and if these changes in blood pressure are associated with vascular alterations.

The IMQ model displays SLE symptoms through an increased TLR-7 activity and its associated type I interferon (IFN) production. Moreover, this model has been shown to develop autoantibodies, splenomegaly and similar immune alterations characteristic of SLE (Yokogawa *et al.,* 2014). Additionally, at the vascular level, TLR-7 activation through IMQ has been proven to cause endothelial dysfunction (Liu *et al.,* 2018). This inducible model, like other models of the disease (Zhang *et al.,* 2014; Luo *et al.,* 2018), develops a shift in bacterial communities in the gut that parts from physiological conditions, commonly known as dysbiosis (Zegarra-Ruiz *et al.,* 2019). Since probiotics have been proven to be effective in the treatment of SLE in other models that also present dysbiosis (de la Visitacion *et al.,* 2019), the last objective of the thesis was:

IV) To determine whether *Lactobacillus fermentum* CECT5716 (LC40) and/or *Bifidobacterium breve CECT7263* (BFM) can prevent hypertension, endothelial dysfunction and intestinal dysbiosis in a female mouse inducible model of lupus.

MATERIALS AND METHODS

MATERIALS AND METHODS

1. Animals and experimental groups

Female NZBW/F1 mice, their adequate healthy controls NZW/LacJ, BALB/c and C57BL/6 were obtained from Janvier (St Berthevin Cedex, France). All mice were maintained at a constant temperature (24 ± 1ºC), with a 12-hour dark/light cycle, and they were provided with free access to tap water and food. Animal body weight, food and water intake were controlled regularly. All experiments were performed in accordance with the Guide for the Care and Use of Laboratory Animals (National Institutes of Health (NIH) publication no. 85-23, revised 1996) and approved by our Institutional Committee for the ethical care of animals. Six different experiments were performed, at the end of each one, mice were sacrificed to collect blood and tissue samples for further processing. Stool samples were collected during different stages in the treatments.

1.1. Role of Gut microbiota in the development of hypertension in a genetic mouse model of SLE

1.1.1. Experiment 1: 30 26-week-old NZBW/F1 mice, and 10 of its respective healthy controls, NZW/LacJ mice, were sorted into to four different groups: control, SLE, SLE-treated with a broad-spectrum antibiotic mixture (SLE+MIX), and SLE-treated with vancomycin (2 g/L) (SLE-VANCO):

I) Control.

II) SLE.

III) SLE-VANCO.

IV) SLE-MIX.

Broad-spectrum antibiotic administration consisted of metronidazole (1 g/L), neomycin (1 g/L), ampicillin (1 g/L) and vancomycin (0.5 g/L, Pfizer, Madrid, Spain) in the drinking water (Manfredo Viera *et al*., 2018). Treatments were maintained for 6 weeks.

1.1.2. Experiment 2: To explore whether microbiota from hypertensive SLE mice is involved in BP regulation, a faecal microbiota transplantation (FMT) experiment was performed, as previously described (Toral *et al*., 2019). 20 10-week-old female C57BL/6J mice were sorted into two groups:

I) Control-Control.
II) Control-SLE.

For this FMT experiment, animals were treated with ceftriaxone as already explained and then, similarly to the previous FMT protocol, were orally gavaged a suspension of Control mice (Control-Control) or NZBW/F1 faeces (Control-SLE). Faecal microbiota transplantation (FMT) to recipient mice was carried out as previously reported with several modifications (Bruce-Keller *et al*., 2015). Briefly, faecal contents were isolated and pooled from donors for each experiment. Faecal contents were diluted 1:20 in sterile PBS and centrifuged at 800 revolutions per minute (rpm) for 5 minutes. The supernatant was aliquoted and stored at -80ºC. Starting 1 week before the administration, recipient mice were administered with 100 µL ceftriaxone sodium (400 mg/kg/day) daily for 5 consecutive days by oral gavage. The purpose of the antibiotic treatment was to reduce the pre-existing microbiota and to facilitate the recovery of the population and diversity of intestinal microbiota from donor rodents after FMT (Li *et al*., 2015). Forty-eight hours after the last antibiotic treatment recipient mice were orally gavaged with donor faecal contents (100 µL) for the time indicated above.

1.2. Effects of probiotic supplementation on cardiovascular and renal complications in SLE

16 18-week-old female NZBW/F1 and 12 age-matched NZW/LacJ mice were divided into the following groups:

I) Control.
II) Control-LC40.
III) SLE.
IV) SLE-LC40.

All treated groups received through oral gavage the probiotic *Lactobacillusfermentum* CECT5716 (LC40, Biosearch, Granada, Spain) at a dose of 5×10^8 colony-forming units (CFU) /day for 15 weeks.

1.3. TLR-7-driven lupus autoimmunity induces hypertension and vascular alterations in mice.

To study these effects, we performed 3 experiments:

1.3.1. Experiment 1: Taking advantage of their higher predisposition to TLR-7-driven functional responses and autoimmunity, we used 32 female7-9-week-old BALB/c mice, randomly sorted into the following experimental groups:

I) Control.
II) IMQ.

IMQ-treated groups were administered topically the TLR-7 agonist (Aldara®, Meda Salu, Madrid) three non-consecutive times a week at a dose of 1.25 mg per mouse for 4 or 8 weeks.

1.3.2. Experiment 2: In order to study the role of ROS on the effects induced by IMQ in hypertension, vascular inflammatory and endothelial dysfunction, a combination of the antioxidants (Antiox) was co-administrated along with IMQ. Briefly, 16 female 7-9-week-old BALB/c mice were randomly assigned to two different groups.

I) IMQ.
II) IMQ-Antiox.

The IMQ-Antiox group was treated with a combination of apocynin (1.5 mM) and tempol (2 mM) in drinking water. Non-treated mice received the corresponding oral vehicles of the active treatments. Treatments were followed for 8 weeks.

1.3.3. Experiment 3: In a separate experiment, we sought to determine whether IL-17 plays a role in hypertension induced by IMQ. Paralleling the antioxidants experiment, mice were assigned to 2 groups: IMQ-treated, and IMQ-treated plus IL-17-neutralizing antibody (IMQ+nIL-17). IP injections of either IL-17–neutralizing antibody (10 µg/mouse; R&D Systems, MN, USA) or the isotype control (10 µg/mouse; R&D Systems, MN, USA) were started on week 6 after IMQ treatment and the treatment lasted until week 8, and every 3 days.

I) IMQ.
II) IMQ-nIL-17.

1.4. Effects of probiotic supplementation on cardiovascular and renal complications in an inducible model of SLE.

One additional experiment using probiotics was performed on the IMQ model. 40 BALB/c mice were divided into 4 groups:

I) Control.
II) IMQ.
III) IMQ-LC40

IV) IMQ-BFM

All IMQ groups received the agonist in the same fashion as described in the previous set of experiments. Both *Lactobacillus fermentum* CECT5716 (LC40, Biosearch, Granada, Spain) and *Bifidobacterium breve* CECT7263 (BFM, Biosearch, Granada, Spain) were orally gavaged at a dose of 10^9 CFU/day for 8 weeks.

2. Blood pressure (BP) measurements

Systolic blood pressure (SBP) was determined on alternative weeks, in the morning in conscious, pre-warmed, restrained mice by tail-cuff plethysmography (digital pressure meter, LE 5001; Letica S.A., Barcelona, Spain). At least seven determinations per mouse were made in every session and the mean was taken as the SBP level (Toral *et al.*, 2014).

3. Plasma and urine determinations

At the end of each treatment, mice were killed under isoflurane anaesthesia. Blood samples were chilled on ice and centrifuged for 10 min at 3500 rpm and 4 ºC, and the plasma frozen at -80 °C. IFN-γ, IL-2, IL-10, IL-17a, IL-6, IL-21 and TNF-α concentrations were measured by multiplex ELISA using Luminex technology (Merk Millipore, Darmstadt, Germany). Plasma anti-dsDNA antibody concentration levels were quantified using a Mouse Anti-dsDNA IgG ELISA Kit (Alpha Diagnostic International, San Antonio, Texas, USA). Plasma LPS concentration was measured using the Pierce LAL chromogenic endotoxin quantitation Kit (Thermo Fisher Scientific S.L.U, Alcobendas, Madrid, Spain).

To determine proteinuria, we used the Combur^3 Test ® three-patch test strips (Roche Diagnostics, Mannheim, Germany), depositing a few drops of urine on top of the reactive patches.

4. Morphological variables

The heart, kidneys, liver, spleen, colon and small intestine were excised, cleaned and weighed. The heart, kidney, liver and spleen weight indices were calculated by dividing by the tibia length. Colon and small intestine ratios were obtained from dividing their weight by their length. All tissue samples were frozen in liquid nitrogen and then stored at -80ºC, save for a segment of spleen for other determinations.

5. Vascular reactivity

Descending thoracic aortic rings were dissected from animals and were suspended in a wire myograph (model 610M, Danish Myo Technology, Aarhus, Denmark) for isometric tension measurement as previously described (Toral *et al.*, 2014). The organ chamber was filled with Krebs solution (composition in mM: 118 NaCl, 4.75 KCl, 25 NaHCO3, 1.2 MgSO4, 2 CaCl 2, 1.2 KH 2PO4 and 11 glucose) at 37ºC and gassed with 95% O2 and 5% CO2 (pH ~7.4). Length-tension characteristics were obtained via the myograph software (Myodaq 2.01) and the aortae were loaded to a tension of 5 mN.

The concentration-relaxation response curves to acetylcholine (ACh) (1 nM - 10 µM) were performed in intact rings pre-contracted by the thromboxane A2 analogous U46619 (10 nM) to obtain similar level of pre-contraction in all aortic rings. The relaxant responses to the NO donor sodium nitroprusside (SNP) (1 nM - 10 µM), the endothelial nitric oxide (NO) synthase (eNOS) inhibitor N(v)-nitro-L-arginine methyl ester (L-NAME, 100mmol/l), or the nonselective nicotinamide adenine dinucleotide phosphate (NADPH) oxidase inhibitor VAS2870 (10mmol/l) were studied in the dark in endothelium-denuded vessels pre-contracted by U46619 (1 µM). In some experiments, responses to ACh were studied after incubation with IL-10- or IL.17a-neutralizing agents at 10 µg/mL (AF519 anf MAB4481 respectively, R&D systems, Minneapolis, Minnesota, USA) for 6 hours. Relaxant responses to ACh were expressed as a percentage of pre-contraction.

6. Histopathological analysis

Sections of the kidney and the superior mesenteric artery were obtained from each mouse by dissection. Sections were immersed in free-calcium Krebs solution for 30min. Then, sections were fixed in 10% buffered formalin for 24h, dehydrated in graded ethanol solutions and embedded in paraffin. For each artery, a series of four 5mm cross sections were obtained with a precision microtome (Microm International ModelHM500OM). These sections were stained with haematoxylin–eosin to visualize the structure of the vascular wall. Arterial media thickness, lumen diameter, media cross-sectional area (MCSA) and media–lumen ratio (M/L) were measured as previously described (Castro *et al.,* 2009) using a computer equipped with a Leica Q500MC image analyser connected to a video camera of a Leica Leitz DMRB microscope (Leica, Wetzlar, Germany). For the evaluation of kidney histopathology, 4mm sections were cut along the central axis of the biopsies. Then, samples were dewaxed and rehydrated for staining with haematoxylin–eosin, periodic acid–Schiff and Masson's trichrome. A morphological study on light microscopy was performed in a blinded fashion and the presence of SLE-like lesions was studied. Glomerular cellularity (proliferation) was evaluated by counting the number of nuclei per glomerular cross section (20 glomerular cross sections per mouse) (Wang *et al*., 2014). We considered proliferative glomeruli when the number of cells was more than 30.

7. In-situ detection of vascular reactive oxygen species levels

Ex-vivo vascular ROS content was measured using the oxidative fluorescent dye dihydroethidium (DHE) in aortic segments as previously described (Gomez-Guzman *et al*., 2014). Briefly, unfixed thoracic aortic rings were cryopreserved (0.1 M PBS with 30% sucrose for 1–2h), embedded in optimum cutting temperature compound (Tissue-Tek; Sakura Finetechnical, Tokyo, Japan) and frozen (-80ºC) until use. Cross-sections of 10mm thickness were obtained in a cryostat (Microm International Model HM500 OM)

and incubated for 30 min in HEPES buffer solution, containing DHE (10 mM), counterstained with the nuclear stain 4,6-diamidino-2-phenylindoledichlorohydrate (DAPI, 30 nM). In the following 24h, sections were examined on a fluorescence microscope (Leica DM IRB, Wetzlar, Germany) and photographed. Ethidium and DAPI fluorescence were quantified using ImageJ (version 1.32j, NIH, http://rsb.info.nih/ij/). ROS production was estimated from the ratio of ethidium/DAPI fluorescence. In preliminary experiments, before incubation with DHE, serial sections were treated with either the O_2^- scavenger polyethylene glycol-modified superoxide dismutase (PEG-SOD, 25 U/ml) for 30 min at 37°C, indicating the specificity of this reaction.

8. NAPDH oxidase activity

NADPH oxidase activity in intact aortic rings was determined using the lucigenin-enhanced chemiluminescence assay as previously described (Gomez-Guzman *et al.*, 2014). Briefly, aortic rings from all experimental groups were incubated for 30min at 37ºC in HEPES containing a physiological salt solution (pH 7.4) with the following composition (in mM): NaCl 119, HEPES 20, KCl 4.6, $MgSO_4$ 1, Na_2HPO_4 0.15, KH_2PO_4 0.4, $NaHCO_3$ 1, $CaCl_2$ 1.2 and glucose 5.5. Then, rings were placed in tubes containing the physiological salt solution, with or without NADPH (100mM) to stimulate aortic production of O_2^- and lucigenin was injected automatically at a final concentration of 5mM. NADPH oxidase activity was determined by measuring luminescence over 200s in a scintillation counter (Lumat LB 9507, Berthold, Germany) in 5s intervals and calculated by subtracting the basal values from those values found in the absence of NADPH. The vessels were then dried, and the dry weight was determined. NADPH oxidase activity was expressed as relative luminescence units (RLU) per min per mg of dry aortic tissue.

In another set of experiments, the NADPH-stimulated ROS production in homogenates from mesenteric arteries was also measured by DHE fluorescence in a microplate reader as previously described (Fernandes *et al.,* 2007). Succinctly explained, tissues and organs were homogenized in cold lysis buffer (pH~7,4) containing: 50 mM Tris-HCl, 150 mM NaCl, 2 mM EDTA, 50 mM NaF, 0.1 % sodium dodecyl sulphate

(SDS), 0.5% Na-deoxycholate, 1% Triton X-100, 1 mM PMSF, 0.5 µg/mL aprotinin, 0.5 µg/mL leupeptin and 0.2 mM Na_3VO_4. The homogenates were incubated in a 96well plate for 30 min at 37ºC in DHE 10 µM (PBS/DTPA 100 µM), DNA (1.25 ug/mL) was used to intensify the signal. After this step, NADPH (50 µM) was added to each well, followed by another 30 min incubation. Finally, fluorescence was measured (excitation:490 nm; emission: 525 nm).

9. Quantitative polymerase chain reaction

For quantitative polymerase chain reaction (qPCR) analysis, total RNA was extracted from different tissues and organs by homogenization and converted to cDNA using standard methods. PCR was performed with a Techne Techgene thermocycler (Techne, Cambridge, UK). A real-time (RT)-PCR technique was used to analyse mRNA expression. Preliminary experiments were carried out with various amounts of cDNA to determine non-saturating conditions of PCR amplification for all the genes studied. Therefore, under these conditions, relative quantification of mRNA was assessed by the SYBR Green based-RT-PCR method. The efficiency of the PCR reaction was determined using a dilution series of a standard tissue sample. Quantification was performed using the $\Delta\Delta$Ct method. The housekeeping genes ribosomal protein L13a (RPL13a), β-actin or glyceraldehyde-3-phosphate dehydrogenase (GADPH) were used for internal normalisation (**Table 4**).

Table 4. Oligonucleotides for qPCR.

mRNA targets	Sense	Antisense
TNF-α	ACGATGCTCAGAAACACACG	CAGTCTGGGAAGCTCTGAGG
IFN-α	GACTTTGGATTTCCCCTGGAG	AAGCCTTTGATGTGAAGAGGTTC
TGF-β	AGGGCTACCATGCCAACTTC	CCACGTAGTAGACGATGGC
IL-1β	GTCACTCATTGTGGCTGTGG	GCAGTGCAGCTGTCTAATGG
IL-6	GATGGATGCTTCCAAACTGG	AGGAGAGCATTGGAAGTTGG
NOX-1	TCTTGCTGGTTGACACTTGC	TATGGGAGTGGGAATCTTGG
NOX-2	ATGCAGGAAAGGAACAATGC	TTGCAATGGTCTTGAACTCG
p22phox	GCGGTGTGGACAGAAGTACC	CTTGGGTTTAGGCTCAATGG
p47phox	ATGACAGCCAGGTGAAGAAGC	CGATAGGTCTGAAGGCTGATGG
FoxP3	AGGCACTTCTCCAGGACAGA	CTGGACACCCATTCCAGACT
eNOS	ATGGATGAGCCAACTCAAGG	TGTCGTGTAATCGGTCTTGC
C1qa	CGGGTCTCAAAGGAGAGAGA	TATTGCCTGGATTGCCTTTC
C1qb	CAGGGATAAAGGGGGAGAAA	TCTGTGTAGCCCCGTAGTCC
Tsp-1	GCAGCACACACAGAAGCATT	CAATCAGCTCTCACCAGCAG
Mfge-8	AAAGCTGTACCCTGTTTCGTG	GGAGGCTGACATCTGGT
IFNϒ	GCCCTCTCTGGCTGTTACTG	CCAAGAGGAGGCTCTTTCCT
IL-10	CCAGCTGGACAACATACTGC	AGGGTCTTCAGCTTCTCACC
T-bet	CAACCAGCACCAGACAGAGA	AACATCCTGTAATGGCTCGTG
GATA-3	GCCTGCGGACTCTACCATAA	GTCTGACAGTTCGCACAGGA
RORγ	GCCTACAATGCCAACAACCACACA	TGATGAGAACCAAGGCCGTGTAGA
IL-17a	TCAGACTACCTCAACCGTTCC	CAGTTTCCCTCCGCATT
TLR-4	GCCTTTCAGGGAATTAAGCTCC	AGATCAACCGATGGACGTGTAA
IAP	CAT GGA CCG CTT CCC ATA	CTT GCA CTG TCT GGA ACC TG
VCAM-1	CTTCCAGAACCCTTCTCA	GGGACCATTCCAGTCACACTTC
TLR7	GCCATCCAGCTTACATCTTCT	TTTGACCCAGGTAGAGTGTTTC
TLR9	CTACAACAGCCAGCCCTTTA	GGACACACGGGTATGAATGT
IL-18	GACTCTTGCGTCAACTTCAAGG	CAGGCTGTCTTTTGTCAACGA
Occludin	ACGGACCCTGACCACTATGA	TGGAGATGAGGCTTCTGCTT
Muc-2	GATAGGTGGCAGACAGGAGA	GCTGACGAGTGGTTGGTGAATG
Muc-3	CGTGGTCAACTGCGAGAATGG	CGGCTCTATCTCTACGCTCTCC
ZO-1	GGGGCCTACACTGATCAAGA	TGGAGATGAGGCTTCTGCTT
RPL13	CCTGCTGCTCTCAAGGTTGTT	TGGTTGTCACTGCCTGGTACTT
GAPDH	TGCACCACCAACTGCTTAGC	GGATGCAGGGATGATGTTCT

Abbreviations: TNF-α, Tumor necrosis factor-alpha; IFN-α, Interferon alpha; TGF-β, Transforming growth factor beta; IL-1β, Interleukin-1beta; IL-6, Interleukin-6; NOX-1, NOX-1 subunit of NADPH oxidase; NOX-2, NOX-2 subunit of NADPH oxidase; p22phox, p22phox subunit of NADPH oxidase; p47phox, p47phox subunit of NADPH oxidase; FoxP3, Forkhead box P3; eNOS, Endothelial nitric oxide synthase; T-bet, T-box expressed in T cells; C1qa, Complement C1q subcomponent subunit a; C1qb, Complement C1q subcomponent subunit b; Tsp-1, Thrombospondin- 1; Mfge-8, Milk fat globule-EGF factor 8 protein; IFNϒ, Interferon gamma; IL-10, Interleukin-10; RORγ, ROR-gamma; IL-17a, Interleukin-17a; TLR, Toll-like receptor-4; IAP,

Intestinal alkaline phosphatase; VCAM-1, Vascular cell adhesion molecule-1; IL-18, Interleukin-18; Muc-2, Mucin-2; ZO-1, Zonula occludens-1; RPL13, Ribosomal protein L13; GAPDH, Glyceraldehyde-3-phosphate dehydrogenase.

10. Western blotting analysis

Tissues and organs were homogenized in cold lysis buffer (pH~7,4) containing: 50 mM Tris-HCl, 150 mM NaCl, 2 mM EDTA, 50 mM NaF, 0.1 % sodium dodecyl sulphate (SDS), 0.5% Na-deoxycholate, 1% Triton X-100, 1 mM PMSF, 0.5 µg/mL aprotinin, 0.5 µg/mL leupeptin and 0.2 mM Na3VO4. All homogenates were run on an SDS-polyacrilamide gel electrophoresis (PAGE) (40 µg of protein per lane). Then, proteins were transferred to polyvinylidene difluoride membranes, incubated overnight at 4°C with primary antibodies (1:1000). Afterwards, the membranes were washed three times for 10 min in Tris-buffered saline (containing 0.1% Tween 20) and were incubated with the correspondent secondary peroxidase conjugated antibodies (1:3000) (**Table 5)** at room temperature for 1 h. After washing the membranes, antibody binding was detected by an electrochemiluminescent (ECL) system (Amersham Pharmacia Biotech, Amersham, UK). Films were scanned and densitometric analysis was performed using Scion Image-Release Beta 4.02 software (http://www.scioncorp.com) (Quintela *et al*., 2014). The primary antibodies used include: a mouse monoclonal anti-eNOS antibody (Transduction Laboratories, San Diego, California, USA), a rabbit monoclonal anti-p-eNOS-Ser1177 antibody (Cell Signaling Technology, Danvers, MA, USA), a rabbit monoclonal anti-p-eNOS-Thr495 (MilliporeSigma), and rabbit polyclonal anti-RhoA (Abcam, Cambridge, United Kingdom). All were complemented with the proper secondary antibody.

For phosphorylated proteins, abundance ratio was calculated and data are expressed as a percentage of the values in control tissue from the same gel. All samples were re-probed for expression of α-actin (mouse monoclonal anti-α-actin, Merk) or β-actin (mouse monoclonal anti-β-actin, Merk).

11. Flow cytometry

MLN, spleens, blood and the abdominal aorta were collected from mice. The tissues were properly mashed with wet slides to decrease friction. The solutions were then filtered through a cell strainer of 70 µm. Cells from spleens were isolated, and then the red blood cells were lysed with Gey's solution. For intracellular staining, 10^6 cells were counted and incubated with a protein transport inhibitor (BD GolgiPlug; BD Biosciences) for an optimum detection of intracellular cytokines by flow cytometry, and cells were stimulated with 50 ng/mL phorbol 12-myristate 13-acetate plus 1 µg/mL ionomycin. After 4.5 h, cell aliquots from each sample were blocked with Fc-γ receptors to avoid nonspecific binding to these receptors (Miltenyi Biotec), and were stained with the live/dead stain as a viability dye, incubating for 30 min at 4°C. After that, cells were transferred to polystyrene tubes for surface staining for 20 min at 4°C in the dark. Cells were then fixed, permeabilized, and intracellular staining was conducted for 30 min at 4°C in the dark (**Table 5**). Data collection was performed using a flow cytometer Canto II (BD Biosciences) as previously described (Romero. *et al.*, 2017).

Table 5. Antibodies used for cytometry.

Antigen	Fluorochrome	Clone	Purveyor	Panel
Live/Dead	AmCyan	LIVE/DEAD® Fixable Aqua Dead Cell Stain	Thermo Fisher	1, 2, 3, 4
CD45	FITC	30F11	Miltenyi Biotec	1, 2, 3, 4
CD3	PE	REA641	Miltenyi Biotec	1, 2, 3
CD4	PerCP-Cy5.5	RM4-5	Invitrogen	1, 2, 3
CD25	PE-VIO770	7D4	Miltenyi Biotec	1
B220	APC	RA3-6B2	BD Bioscience	1
IL17a	PE-Cy7	eBio17B7	Thermo Fisher	2
IFN-γ	PE-VIO770	XMG1.2	BD Bioscience	3
CD11b	APC	REA592	Miltenyi Biotec	4
CD68	PerCP-VIO700	REA835	Miltenyi Biotec	4

Abbreviations: CD, Cluster of differentiation; IL-17a, Interleukin-17a; IFN-γ, Interferon gamma.

The technique was performed for a total of four panels following this strategy **(Figure 4 and 5)**:

I) B cells (CD45+ B220+) and Tregs (CD45+ CD3+ CD4+ CD25+).

II) Th17 (CD45+ CD3+ CD4+ IL17a+).

III) Th1 (CD45+ CD3+ CD4+ IFNγ+).

IV) Activated macrophages (CD45+ CD11b+ CD68+).

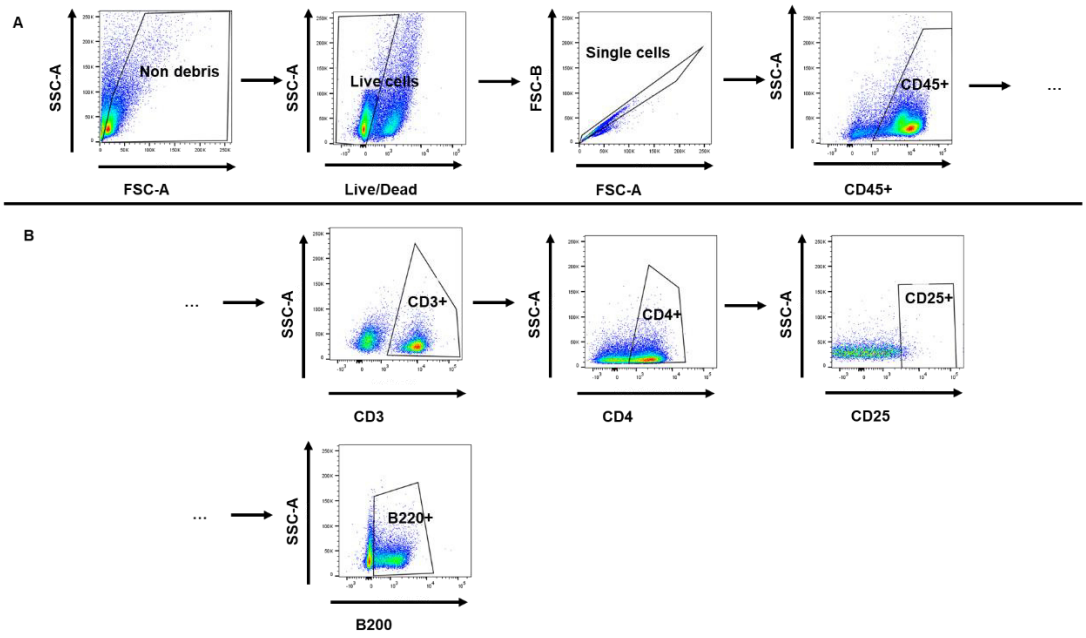

Figure 4. *Common steps for all panels studied (A). Specific gating from CD45+ cells for panel I(B).*

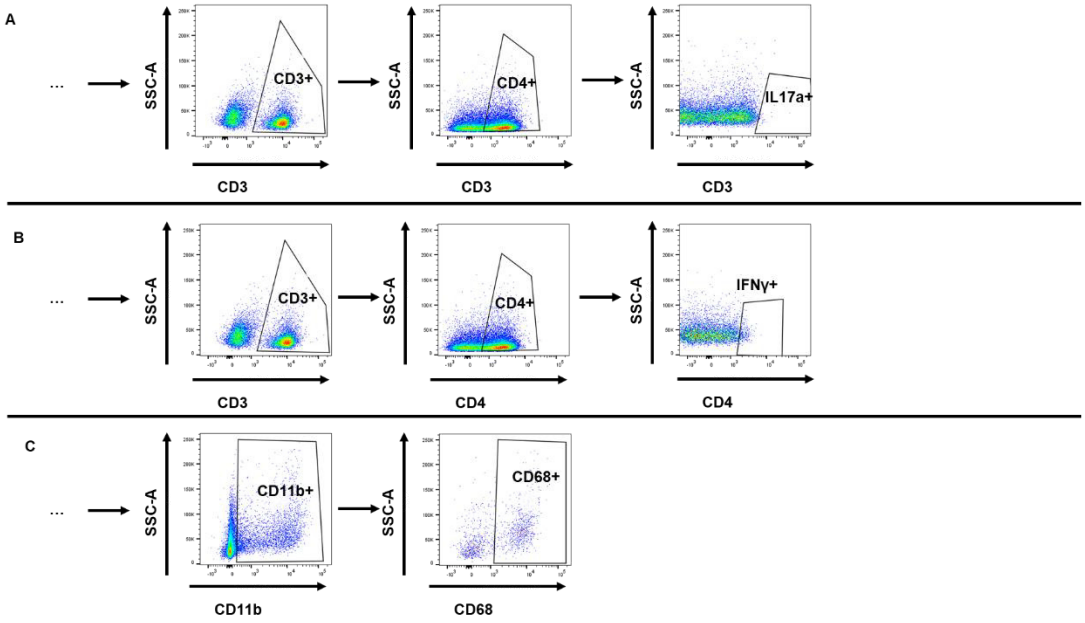

Figure 5. *Specific gatings from CD45+ cells for panels II (A), III (B) and IV (C).*

12. DNA extraction, 16s rRNA gene amplification and bioinformatics

Faecal samples were collected from 4 to 8 animals/group at the end of the experimental period. DNA was extracted from faecal samples using G-spin columns (Intron Biotechnology, Gyeonggi-do, Korea) starting from 30 mg of samples resuspended in PBS and treated with proteinase K and RNAses (Dole. *et al.,* 2013). DNA concentration was determined in the samples using Quant-IT PicoGreen reagent (Thermo Fisher Scientific), and DNA samples (about 3ng) were used to amplify the V3–V4 region of 16S rRNA gene (Caporaso *et al*., 2011). PCR products (around 450 base pair included extension tails, which allowed sample barcoding and the addition of specific Illumina sequences in a second low-cycle number PCR. Individual amplicon libraries were analysed using a Bioanalyzer2100 (Agilent Technologies, Santa Clara, CA, USA), and a pool of samples was made in equimolar amounts. The pool was further cleaned and quantified, and the exact concentration estimated by real-time PCR (Roche). Finally,

DNA samples were sequenced on a MiSeq instrument (Illumina, San Diego, CA, USA) with 23300 paired-end read sequencing at the Unidad de Genomica (Parque Cientifico de Madrid, Madrid, Spain). We used the barcoded Illumina paired-end sequencing pipeline to process the raw sequences (Zhou *et al*., 2011). First, the barcode primers were trimmed and filtered if they contained ambiguous bases or mismatches in the primer regions according to the bar-coded Illumina paired-end sequencing protocol. Second, we removed any sequences with more than 1 mismatch within the 40–70 base pair region at each end. Third, we used 30 Ns to concentrate the 2 single-ended sequences for the downstream sequence analysis. A detailed description of these methods was reported previously (Liu, 2017). Fourth, we performed UCHIME (implemented in USEARCH, v.6.1) to screen out and remove chimeras in the *de novo* mode (using-minchunk 20-xn 7-noskip-gaps 2) (Edgar, 2015). Between 90,000 and 220,000 sequences were identified in each sample. All subsequent analyses were performed using 16SMetagenomics (v.1.0.1.0) from Illumina. The sequences were then clustered to an operational taxonomic unit (OTU) using USEARCH with default parameters (USERACH v.61). The threshold distance was set to 0.03. Thus, when the similarity between 2 16S rRNA sequences was 97%, the sequences were classified as the same OTU. Quantitative Insights into Microbial Ecology (QIIME)-based alignments of representative sequences were performed using PyNAST, and the Greengenes 13_8 database was used as the template file. The Ribosome Database project algorithm was applied to classify the representative sequences into specific taxa using the default database (Edgar, 2015). The Taxonomy Database (National Centre for Biotechnology Information) was used for classification and nomenclature. Bacteria were classified based on the short-chain fatty acids' end-product, as previously described (Wang *et al*., 2007; Antharam *et al*., 2013).

13. Reagents

All chemicals were obtained from Merk (Barcelona, Spain), unless otherwise stated.

14. Statistical analysis

The Shannon diversity, Chao richness, and Pielou evenness, and observed species indexes were calculated using the QIIME pipeline (PAST ×3). Reads in each OTU were normalized to total reads in each sample. Only taxa with a percentage of reads >0.001% were used for the analysis. Principal Component Analysis (PCA) was also applied to these data to identify significant differences between groups. Linear discriminant analysis (LDA) scores above 2 were displayed. Taxonomy was summarized at the genus level within QIIME v.1.9.0 and uploaded to the Galaxy platform (Segata *et al*., 2011) to generate LEfSe/cladogram enrichment plots that considered significant enrichment at a value of $P < 0.05$, LDA score >2.

Results are expressed as means ± SEM. Statistical analyses were performed using Graph Pad Prism 7 software. A two-factor ANOVA was used to test for drug or group interactions. When a significant interaction was detected, one-way ANOVA with a Student Newman-Keuls post hoc test was used to discern individual differences between groups. Significance was accepted at $P<0.05$.

RESULTS

RESULTS

1. Gut microbiota is involved in the development of hypertension in a mouse model of systemic lupus erythematosus

1.1. Changes in microbiota composition with the development of hypertension in SLE mice

To determine the dynamics of the gut microbiota during BP increase associated with lupus progression in female NZBW/F1 mice, we analysed faecal pellets collected at 26 (prehypertensive) and 32 (hypertensive) weeks of age, and compared to aged-matched control mice. At 26 weeks, several bacterial taxa (class, order, family, and genus) were altered in SLE mice. According to the LDA, the relative abundance of 23 taxa was increased (green) and 18 taxa were decreased (red) as compared to control (**Figure 6**). PCA, at the genus levels, showed a clear separation between the two clusters, indicating two different gut environments. When we evaluated the phyla composition, faecal samples were dominated by *Firmicutes* and *Bacteroidetes*, with smaller proportions of *Verrucomicrobia*, *Proteobacteria*, *Tenericutes*, and *Actinobacteria*, (**Figure 7A, B**). We showed increased *Firmicutes* and reduced *Bacteroidetes* proportions in SLE as compared to control, which result in a significant increase in the F/B ratio (**Figure 7C**). At 32 weeks of age, both control and SLE mice alter the phyla proportion of the microbiota. A significant increase in the bacteria belonging to *Verrucomicrobia* and *Proteobacteria*, with tendency (0.065) to reduce *Firmicutes* was detected in control mice, whereas in SLE the dynamic is different, with significant increases in *Bacteroidetes* and *Proteobacteria*, and a reduction of *Firmicutes* (**Figure 7B**).

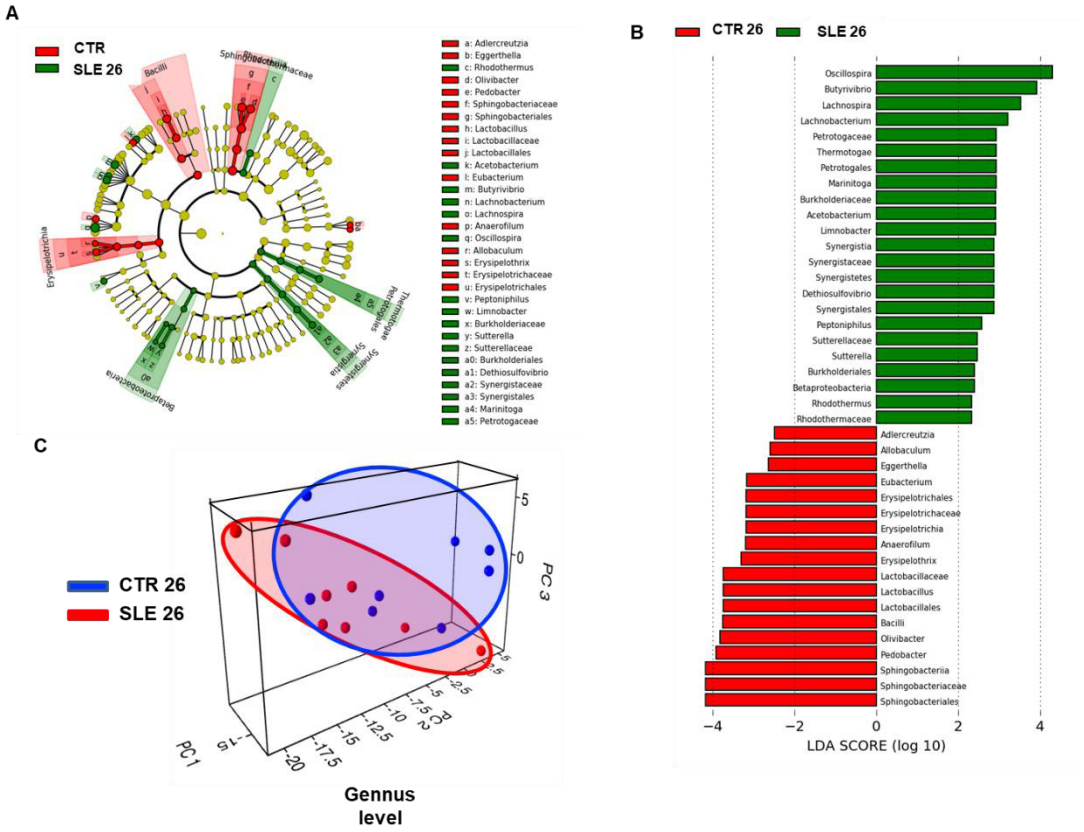

Figure 6. Analysis of gut microbiota composition in control (CTR) and systemic lupus erythematosus (SLE) mice at 26 weeks of age. *(**A**) The cladogram shows the significantly enriched taxa, the taxa are identified in the key to the right of the panel. Larger circles represent greater differences in abundance between groups. (**B**) Linear discriminant analysis effect size (LEfSe) identified significantly different bacterial taxa enriched in each cohort at LDA Score > 2, p<0.05 (red bars CTR enriched, green bars SLE enriched). (**C**) Principal components analysis comparing the diversity of both groups. n = 8 mice per treatment group for each comparison*

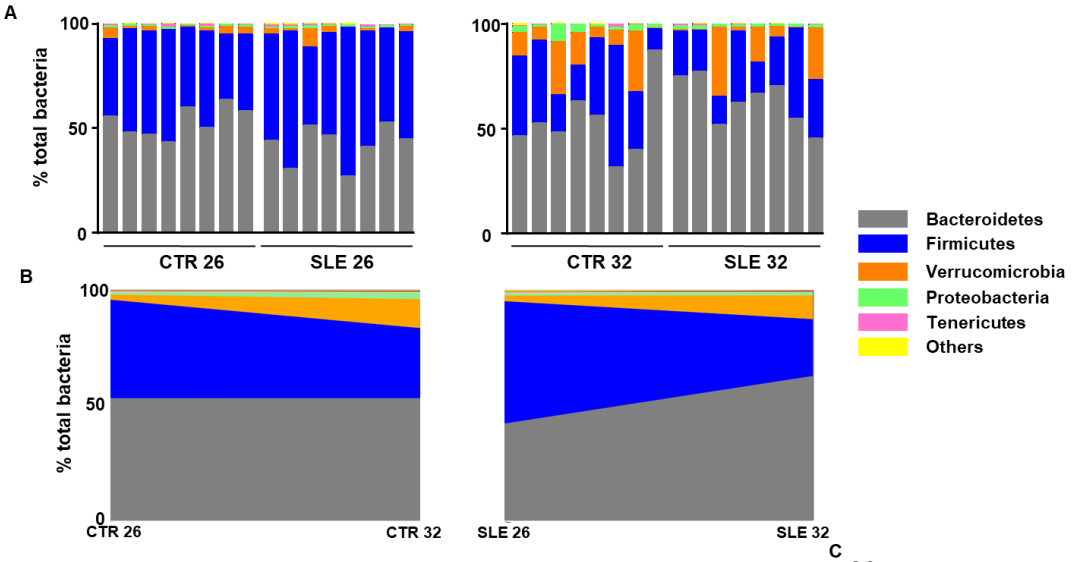

	26 weeks-old			32 weeks-old				
	Ctr (n = 8)	**SLE** (n = 8)	P value (SLE vs Ctr)	**Ctr** (n = 8)	P value (vs Ctr 26)	**SLE** (n = 8)	P value (vs SLE 26)	P value (SLE vs Ctr)
Actinobacteria	0.08 ± 0.00	0.09 ± 0.01	0.214	0.10 ± 0.03	0.216	0.11 ± 0.02	0.485	0.902
Bacteroidetes	53.13 ± 2.71	42.19 ± 3.46	0.019 *	53.16 ± 6.35	0.996	62.89 ± 4.33	0.001##	0.197
Firmicutes	42.82 ± 3.02	53.16 ± 4.11	0.048*	30.49 ± 5.86	0.065	24.64 ± 3.80	0.001##	0.385
Verrucomicrobia	2.12 ± 0.65	2.41 ± 1.06	0.806	12.47 ± 3.82	0.013*	10.30 ± 4.81	0.109	0.712
Proteobacteria	0.93 ± 0.03	0.94 ± 0.06	0.911	2.96 ± 0.89	0.029*	1.39 ± 0.09	0.001##	0.083
Tenericutes	0.64 ± 0.21	0.61 ± 0.15	0.916	0.32 ± 0.17	0.225	0.28 ± 0.10	0.065	0.838
Others	0.25 ± 0.02	0.67 ± 0.09		0.48 ± 0.10		0.39 ± 0.03		

Figure 7. Composition and evolution of gut microbiota in control (CTR) and systemic lupus erythematosus (SLE) mice. *(**A**) Proportion of bacterial phyla as percentages of the total population. (**B**) Evolution of phyla during the treatment. (**C**) Firmicutes/Bacteroidetes (F/B) ratios at 26 and 32 weeks of age. Values are expressed as means ± SEM. n = 8 mice per treatment group for each comparison. *P < 0.05 compared to the CTR group; #P < 0.05 and ##P < 0.01 compared to the untreated SLE group.*

When we compare the normotensive control with the hypertensive SLE at 32 weeks of age, no significant differences in the proportion of bacteria belonging to each phylum was observed, with no change in the F/B ratio. Moreover, no significant changes were observed between control and SLE at 32 weeks of age in three major ecological parameters, including Chao's richness (an estimate of a total number of operational taxonomic units present in the given community), Shannon's diversity (the combined parameters of richness and evenness), and Pielou's evenness (to show how evenly the individuals in the community are distributed over different operational

taxonomic units) (**Figure 8A**). However, at family level, a significant increase of bacteria from *Porphyromonadaceae* and *Sphingobacteriaceae* was detected in hypertensive SLE as compared to normotensive aged-matched control mice (**Figure 9**). At genus levels, PCA also showed a clear separation between the two clusters, and the proportions of several genus, such as *Parabacteroides*, *Pedobacter*, *Olivibacter* and *Clostridium* were also increased in SLE (**Figure 10**). It is interesting to note that at 26 weeks of age no significant differences were found in *Parabacteroides* and *Clostridium* abundance between SLE and control mice (not shown).

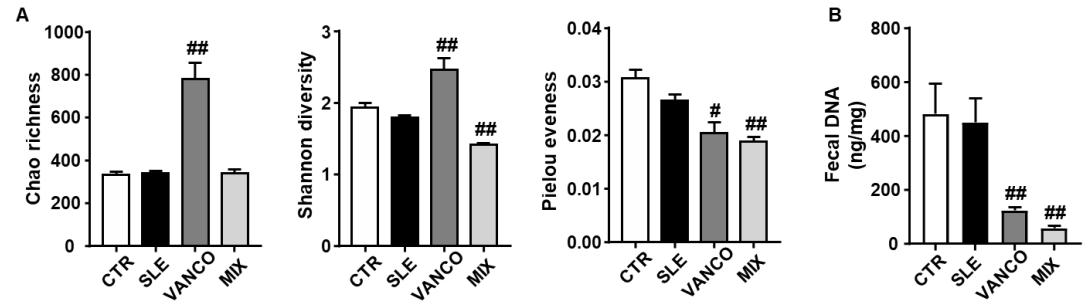

	Ctr (n = 8)	SLE (n = 8)	P value (SLE vs Ctr)	VANCO (n = 6)	P value (vs SLE)	MIX (n = 8)	P value (vs SLE)
Actinobacteria	0.10 ± 0.03	0.11 ± 0.02	0.902	4.26 ± 2.88	0.089	0.06 ± 0.01	0.025#
Bacteroidetes	53.16 ± 6.35	62.89 ± 4.33	0.197	21.99 ± 4.45	0.001##	0.34 ± 0.03	0.001##
Firmicutes	30.49 ± 5.86	24.64 ± 3.80	0.385	34.13 ± 6.56	0.175	5.60 ± 1.42	0.001##
Verrucomicrobia	12.47 ± 3.82	10.30 ± 4.81	0.712	10.71 ± 4.17	0.947	58.64 ± 2.64	0.001##
Proteobacteria	2.96 ± 0.89	1.39 ± 0.09	0.083	26.54 ± 8.72	0.003##	33.18 ± 4.26	0.001##
Tenericutes	0.32 ± 0.17	0.28 ± 0.10	0.838	0.14 ± 0.07	0.253	2.06 ± 0.84	0.040#
Others	0.48 ± 0.10	0.39 ± 0.03		2.22 ± 0.27		0.11 ± 0.01	

Figure 8. Phyla changes in the microecological parameters and gut microbiota composition in control (CTR) and hypertensive 32-week-old systemic lupus erythematosus (SLE). *(**A**) Ecological parameters. (**B**) Bacterial charge. (**C**) Proportion of bacterial phyla. (**D**) Firmicutes/Bacteroidetes (F/B) ratios calculated as a biomarker of dysbiosis in the gut microbiota in CTR, SLE and SLE- groups treated with Vancomycin (VANCO) or*

antibiotic mix (MIX). Values are expressed as means ± SEM. n = 6-8 mice per treatment group for each comparison. #P < 0.05 and ##P < 0.01 compared to the untreated SLE group.

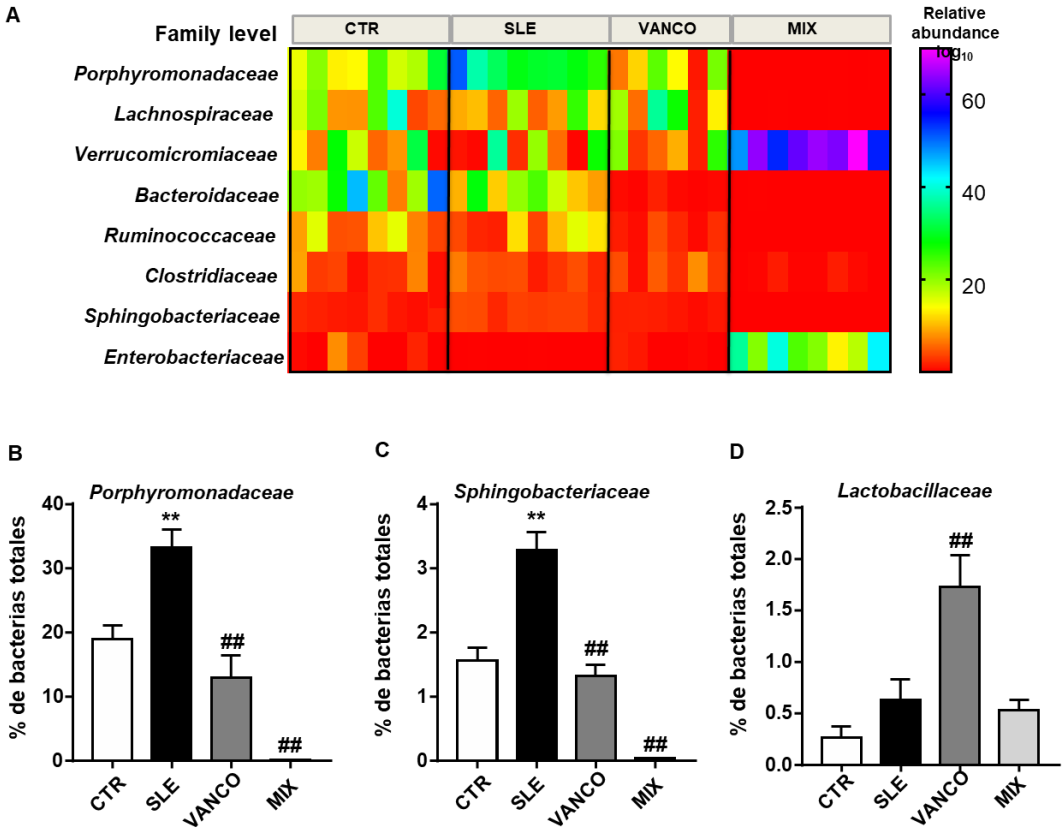

Figure 9. Family changes in the gut microbiota composition in control (CTR) and hypertensive 32-week-old systemic lupus erythematosus (SLE). *(**A**) Heat map of bacterial families. The heatmap colours represent the relative percentage of microbial genus assigned within each sample. (**B**) Relative abundance of bacterial families in CTR, SLE and SLE- groups treated with Vancomycin (VANCO) or antibiotic mix (MIX). Values are expressed as means ± SEM. n = 6-8 mice per treatment group for each comparison. **P < 0.01 compared to the CTR group; ##P < 0.01 compared to the untreated SLE group.*

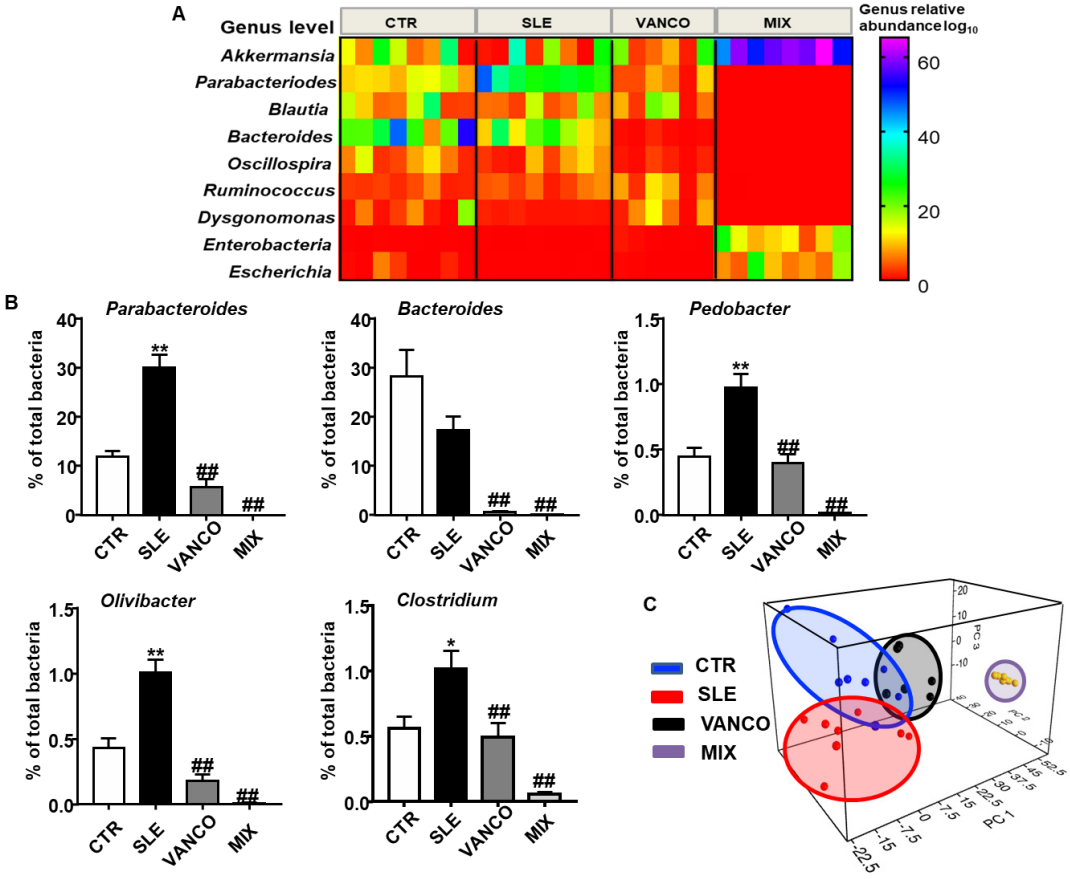

Figure 10. Genera changes in the gut microbiota composition in control (CTR) and hypertensive 32-week-old systemic lupus erythematosus (SLE). *(**A**) Heatmap shows the bacterial genera most differing in abundance between different groups. The heatmap colours represent the relative percentage of microbial genus assigned within each sample. (**B**) Main significantly modified bacterial genera in the gut microbiota in CTR, SLE and SLE-groups treated with Vancomycin (VANCO) or antibiotic mix (MIX). (**C**) Principal coordinate analysis in the gut microbiota from all experimental groups. Values are expressed as means ± SEM. n = 8 mice per treatment group for each comparison. *P<0.05 and **P < 0.01 compared to the CTR group; ##P < 0.01 compared to the untreated SLE group.*

Finally, we evaluated gut microbial functions across experimental groups and expressed as Z-score using the Kyoto Encyclopaedia of Genes and Genomes (KEGG) database (**Figure 11**). At 26 weeks of age, modules related to energy metabolism and metabolisms of cofactors and vitamins were increased 16% and 21%, respectively, in SLE as compared to control. It is interesting to note that modules involved in LPS

biosynthesis tended (P = 0.054) to increase in SLE group. However, no significant differences were observed among groups in KEGG modules at the end of the experiment between SLE and control groups, but modules related to LPS export tended to increase in SLE.

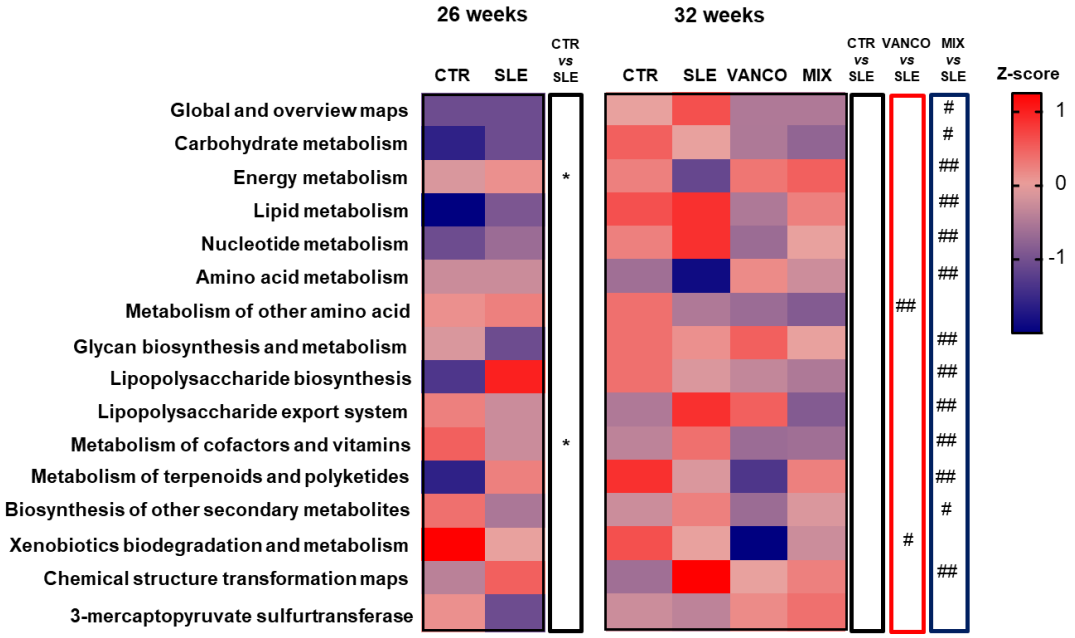

Figure 11. Z-score for predictive functional profiling for microbial communities. *n = 6-8 mice per treatment group for each comparison. *P < 0.05 compared to the control (CTR) group; #P < 0.05 and ##P < 0.01 compared to the untreated systemic lupus erythematosus (SLE) group. Treated SLE groups: vancomycin (VANCO) and antibiotic mix (MIX).*

1.2. Antibiotic treatments induced changes in gut microbiota, and inhibited the increment of blood pressure, target organ hypertrophy, and disease activity in lupus-prone mice

Vancomycin is a non-absorbable antibiotic that kills primarily gram-positive organisms. The qPCR analysis showed that vancomycin or MIX treatment reduced total DNA levels in the faeces by ≈ 72% and ≈ 87, respectively (**Figure 8B**). The

vancomycin treatment increased richness and diversity, but decreased evenness, whereas the broad-spectrum antibiotic mixture treatment reduced diversity and evenness. Profound changes in phyla composition were observed, especially with MIX treatment (**Figure 8C**). The proportion of bacteria belonging to *Bacteroidetes* and *Proteobacteria* were reduced and increased, respectively, in the SLE-VAN group as compared to SLE, whereas bacteria belonging to *Verrucomicrobia* and *Proteobacteria* dominated the composition of gut microbiota in SLE-MIX, with intense reductions of *Bacteroidetes* and *Firmicutes*. This result in both treatments in a significant increase of F/B ratio, mainly associated with a *Bacteroidetes* decrease (**Figure 8D**). Vancomycin normalized the proportion of the bacteria from *Porphyromonadaceae* and *Sphingobacteriaceae*, whereas SLE-MIX almost suppressed these bacteria. Interestingly, vancomycin increased by ≈ 2.7-fold *Lactobacillaceae* family (**Figure 9**). At genus level, the PCA analysis showed that vancomycin separates its cluster from SLE, which is closer than control, whereas bacteria from SLE-MIX were far from the rest of groups. In fact, the proportion of *Parabacteroides*, *Pedobacter*, *Olivibacter* and *Clostridium* were normalized by vancomycin, and almost abolished by MIX. *Bacteriodes* were also almost suppressed by both groups of treatment with antibiotics (**Figure 10**). In addition, the vancomycin treatment significantly reduced the modules relates to the metabolism of other amino acid and xenobiotics biodegradation and metabolism (**Figure 11**). By contrast, the MIX treatment induced profound changes in microbial functions. Interestingly, MIX evoked a significant reduction in the capacity of gut microbiome to synthetize and export LPS, whereas vancomycin did not change these modules.

At twenty-six weeks of age, SBP was similar among all experimental groups (not shown). At thirty-two-week old, SBP was significantly higher in SLE mice in comparison to control mice in approximately 55 mmHg and this change was partially prevented by both the vancomycin (≈ 40 %, $P < 0.05$) and MIX (≈ 44 %, $P < 0.01$) treatments (**Figure 12A**). At 26-week old, SLE mice showed higher protein excretion than control mice, despite similar SBP (**Figure 12B**). Protein excretion increased in untreated SLE mice with ageing, whereas six weeks of treatment with vancomycin, or MIX reduced by ≈ 45

% and ≈ 63 %, respectively this parameter. At the end of the experiment, a significant increase in body weight of SLE mice (35.8 ± 2.3 g, n = 10) in comparison to weight of control animals (30.2 ± 1.3 g, n = 10, $P < 0.05$) was found, and neither vancomycin (35.8 ± 1.6 g, n = 8), nor the MIX (32.0 ± 1.5 g, n = 10) treatment changed it significantly. Anatomical analysis revealed that left ventricle weight/tibia length, and kidney weight/tibia length indices were higher ≈ 47 % and ≈ 45%, respectively, in SLE mice than in control mice (**Figure 12C**). Both antibiotics treatments prevented the increase of renal and cardiac indices found in SLE mice. We measured SLE disease activity by plasma levels of autoantibodies and we found a significant increase in SLE mice compared to control mice (**Figure 12D**), as previously reported (Gómez-Guzmán *et al*., 2014). Vancomycin did not change disease activity but MIX treatment reduced plasma anti-dsDNA levels. Moreover, disease progression has been associated with splenomegaly, most probably because of a lymphoproliferative disorder (Wofsy *et al*., 1988). We have also observed splenomegaly in lupus mice, which was abolished by MIX treatment, whereas vancomycin was unable to change spleen weight (**Figure 13**).

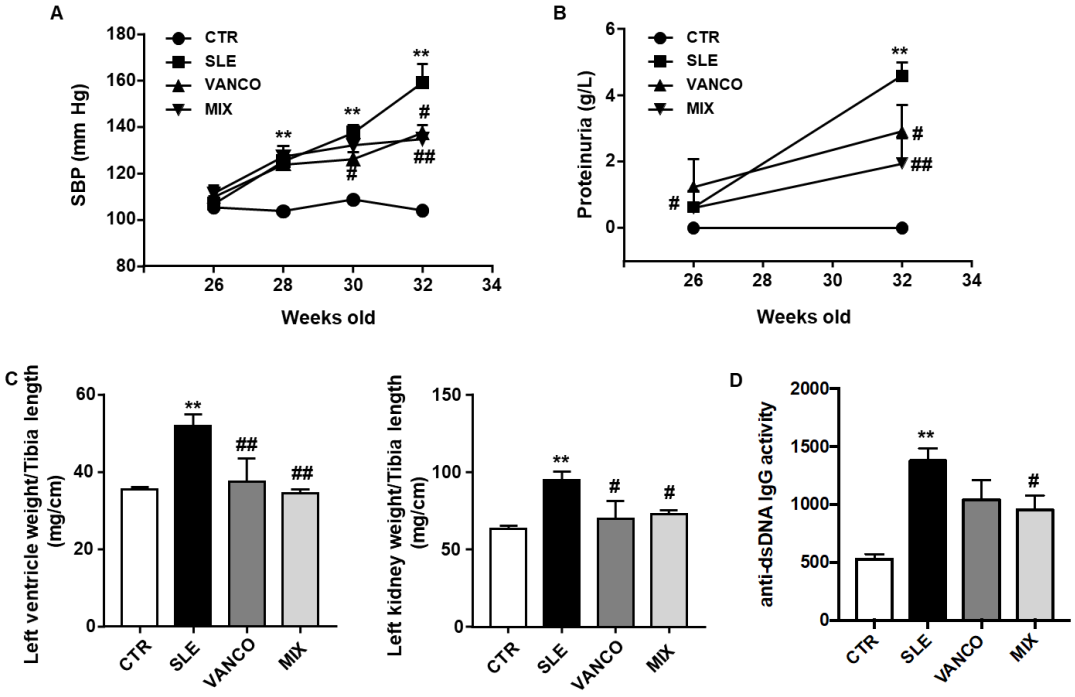

Figure 12. Antibiotic treatments inhibited the increase of blood pressure, target organ hypertrophy and disease activity in systemic lupus erythematosus (SLE) mice. *(**A**) Systolic blood pressure (SBP) measured by tail-cuff plethysmography, (**B**) proteinuria, (**C**) morphological parameters and (**D**) circulating double-stranded DNA autoantibodies levels as antibody in control (CTR), SLE and SLE- groups treated with Vancomycin (VANCO) or antibiotic mix (MIX). Values are expressed as means ± SEM (n = 6-8). **P < 0.01 compared to the CTR group; #P < 0.05 and ##P < 0.01 compared to the untreated SLE group.*

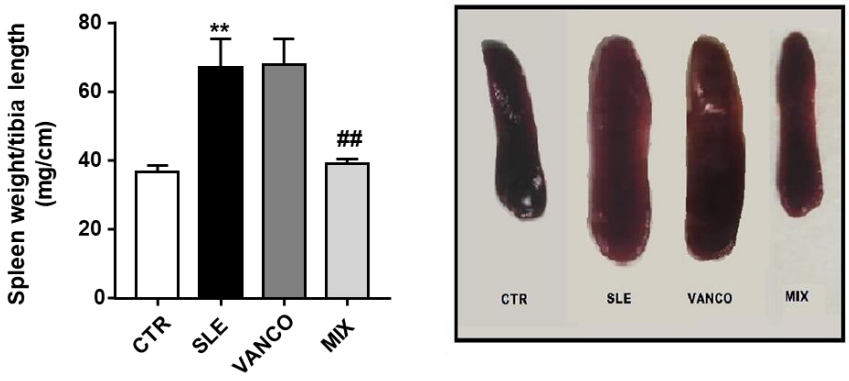

Figure 13. Effects of antibiotic treatments on splenomegaly in activity in systemic lupus erythematosus (SLE) mice. *Splenomegaly in all experimental groups. Experimental groups:*

*control (CTR), SLE and SLE- groups treated with Vancomycin (VANCO) or antibiotic mix (MIX). Values are expressed as means ± SEM (n = 6-8). **P < 0.01 compared to the CTR group; ##P < 0.01 compared to the untreated SLE group.*

1.3. Antibiotic treatments induced changes in intestinal integrity and permeability.

The integrity of the gut barrier was analysed by the colonic mRNA expression of barrier-forming junction transcripts (**Figure 14A**), such as occludin and ZO-1 and of the mucins (**Figure 14B**), mucin (MUC)-2, and MUC-3. No significant changes in these parameters were observed between control and SLE groups. However, the vancomycin treatment increased ZO-1 and MUC-2, by ≈ 2.8- and 3.5-fold, respectively. The improvement in gut barrier integrity induced by vancomycin was accompanied by a 63% reduction in gut permeability measured by FITC-dextran (**Figure 14C**). The plasma endotoxin levels were significantly higher in SLE mice than in the control group (**Figure 14D**). Surprisingly, the long-term treatment with vancomycin or MIX did not change endotoxemia in lupus mice.

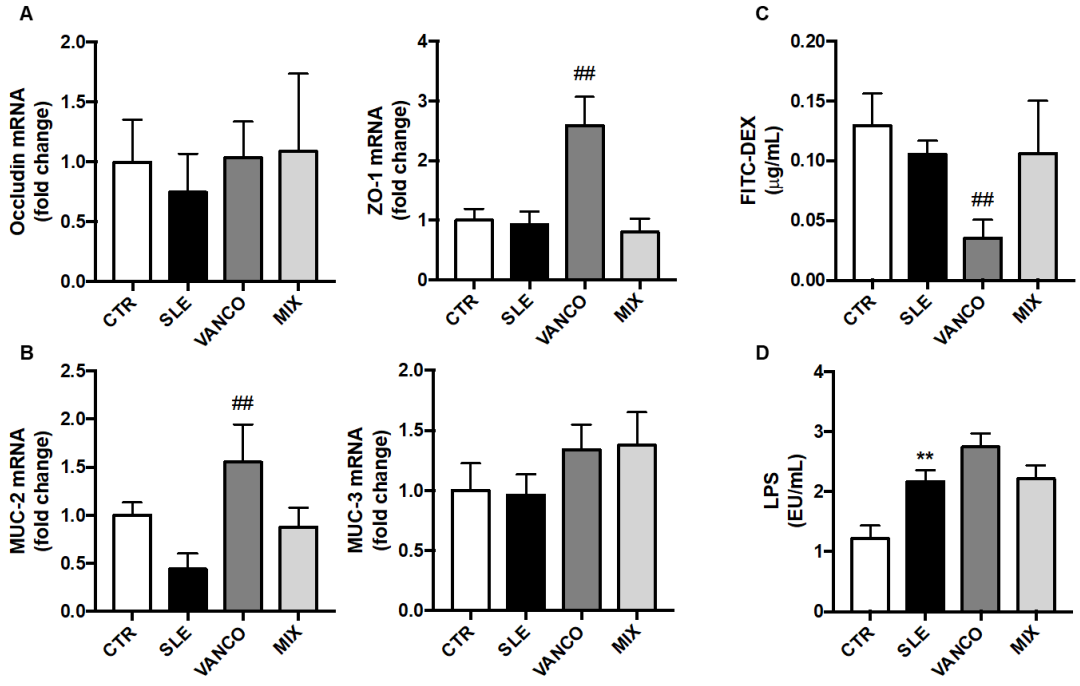

Figure 14. Effects of antibiotic treatments on epithelial integrity markers and permeability in systemic lupus erythematosus (SLE) mice. *Colonic mRNA expression levels of (**A**) barrier-forming proteins occludin, zonula occludens-1 (ZO-1) and (**B**) mucins (MUC)-2 and MUC-3. (**C**) Intestinal permeability measured by FITC-dextran. (**D**) Plasma LPS levels in control (CTR), SLE and SLE- groups treated with Vancomycin (VANCO) or antibiotic mix (MIX). Values are expressed as means ± SEM (n = 6-8). **P < 0.01 compared to the CTR group; ##P < 0.01 compared to the untreated SLE group.*

1.4. Antibiotic treatments attenuate T cells imbalance

Increased production of autoantibodies and progressive lupus-like autoimmune disease are associated with an imbalance of T cells (Talaat *et al.*, 2015) and increased B cells (Dar *et al.*, 1988). We measured the levels of B and T cells in MLN, spleen, and blood from all experimental groups. The percentage of B was higher in both secondary lymphoid organs from SLE mice than in the control group, whereas the proportion of T cells was only increased in spleen (**Figure 15A and 15B**).The vancomycin treatment did not change the levels of B and T cells in both lymphatic organs, whereas MIX decreased T cells in the spleen (**Figure 15B**). As expected, the percentages of Treg

cells, Th17 cells and Th1 cells increased in SLE mice in mesenteric lymph nodes (**Figure 15A**), whereas only Treg and Th1 increased by lupus disease in the spleen (**Figure 16**). Vancomycin and MIX treatments prevented the increase of Th17 cell content induced by SLE only in mesenteric lymph nodes (**Figure 15A**).

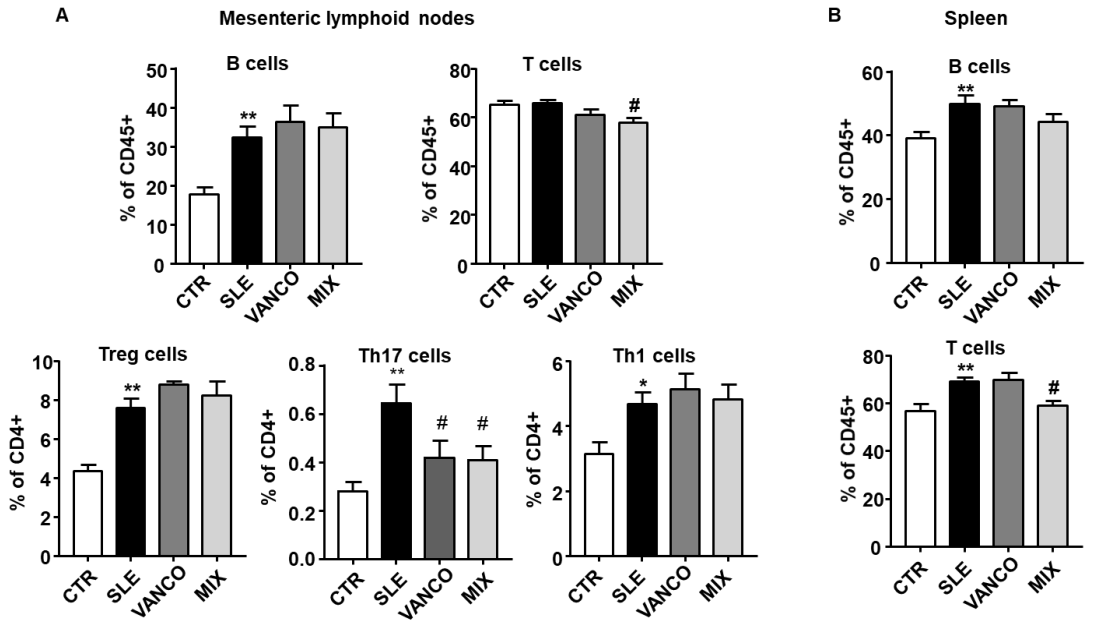

Figure 15. Effects of antibiotic treatments on lymphocytes populations. in systemic lupus erythematosus (SLE) mice*. (**A**) Total B lymphocytes, T cells, Regulatory T cells (Treg), T helper (h)17, and Th1 cells measured by flow cytometry in mesenteric lymphoid nodes and (**B**) B and T cells in spleen from control (CTR), SLE and SLE- groups treated with Vancomycin (VANCO) or antibiotic mix (MIX). . Values are expressed as means ± SEM (n = 6-8). *P<0.05 and **P < 0.01 compared to the CTR group; #P<0.05 compared to the untreated SLE group.*

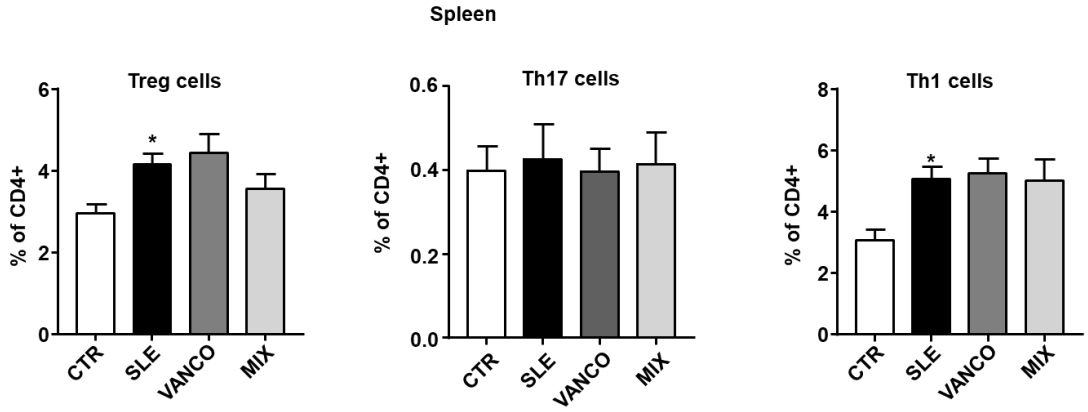

Figure 16. Effects of antibiotic treatments on splenocytic populations in systemic lupus erythematosus (SLE) mice*. Total Regulatory T cells (Treg), T helper (h)17, and Th1 cells measured by flow cytometry in spleen from control (CTR), SLE and SLE- groups treated with Vancomycin (VANCO) or antibiotic mix (MIX). Values are expressed as means ± SEM (n = 6-8). *P<0.05, compared to the CTR group.*

Circulating B, Treg, and Th17 cells were higher in SLE than in control mice (**Figure 17A**). In concordance with changes induced by antibiotic treatments in mesenteric lymph nodes, vancomycin and MIX reduced the proportion of circulating Th17 cells. Plasma levels of IL-6, IL-17a, and IFN-γ were increased in SLE mice compared to control mice (**Figure 17B**), Both antibiotic treatments normalized plasma levels of pro-inflammatory cytokines IL-6 and IL-17a, being without significant effects in IL-10 and IFN-γ.

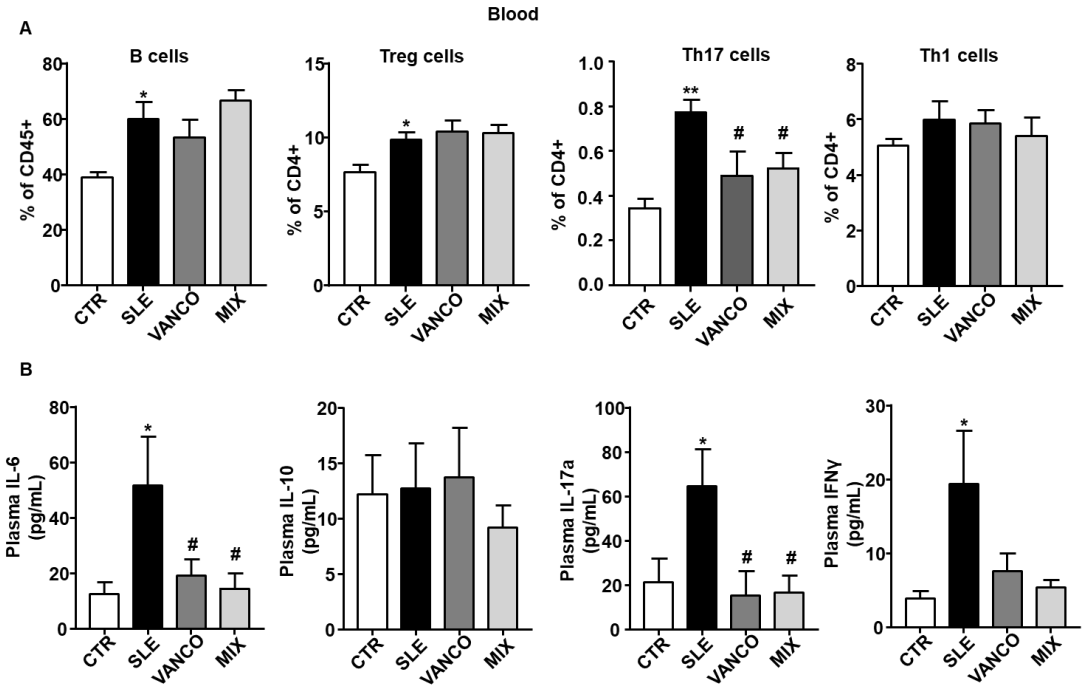

Figure 17. Effects of antibiotic treatments on blood lymphocyte population in systemic lupus erythematosus (SLE) mice*. (**A**) Total B lymphocytes, Regulatory T cells (Treg), T helper (h)17, and Th1 cells measured by flow cytometry in blood. (**B**) Analysis of cytokines in plasma through the multiplex ELISA method in control (CTR), SLE and SLE- groups treated with Vancomycin (VANCO) or antibiotic mix (MIX). Values are expressed as means ± SEM (n = 6-8). *P<0.05 and **P < 0.01 compared to the CTR group; #P<0.05 compared to the untreated SLE group.*

1.5. Antibiotic treatments prevent endothelial dysfunction, vascular oxidative stress and Th17 infiltration in aorta

Aortas from SLE mice had strongly reduced endothelium-dependent vasorelaxant responses to acetylcholine compared with aortas from the control group (Emax= 26.9 ± 5.6 % and 73.2 ± 1.4 %, respectively, P<0.01) (**Figure 18A**). The treatment of SLE mice with both vancomycin and MIX improved the impairment of acetylcholine-induced relaxation. This response induced by acetylcholine was also improved in aortic rings from SLE mice after incubation with the Rho kinase inhibitor Y27632 (**Figure 18A**), showing that the impaired acetylcholine-induced relaxation in aorta is mediated, at

least in part, by Rho kinase activation. ROS-dependent activation of RhoA/Rho kinase has been previously described (MacKay *et al*., 2017). Since NADPH oxidase is the major source of ROS in the vascular wall, we measured NADPH oxidase activity in all experimental groups (**Figure 18B**). NADPH oxidase activity was ≈ 2.8-fold higher in aortic rings of SLE mice than in aortic rings of control mice, and both antibiotic treatments inhibited this activity. Taken to account that inflammatory cells increased vascular ROS production, we measured T-lymphocytes and macrophages infiltration in aorta from all experimental groups. Th17 cells and macrophages were increased in aorta from SLE mice as compared to control mice, being without change Treg and Th1 cells (**Figure 18C**). Both vancomycin and MIX reduced the infiltration on Th17 in aorta, whereas macrophage content was only reduced by MIX treatment.

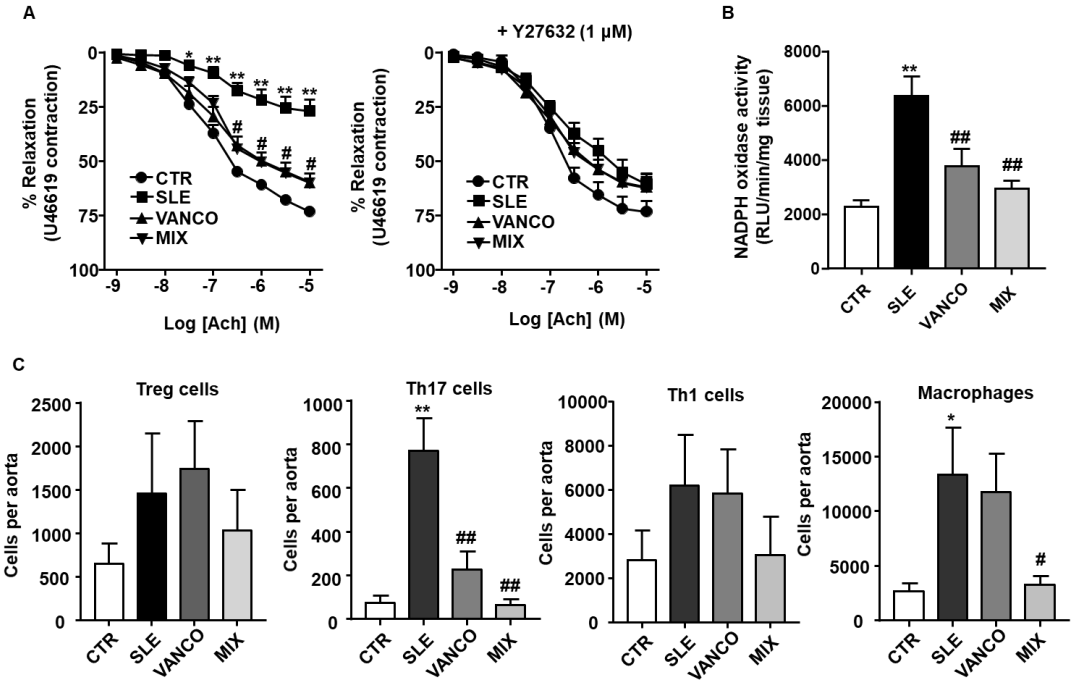

Figure 18. Effects of antibiotic treatments on endothelial function, NADPH oxidase activity and aortic infiltration of immune cells in systemic lupus erythematosus (SLE) mice. *(**A**) Vascular relaxation responses induced by acetylcholine (Ach) in endothelium-intact aortas pre-contracted by U46619 (10 nM) in all experimental groups: control (CTR),*

*SLE, vancomycin (VANCO) and mix antibiotic (MIX) treatments. (**B**) NADPH oxidase activity measured by lucigenin-enhanced chemiluminescence. (**C**) Aortic infiltration of immune cells measured by flow cytometry. Values are expressed as means ± SEM (n = 6-8). *P<0.05 and **P < 0.01 compared to the CTR group; #P<0.05 and ##P<0,01 compared to the untreated SLE group.*

1.6. Gut microbiota from NZBW/F1 mice increased blood pressure and impaired endothelial function in mice without lupus genetic background

To address the question whether lupus mice microbiota could potentially regulate blood pressure and endothelial function, we transferred microbiota from hypertensive NZBW/F1 mice or from normotensive NZW/LacJ control mice to recipient C57BL/6J female mice, for 3 weeks. SLE microbiota raised systolic blood pressure to a maximum of ≈ 16 mmHg, being without effect the FMT from control mice (**Figure 19A**). Interestingly, no significant changes either in spleen weight or plasma levels of anti-dsDNA were observed between C-C and C-SLE groups (**Figure 19B**), showing no change in lupus activity induced by microbiota from SLE mice. Microbiota from SLE increased the Th17 proportion in mesenteric lymph nodes, without changes in B cells, total T cells, Treg and Th1 populations (**Figure 19C**). In addition, endothelium-dependent relaxant responses to Ach in U46619-contracted aortic rings from the C-SLE group were significantly lower than those from the C-C group (Emax: 48.7 ± 4.6% vs 67.7 ± 4.2%, $p < 0.01$, respectively; **Figure 20A**). Incubation during 30 min with the pan-NOX inhibitor VAS2870 abolished differences between groups in relaxation to acetylcholine, showing the involvement of NADPH oxidase in this impaired relaxant response induced by SLE microbiota. Moreover, the stool transfection from SLE mice increased aortic NADPH oxidase activity (**Figure 20B**), as compared to C-C group. Interestingly, Th7 infiltration in aorta was also increased in C-SLE (**Figure 20C**) without changes in Tregs, Th1 and macrophages (not shown). When we incubated the aortic ring from C-SLE for 6 h with nIL17 or vehicle, the neutralization of IL17 improved the relaxation to acetylcholine (**Figure 20D**) showing the key role of Th17 infiltration in endothelial dysfunction induced by SLE microbiota.

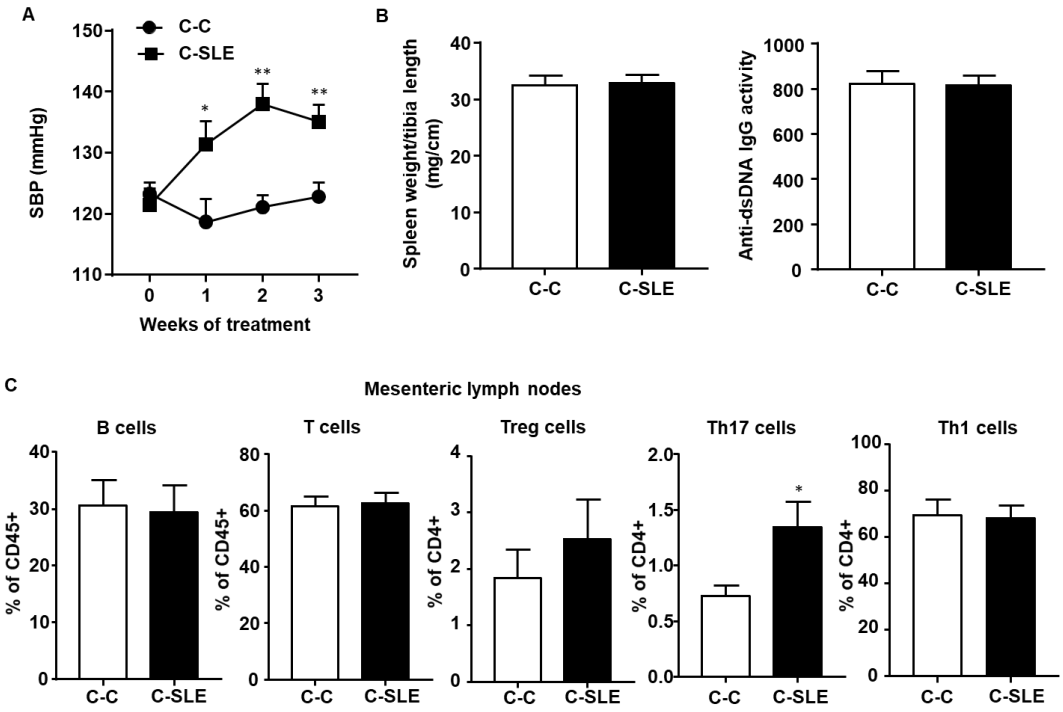

Figure 19. Effects of faecal microbiota transplantation (FMT) on evolution of systolic blood pressure (SBP), disease activity and lymphocytes populations in mesenteric lymph nodes. *(**A**) SBP measured by tail-cuff plethysmography. (**B**) Spleen/tibia ratio and autoantibody levels were measured as markers of the lupus ?? pathology. (**C**) Proportion of different immune cell types in mesenteric lymph nodes: Total B lymphocytes, T cells, Regulatory T cells (Treg), T helper (h)17, and Th1. cells measured by flow cytometry in mesenteric lymphoid nodes. Values are expressed as means ± SEM (n = 8). *P<0.05 and **P < 0.01 compared to the C-C group. SLE, systemic lupus erythematosus*

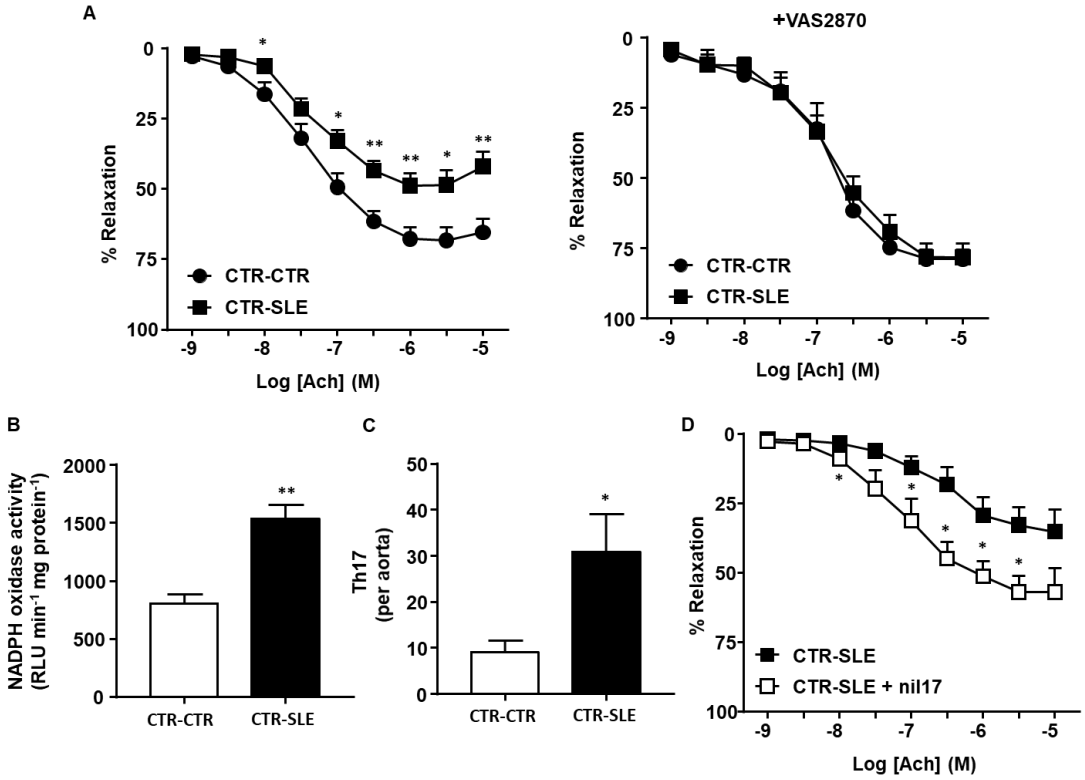

Figure 20. Effects of vancomycin (VANCO) and antibiotic mix (MIX) treatments on the vascular nitric oxide pathway and the role of Th17. *(**A**) Vascular relaxation responses induced by acetylcholine (Ach), in endothelium-intact aortae pre-contracted by U46619 (10 nM), in the absence and in the presence of the NADPH oxidase inhibitor VAS2870 (5 μM). (**B**) NADPH oxidase activity in aorta. (**C**) T helper (h)17 cells infiltration in aorta FMT-linked hypertension is associated with endothelial dysfunction. (**D**) Relaxation curve to Ach in the presence of a neutralising agent for interleukin-17a (nil7a). Values are expressed as means ± SEM (n = 8). *P<0.05 and **P < 0.01 compared to the CTR-CTR group. SLE, systemic lupus erythematosus.*

2. Lactobacillus fermentum CECT5716 is a novel alternative for the prevention of vascular disorders in a genetic mouse model of systemic lupus erythematosus

Since we were able to stablish that there is a link between the onset of SLE and changes in the composition of the gut microbiota, we proceeded to examine the possible beneficial aspects of modulating these bacterial communities through the

administration of probiotics, focusing on the potential preventive rather than curative effects, since, as we observed, the shift in the composition of the microbiota precedes the first signs of the pathology.

2.1. LC40 treatment prevents gut dysbiosis in SLE mice

LC40 was detected alive in faecal samples of 57% and 50% of SLE-LC40 and control-LC40 groups, respectively, demonstrating that this strain is able to survive the conditions of the gastrointestinal tract of these mice. We analysed faecal DNA isolated from all experimental mice groups to determine the dynamics of gut microbiota during lupus disease. In order to compare the bacterial composition of the gut microbiota between SLE mice and control mice, we have evaluated three major ecological parameters, including Shannon's and Simpson's (the combined parameters of richness and evenness) diversity, Chao's richness (an estimate of a total number of operational taxonomic units present in the given community), Pielou's evenness (to show how evenly the individuals in the community are distributed over different operational taxonomic units), and numbers of species. No significant changes among groups were observed regarding microbial richness, diversity, and evenness (**Figure 21A**).

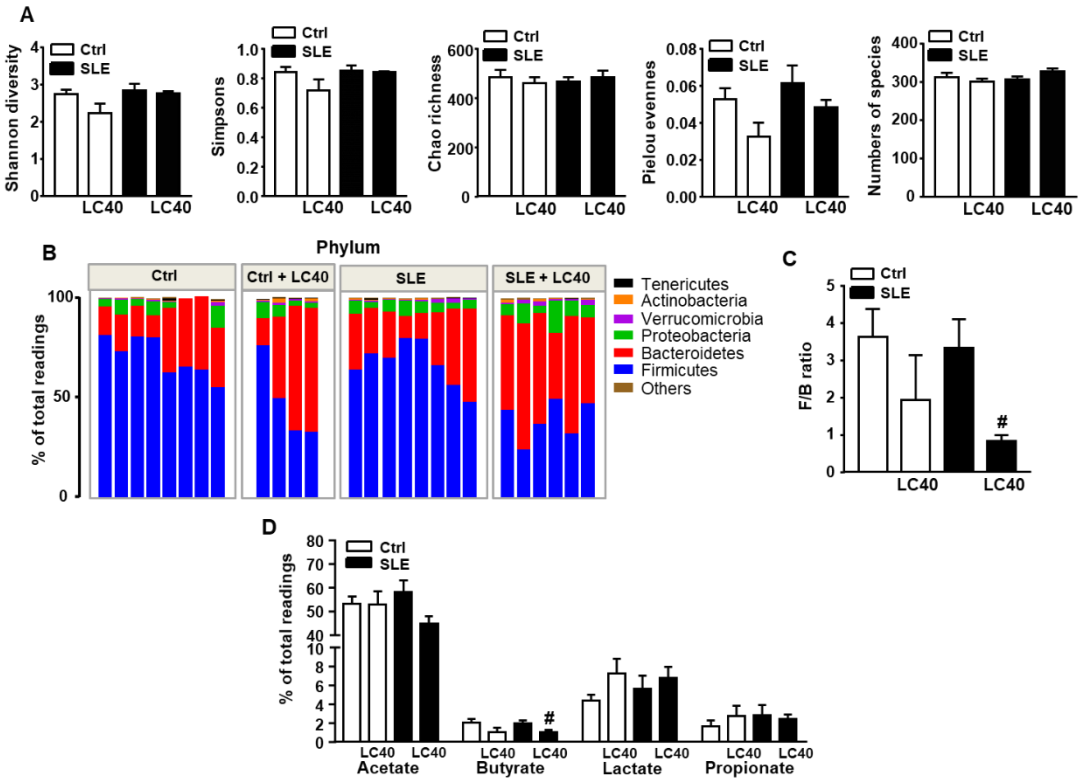

Figure 21. Effects of Lactobacillus fermentum CECT5716 (LC40) treatment on phyla changes in the microecological parameters and gut microbiota composition. *Faecal samples were collected and bacterial 16S ribosomal DNA were amplified and sequenced to analyse the composition of microbial communities. (**A**) Faecal diversity, richness, evenness, and numbers of species were used to evaluate general differences of microbial composition in all experimental groups. (**B**) Phylum breakdown of the most abundant bacterial communities in the faecal samples from all experimental groups. (**C**) The Firmicutes/Bacteroidetes (F/B) ratio was calculated as a biomarker of gut dysbiosis. (**D**) Relative proportions of lactate-, butyrate-, and acetate-producing bacteria in the gut microbiota in control (Ctrl) and systemic lupus erythematosus (SLE) mice. Values are expressed as means ± SEM (n = 4–8). #P < 0.05compared to the untreated SLE group.*

Similarly, when we evaluated the phyla composition, faecal samples were dominated by *Firmicutes* and *Bacteroidetes*, smaller proportions of *Actinobacteria*, *Proteobacteria*, and *Tenericutes* (**Fig. 21B**) were found in the different experimental groups. No significant differences were found between control and SLE group in the two main phyla percentages (**Fig. 21B, Table 6**) and F/B ratio (**Fig. 21C**). Of note, the

administration of the probiotic LC40 to the SLE-treated group was able to reduce the F/B ratio (**Fig. 21C**) as a result of a decrease in the proportion of *Firmicutes* and an increase in the proportion of *Bacteroidetes*. We have also evaluated what genera of bacteria contributed to the alteration of microbiota composition in SLE disease. A significant decrease in the proportion of butyrate- and acetate-producing bacteria has been previously described in both humans and animals with hypertension (Yang *et al*., 2015). However, we did not find any differences in the proportion of butyrate-, acetate- and lactate-producing bacteria between SLE mice and control mice. Only the LC40 treatment reduced the proportion of butyrate-producing bacteria in SLE mice (**Fig. 21D**). **Fig. 22A** shows the bacterial taxa (class, order, family, and genus) that were altered by SLE disease, according to LEfSe analysis. Prominent changes in bacterial taxa occurred, as showed in cladograms comparing control to SLE groups (**Fig. 22A**) and SLE to SLE-LC40 groups (**Fig. 22B**), with minor changes between SLE and control mice (4 increased and 2 decreased) and SLE treated with LC40 vs. SLE (4 increased and 1 decreased) when we compared by LDA score genera representing > 0.1% of total bacteria.

Table 6. Effects of *Lactobacillus fermentum* CECT5716 (LC40) treatment on phyla changes in the gut microbiota.

Phylum	Ctrl (n = 8)	Ctrl+LC40 (n = 4)	SLE (n = 8)	SLE+LC40 (n = 6)
Tenericutes	0.4 ± 0.2	0.2 ± 0.0	0.2 ± 0.1	0.1 ± 0.1
Actinobacteria	0.3 ± 0.0	1.1 ± 0.6*	0.4 ± 0.1	0.6 ± 0.3
Verrucomicrobia	1.1 ± 0.3	0.8 ± 0.1	0.8 ± 0.2	1.4 ± 0.4
Proteobacteria	5.8 ± 1.0	4.7 ± 1.6	5.2 ± 0.6	8.1 ± 1.9
Bacteroidetes	24.4 ± 4.0	44.7 ± 13.3	26.1 ± 4.5	50.2 ± 5.0##
Firmicutes	69.4 ± 3.7	47.2 ± 11.7*	66.0 ± 4.2	37.9 ± 4.4##
Others	14.5 ± 2.6	15.4 ± 0.6	14.0 ± 1.7	19.7 ± 1.7#

*Values are expressed as means ± SEM (n = 4-8). *P< 0.05 compared to the control (Ctrl) group. #P< 0.05 compared to the non-treated systemic lupus erythematosus (SLE) group. *P < 0.05 compared to Ctrl group; #P < 0.05 and ##P < 0.01 compared to SLE group.*

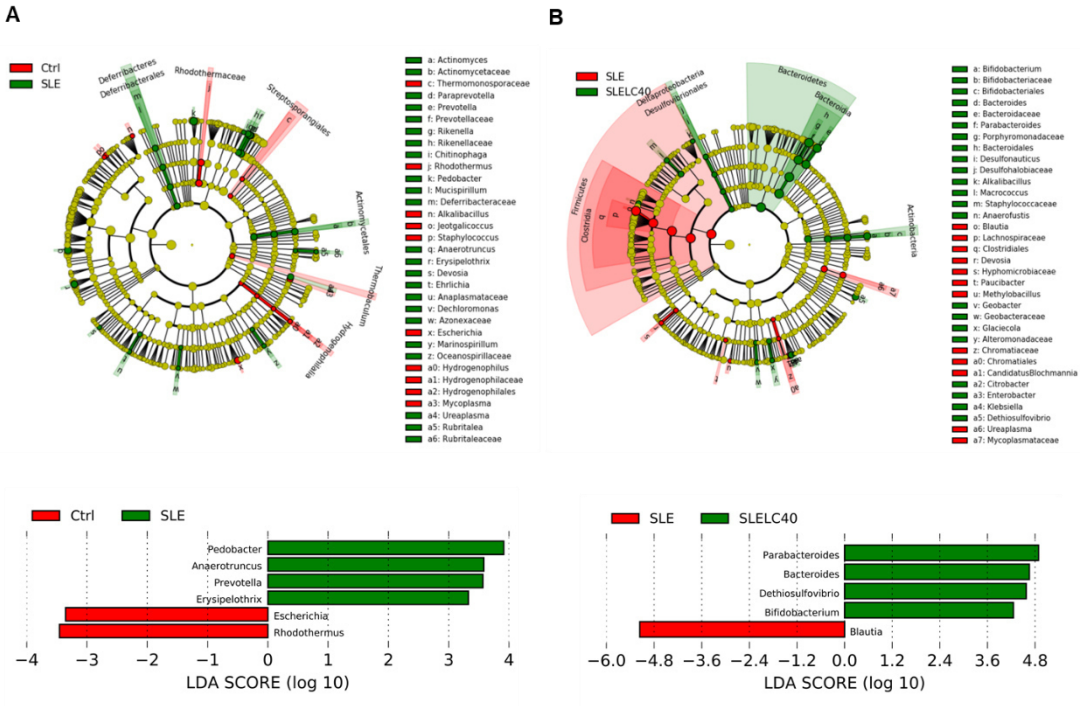

Figure 22. Effects of Lactobacillus fermentum CECT5716 (LC40) treatment on changes in the gut microbiota composition. *Comparisons of microbiome changes in control (Ctrl) versus systemic lupus erythematosus (SLE) mice (**A**). Linear discriminant analysis effect size (LEfSe) identified significantly different bacterial taxa enriched in each cohort at LDA Score > 2, p<0.05 (red bars Ctrl enriched, green bars SLE enriched). Comparisons of microbiome changes in SLE versus SLE+LC40 mice (**B**). Linear discriminant analysis effect size (LEfSe) identified significantly different bacterial genera representing > 0.1% of total bacteria enriched in each cohort at LDA Score > 2, p<0.05 (red bars SLE enriched, green bars SLE+LC40 enriched). Cladograms show the significantly enriched taxa, the taxa are identified in the key to the right of each panel. Larger circles represent greater differences in abundance between groups (**A**, **B**). n= 4-8 mice per treatment group for each comparison.*

We have also evaluated what genera of bacteria were altered within the microbiota (**Fig. 23**). **Figure 23A** shows 3-dimensional scatterplots generated by PCA to visualize whether the experimental groups in the input phylogenetic tree have significantly different microbial communities between each other. The main separation is because of LC40 treatment, control and SLE groups did not separate in genera. Interestingly, and similar to that described in LDA analysis, we found that the gut microbiota of SLE

mice had a significantly higher abundance of only *Pedobacter*, *Lactobacillus*, and *Prevotella* than control group, and no changes in other genera such as *Bifidobacterium* were found (**Fig. 23B and 23C**). LC40 treatment increased the accumulation of *Parabacteroides* or *Bifidobacterium* (**Fig. 23C**) in both control-treated and SLE-treated mice. This modification would be involved in the change in T cells polarization (Zuo *et al.*, 2014) found in mesenteric lymph nodes induced by this probiotic and the improvement of gut epithelial integrity by strengthening tight junctions (Hsieh *et al.*, 2015). Moreover, we observed that the administration of LC40 significantly reduced the abundance of *Blautia* and *Lachnospira* (**Fig. 23C**) in the gut microbiota of SLE-treated mice.

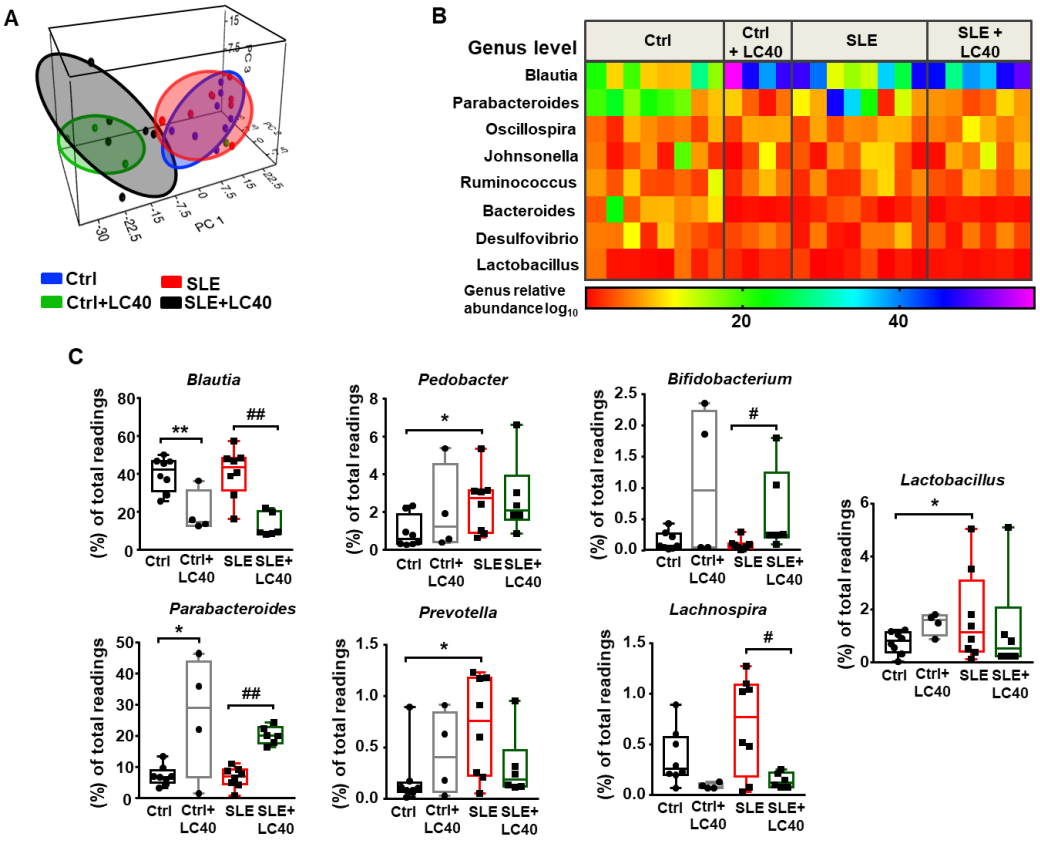

Figure 23. Effects of Lactobacillus fermentum CECT5716 (LC40) treatment on genera changes in the gut microbiota composition. *(**A**) Principal components*

*analysis in the gut microbiota from all experimental groups. (**B**) Heatmap showing the bacterial genera most differing in abundance between different groups. Samples clustered by treatment group demonstrated that the treatments resulted in distinct populations of bacteria at the genus level. The heatmap colours represent the relative percentage of microbial genus assigned within each sample. (**C**) Bacterial genera Blautia, Pedobacter, Bifidobacterium, Lactobacillus, Parabacteroides, Prevotella, and Lachnospira in the gut microbiota in control (Ctrl) and SLE mice. Values are expressed as means ± SEM (n = 4–8).*P < 0.05 and **P < 0.01 compared to the Ctrl group; #P < 0.05 ##P < 0.01 compared to the untreated SLE group.*

2.2. LC40 treatment improves intestinal integrity, inflammation and endotoxemia

We measured endotoxin levels in plasma, we found them significantly higher in SLE mice than in the control group (**Fig. 24A**). Interestingly, the long-term treatment with LC40 significantly decreased endotoxemia in lupus mice. These results suggest that intestinal permeability is increased in this female mouse model of lupus and allow bacterial components (e.g., LPS) to enter the blood stream. Because of this, we tested the integrity of the gut barrier and we found that the treatment with LC40 significantly increased the colonic mRNA expression of barrier-forming junction transcripts (ZO-1 and occludin) and of the mucins, in particular, MUC-2 (**Fig. 24B**). This effect suggests an enhanced barrier function of the intestinal epithelium as a result of the supplementation with *Lactobacillus*. We also found that colonic expression of IL-18 (**Fig. 24C**), a cytokine important for tissue repair (Elinav. *et al*., 2013) and limiting colonic Th17 cell differentiation (Harrison. *et al*., 2015), was higher in SLE-treated mice. Furthermore, the increased mRNA levels of the colonic pro-inflammatory cytokines: TNF-α and IL-1β (**Fig. 24D**) in SLE mice were significantly reduced by LC40 administration. In addition, the colonic expression of intestinal alkaline phosphatase (IAP) was significantly up-regulated after the probiotic treatment in SLE mice compared to untreated lupus mice (**Fig. 24E**). This effect may be associated with the enhanced LPS clearance, since IAP is an enzyme expressed on the microvillus membranes of enterocytes (Geddes and Phillpott, 2008) that can dephosphorylate LPS, leading to an important reduction in LPS toxicity (Bates *et al*., 2007).

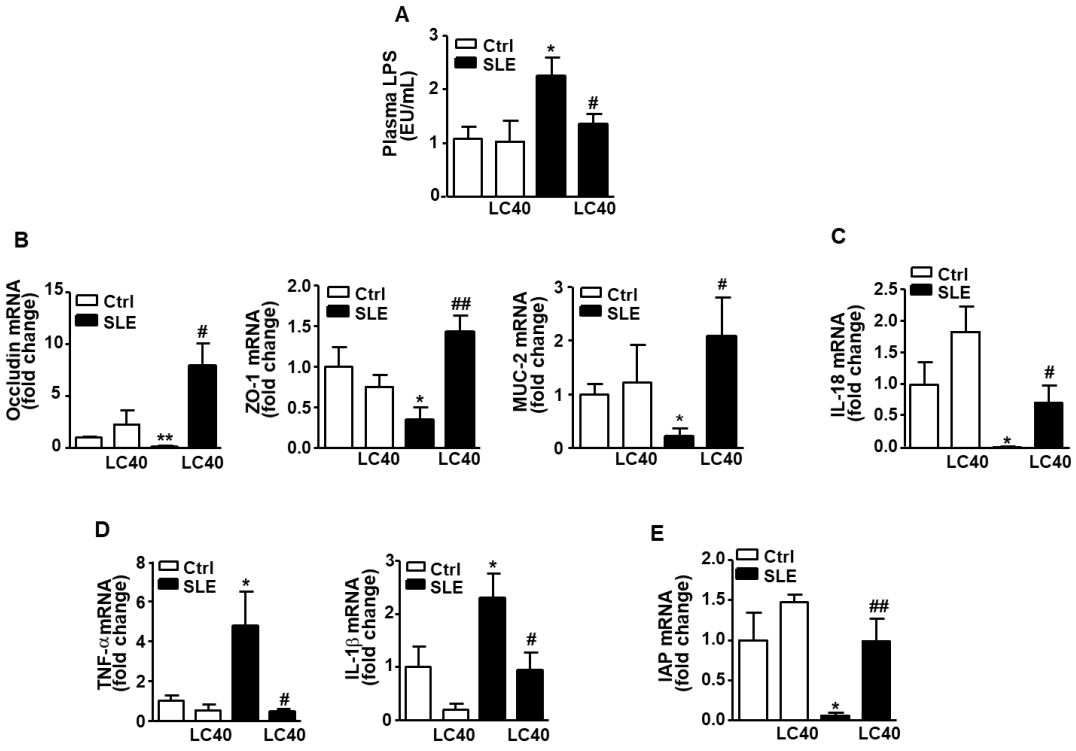

Figure 24. Effects of Lactobacillus fermentum CECT5716 (LC40) treatment on proinflammatory and epithelial integrity markers. *(**A**) Plasma endotoxin concentrations (EU/ml, endotoxin U/ml). **B–D**) Colonic mRNA levels of occludin, zonula occludens-1 (ZO-1), and mucin (MUC)-2 (**B**), tissue repair cytokine interleukin (IL)-18 (**C**), proinflammatory cytokines TNF-α and IL-1β (**D**). (**E**) intestinal alkaline phosphatase (IAP) in control (Ctrl) and systemic lupus erythematosus (SLE) mice. Values are expressed as means ± SEM (n = 4–6). *P < 0.05 and **P < 0.01 compared to the Ctrl group; #P < 0.05 and ##P < 0.01 compared to the untreated SLE group.*

2.3. LC40 treatment improves morphological variables, plasma parameters, and blood pressure

At eighteen-weeks old, SBP was similar among all experimental groups (not shown). At thirty-three-weeks old, SBP was significantly higher in SLE mice in comparison to control mice in approximately 56 mmHg and this change was prevented by chronic LC40 treatment (**Fig. 25A**). Also, these antihypertensive effects were observed using direct intra-arterial recordings in conscious mice (**Fig. 25B**), without

significantly affecting heart rate (HR) (**Fig. 25C**). Regardless the presence or absence of LC40 treatment, a significant increase in body weight of SLE mice in comparison to weight of control animals was found (**Table 7**). Anatomical analysis revealed that left ventricle weight/tibia length, heart weight/tibia length and kidney weight/tibia length indices were higher in SLE mice (**Table 7**) than in control mice. Long-term administration of LC40 significantly reduced both renal and cardiac hypertrophy found in SLE mice. Analysis of metabolic plasma variables (**Table 7**) showed that fasting glycemia and plasma cholesterol were higher in SLE mice than in control mice. However, no effect of LC40 treatment was found on basal glycemia and cholesterol.

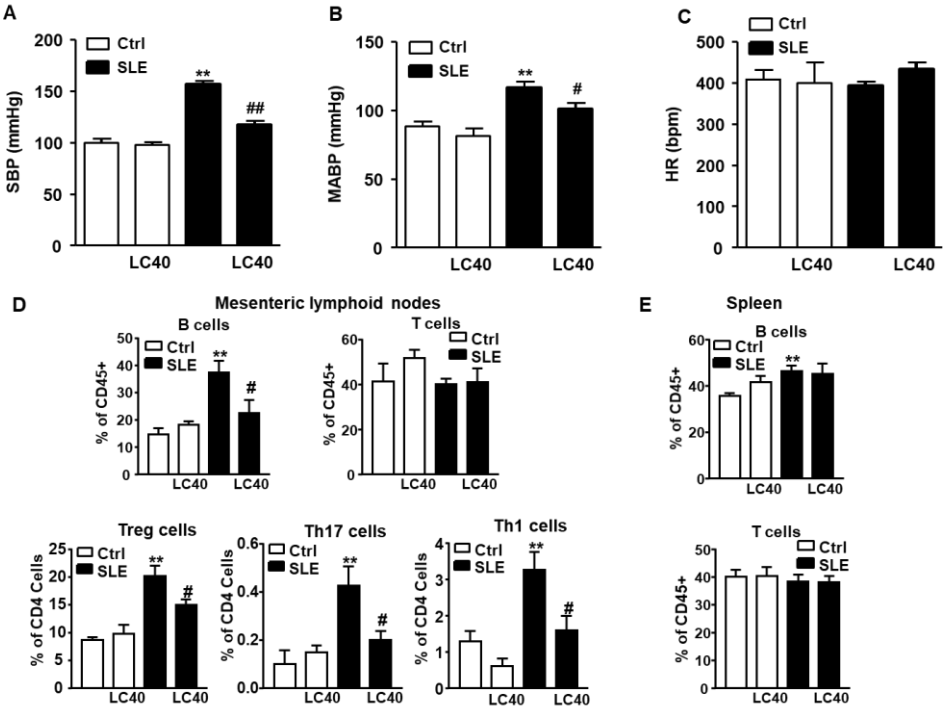

Figure 25. Effects of Lactobacillus fermentum CECT5716 (LC40) treatment on both blood pressure (BP) and lymphocytes populations in mesenteric lymph nodes and spleen*. (**A**) Systolic BP (SBP) was measured by tail-cuff plethysmography. (**B**, **C**) Mean arterial BP (MABP) (**B**) and heart rate (HR) (**C**) were measured in left carotid artery by direct registration in control (Ctrl) and systemic lupus erythematosus (SLE) mice. (**D**, **E**) Total B lymphocytes, T cells, Treg cells, Th17, and Th1 cells measured by flow cytometry in mesenteric lymphoid nodes (**D**), and B and T cells in*

*spleen (**E**) in Ctrl and SLE mice. Values are expressed as means ± SEM (n = 4–8). **P < 0.01 compared to the Ctrl group; #P < 0.05 and ##P < 0.01 compared to the untreated SLE group.*

Table 7. Morphological and plasma parameters of all experimental groups.

Variables	Ctrl (n = 8)	Ctrl+LC40 (n = 4)	SLE (n = 8)	SLE+LC40 (n = 7)
BW (g)	27.1± 0.5	27.0± 0.9	32.1 ± 2.4*	33.2 ± 2.1
HW/TL (mg/cm)	60.3 ± 2.1	56.3 ± 2.7	73.4 ± 3,7*	63.7± 1.2#
LVW/TL (mg/cm)	39.1 ± 2.1	39.1 ± 2.6	54.1 ± 5.5*	44.5 ± 1.1#
Mesenteric fat/ BW (%)	0.34 ± 0.04	0.43 ± 0.01	0.63 ± 0.15	0.46 ± 0.17
Gonadal fat/BW (%)	0.96 ± 0.17	1.27 ± 0.28	1.28 ± 0.15	1.17 ± 0.45
KW/TL (mg/cm)	77.4 ± 3.3	75.9 ± 4.0	115.8 ± 11.6**	89.8 ± 4.4#
Fasting glucose (mg/dL)	116 ± 15	116.9 ± 4.3	261 ± 29**	225.0 ± 22.3
Total cholesterol (mg/dL)	107.3 ± 9.7	115.5 ± 7.3	245.9 ± 41.7*	265.1 ± 45.3
Triglycerides	43.8 ± 3.0	42.5 ± 7	38.9 ± 3.1	42.0 ± 6.2
HDL (mg/dL)	53.5 ± 7.2	52.0 ± 3.4	63.3 ± 4.1	67.1 ± 5.1

*BW, Body weight; HW, Heart weight; KW, Kidney weight; LVW, Left ventricular weight; TL, Tibia length. Results are shown as means ± SEM. All parameters were assessed in mice treated with vehicle or Lactobacillus fermentum CECT5716 (LC40). *P < 0.05 and **P < 0.01. compared to control (Ctrl) group; #P < 0.05 and ##P < 0.01 compared to systemic lupus erythematosus (SLE) group.*

2.4. LC40 treatment attenuates SLE disease activity and T cells imbalance

We measured SLE disease activity by plasma levels of autoantibodies and we found a significant increase in SLE mice compared to control mice (**Fig. 26A**), as previously reported (Gómez-Guzmán. *et al*., 2014). Probiotic treatment significantly reduced the levels of anti-dsDNA in SLE, being without effect in control mice. Moreover, disease progression has been associated with splenomegaly, most probably because of a lymphoproliferative disorder (Wofsy *et al*., 1988). We have also observed splenomegaly in lupus mice, which was considerably reduced by the administration of LC40 (**Fig. 26B**).

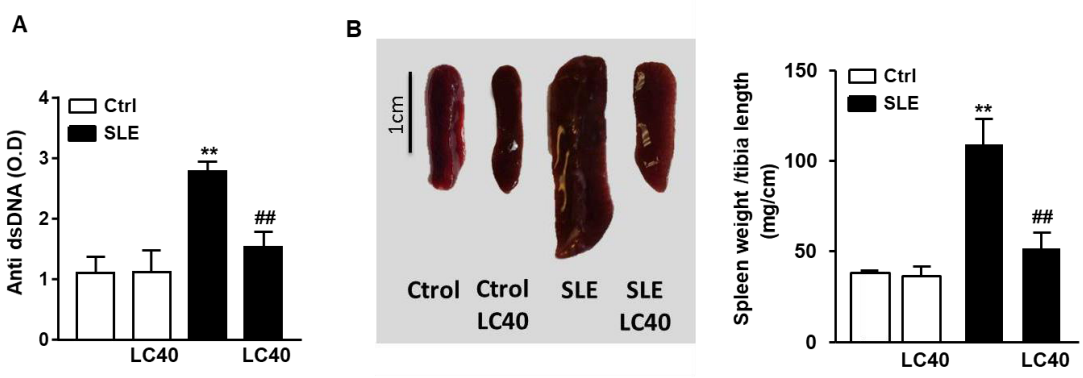

Figure 26. Effects of Lactobacillus fermentum CECT5716 (LC40) treatment on systemic lupus erythematosus (SLE) activity. *Circulating double-stranded DNA autoantibodies (presented as antibody activity index (**A**), and splenomegaly (**B**) in control (Ctrl) and SLE mice. Values are expressed as means ± SEM (n = 4-8). **P< 0.01 compared to the Ctrl group. ##P< 0.01 compared to the SLE group.*

Increased production of autoantibodies and progressive lupus-like autoimmune disease are associated with an imbalance of T cells (Talaat *et al*., 2015) and increased B cells (Dar *et al*., 1988). In order to determine the immunomodulatory actions of the probiotic LC40, we measured the levels of B and T cells in mesenteric lymph nodes and spleen from all experimental groups. The percentage of B cells was higher in both

organs from SLE mice than in the control group, without any change in T cells (**Fig. 25D and 25E**). LC40 treatment of SLE mice led to a significant decrease in the levels of B cells in mesenteric lymph nodes (**Fig. 25D**), whereas this decrease was not found in the spleen (**Fig. 25E**). As expected, the percentages of Treg cells, Th17 cells and Th1 cells increased in SLE mice in mesenteric lymph nodes (**Fig. 25D**), whereas only Treg increased by lupus disease in the spleen (**Fig. 27**). LC40 treatment prevented the altered T-cell polarization induced by SLE only in mesenteric lymph nodes (**Fig. 25D**).

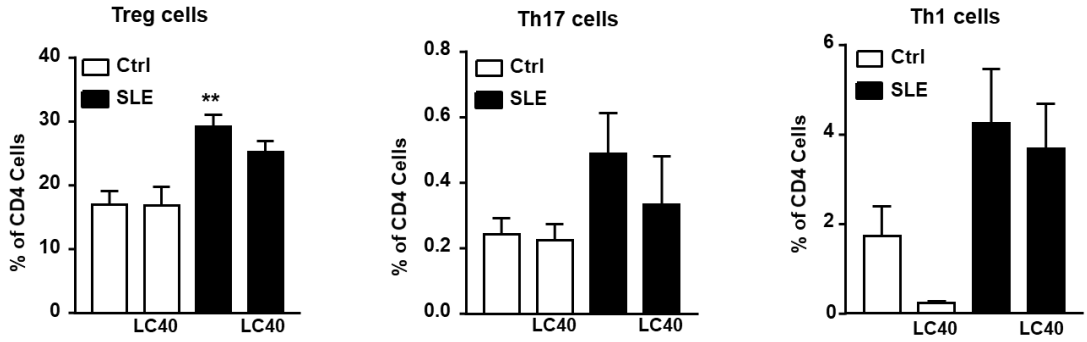

Figure 27. Effects of Lactobacillus fermentum CECT5716 (LC40) treatment on T-cell polarization in spleen*. Treg, Th17, and Th1 cells measured in spleen in control (Ctrl) and systemic lupus erythematosus (SLE) mice. Values are expressed as means ± SEM (n = 4-8). **P< 0.01 compared to the Ctrl group.*

Plasma levels of IL-17a, IL-10, IFN-γ,TNF-α, and IL-21 also increased in SLE mice compared to control mice. Again, probiotic administration led to the return to normal levels of these parameters, except for TNF-α, which tended to decrease but without statistical significance (**Fig. 28**). The lower colonic TNF-α levels found in SLE-LC40 group might be a result of a local anti-inflammatory activity induced by LC40 in the gut.

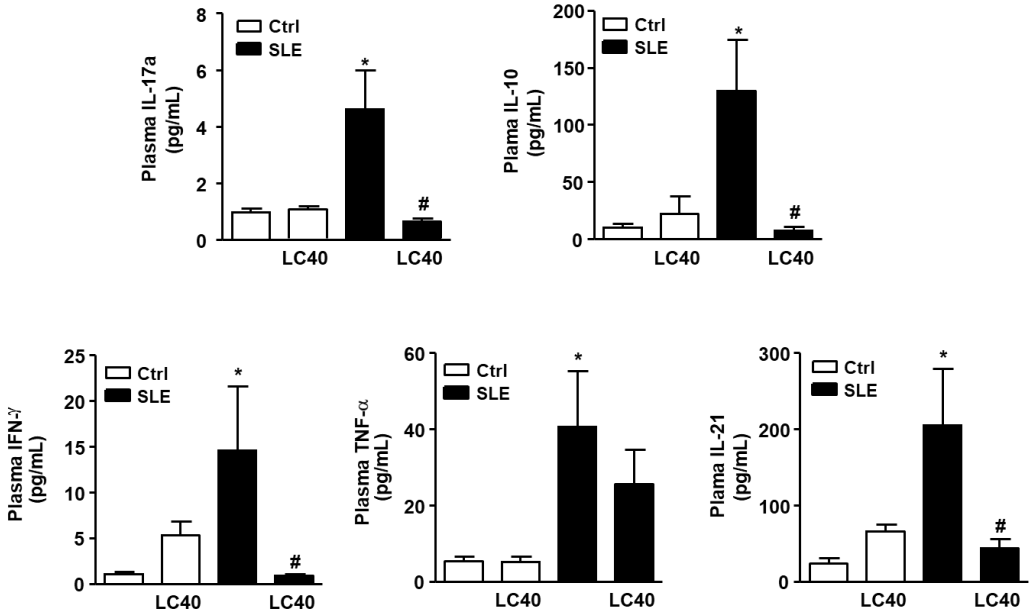

Figure 28. Effects of Lactobacillus fermentum CECT5716 (LC40) treatment on plasma cytokines. *Plasma concentrations of interleukin (IL)-17a, IL-10, interferon-γ (IFN-γ), tumor necrosis factor-α (TNF-α), and IL-21 measured by ELISA in control (Ctrl) and systemic lupus erythematosus (SLE) mice. Values are expressed as means ± SEM (n = 4-8). *P< 0.05 compared to the Ctrl group. #P< 0.05 compared to the untreated SLE group.*

2.5. LC40 treatment prevents endothelial dysfunction and vascular oxidative stress

Aortas from SLE mice had strongly reduced endothelium-dependent vasodilator responses to acetylcholine compared to aortas from the control group. The treatment of SLE mice with the probiotic showed an increase in the acetylcholine-induced vasodilation compared to vehicle-treated SLE mice (**Fig. 29A**). The relaxation response induced by acetylcholine was fully inhibited by L-NAME in all experimental groups (**Fig. 30A**), showing that acetylcholine-induced relaxation of aorta depends entirely on endothelium-derived NO in both control and SLE groups. We determined the effects of SNP to analyse whether the impaired response to endothelium-derived NO is due to a lower bioavailability of NO or to a defect in NO signalling in vascular smooth muscle.

SNP directly activates soluble guanylate cyclase in vascular smooth muscle mimicking the effects of endogenous NO. No differences were observed among all experimental groups in the endothelium-independent relaxation response to SNP (**Fig. 30B**).

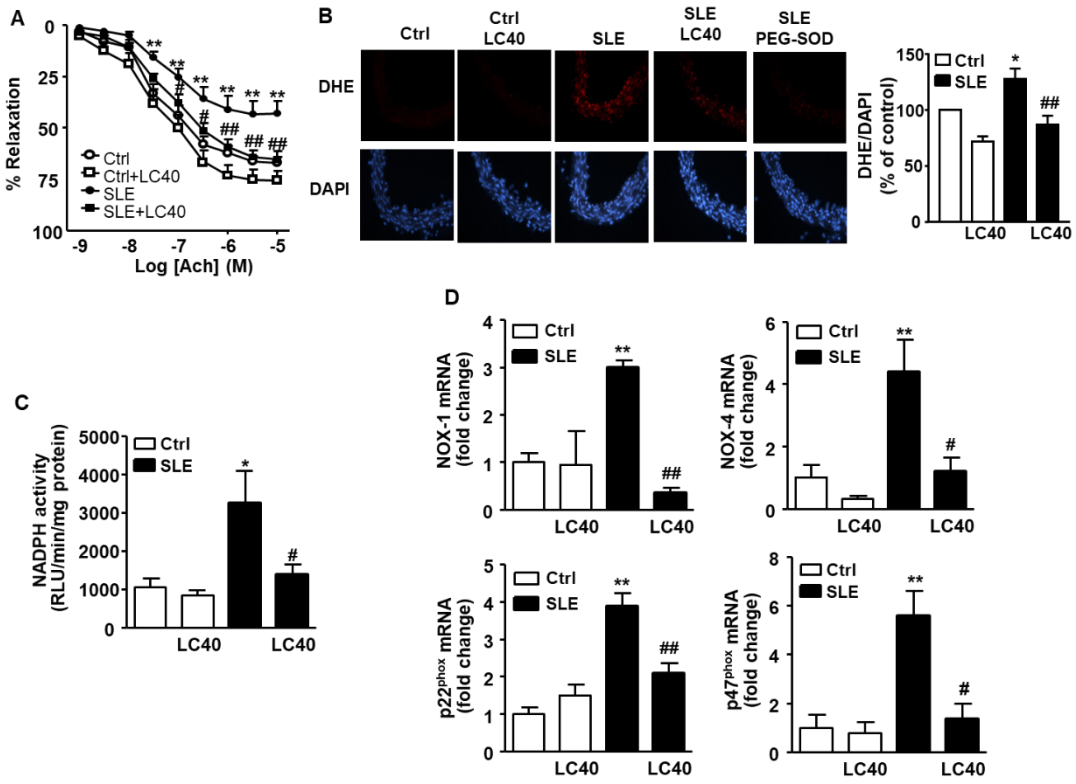

Figure 29. Effects of Lactobacillus fermentum CECT5716 (LC40) treatment on endothelial function, vascular oxidative stress, and NOX pathway. *(**A**) Vascular relaxation responses induced by acetylcholine (Ach) in endothelium-intact aortas precontracted by U46619 (10 nM) in control (Ctrl) and systemic lupus erythematosus (SLE) mice. (**B**) Top pictures show arteries incubated in the presence of dihydroethidium (DHE), which produces a red fluorescence when oxidized to ethidium by reactive oxygen species (ROS). Bottom pictures show the blue fluorescence of the nuclear dye DAPI (original magnification, ×400). Averaged values, means ± SEM (n = 4–8 rings from different mice) of the red ethidium fluorescence normalized to the blue DAPI fluorescence. (**C**, **D**) NOX activity measured by lucigenin-ECL (**C**) and expression of NOX subunits NOX-1, NOX-4, p47phox, and p22phox (**D**) at the level of mRNA by RT-PCR in Ctrl and SLE mice. Values are expressed as means ± sem (n = 4–8). *P < 0.05 and **P < 0.01 compared to the Ctrl group; #P < 0.05and ##P < 0.01 compared to the untreated SLE group.*

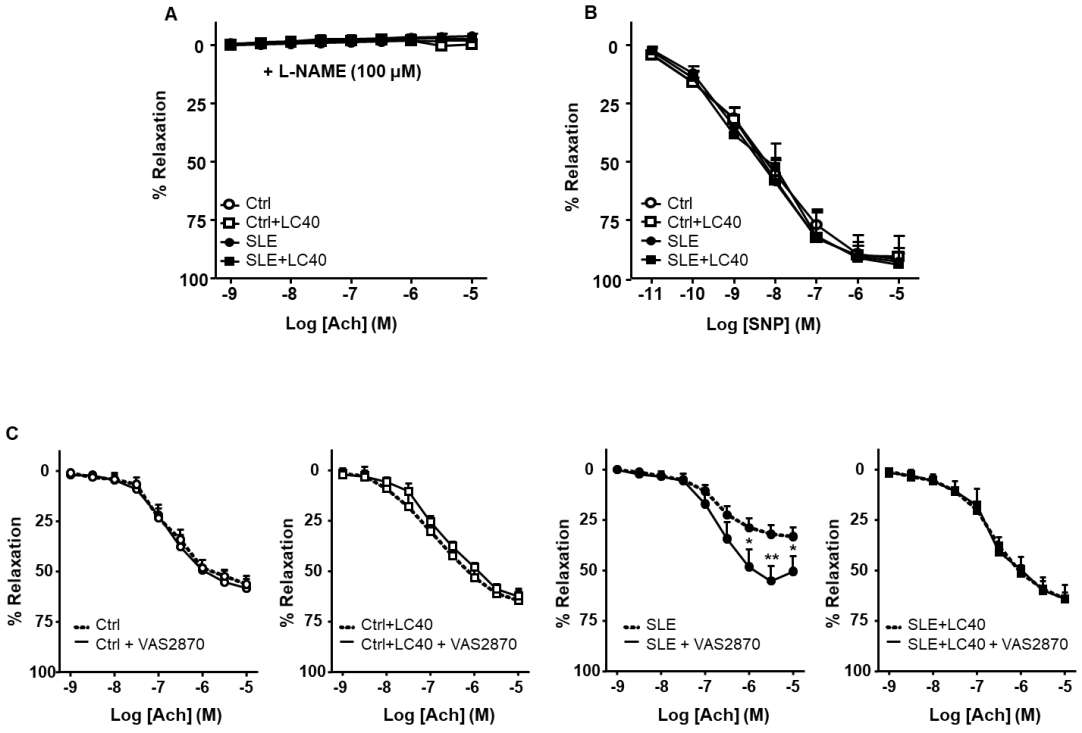

Figure 30. Effects of Lactobacillus fermentum CECT5716 (LC40) treatment on vascular nitric oxide pathway*. Vascular relaxation responses induced by acetylcholine (Ach), in endothelium-intact aortae pre-contracted by U46619 (10 nM) in the absence and in the presence of NG-nitro-L-arginine methyl (L-NAME;* ***A****), or the NADPH oxidase inhibitor VAS2870 (5 µM;* ***C****). Endothelium-independent vasodilator responses to sodium nitroprusside (SNP;* ***B****) in endothelium-denuded aortae pre-contracted by U46619 (10 nM) in control (Ctrl) and systemic lupus erythematosus (SLE) mice. Values are expressed as means ± SEM (n = 4-7). *P< 0.05 and **P< 0.01 compared to the untreated SLE group.*

Ethidium red fluorescence was measured in sections of aortas incubated with DHE to characterize and localize ROS levels within the vascular wall. Positive red nuclei were observed in adventitial, medial and endothelial cells from sections of aorta incubated with DHE (**Fig. 29B**). Nuclear ethidium red fluorescence was quantified and normalized to the blue fluorescence of the DAPI nuclear stain, allowing comparisons between different sections. Aortic rings from SLE group showed A marked staining in adventitial, medial and endothelial cells was found in aortic rings from the SLE group, whereas a slighter staining was found in aortic rings from the control group because it

was almost suppressed in this group by the O_2^- scavenger PEG-SOD. These effects on ROS levels were prevented by LC40 treatment (**Fig. 29B**). Since NADPH oxidase is the major source of ROS in the vascular wall, we investigated the role of NADPH oxidase-driven ROS production in endothelial function. We tested endothelium-dependent relaxation to acetylcholine in the presence of the pan-NOX inhibitor VAS2870. No significant differences were observed after incubation with VAS2870, in control and LC40 treated groups, but this agent increased the relaxant response to acetylcholine in SLE group, showing the critical role of increased NADPH oxidase in the endothelial dysfunction found in aortas from SLE mice (**Fig. 30C**). In addition, NADPH oxidase activity was higher in aortic rings of SLE mice than in aortic rings of control mice (**Fig. 29C**). This activity was associated with a significant mRNA increase of the main NADPH oxidase subunits in aortas obtained from all experimental groups (**Fig. 29D**). Chronic administration of LC40 reduced significantly both the up-regulation of NADPH oxidase subunits and the increased NADPH oxidase activity in SLE mice, but not in control mice (**Fig. 29C and 29D**).

2.6. LC40 treatment reduces IL17/ROCK/eNOS pathway and vascular inflammation

We measured the mRNA level of FoxP3 (a marker of Treg) and RORγ (a marker of Th17) to determine whether these vascular effects were associated with T-lymphocytes infiltration in aorta. In addition, mRNA of IL-10 and IL17a, cytokines released by Treg and Th17, respectively, were also measured. mRNA levels of FoxP3 and IL-10 were higher in SLE mice than in control mice. These mRNA levels were restored to normal values when SLE mice were treated with LC40 (**Fig. 31A**). Moreover, RORγ and IL-17a mRNA levels were markedly higher in SLE mice than in control mice; whereas the chronic administration of LC40 decreased these high mRNA levels (**Fig. 31B**). IL-17a activates Rho A/ROCK leading to increased phosphorylation of the inhibitory eNOS residue Thr495 and endothelial dysfunction (Nguyen*et al.*, 2013). In consistency with these data, we found that the protein expression of RhoA (**Fig. 31C**) (an upstream

ROCK activator) and eNOS phosphorylation at the inhibitory Thr495 were higher in SLE mice than in control mice; whereas the phosphorylation of eNOS at the activation site Ser1177 was lower in aortas of the SLE group than in aortas of the control group. These effects on SLE mice were restored to values similar to control mice when SLE mice were treated with LC40 (**Fig. 31D**).

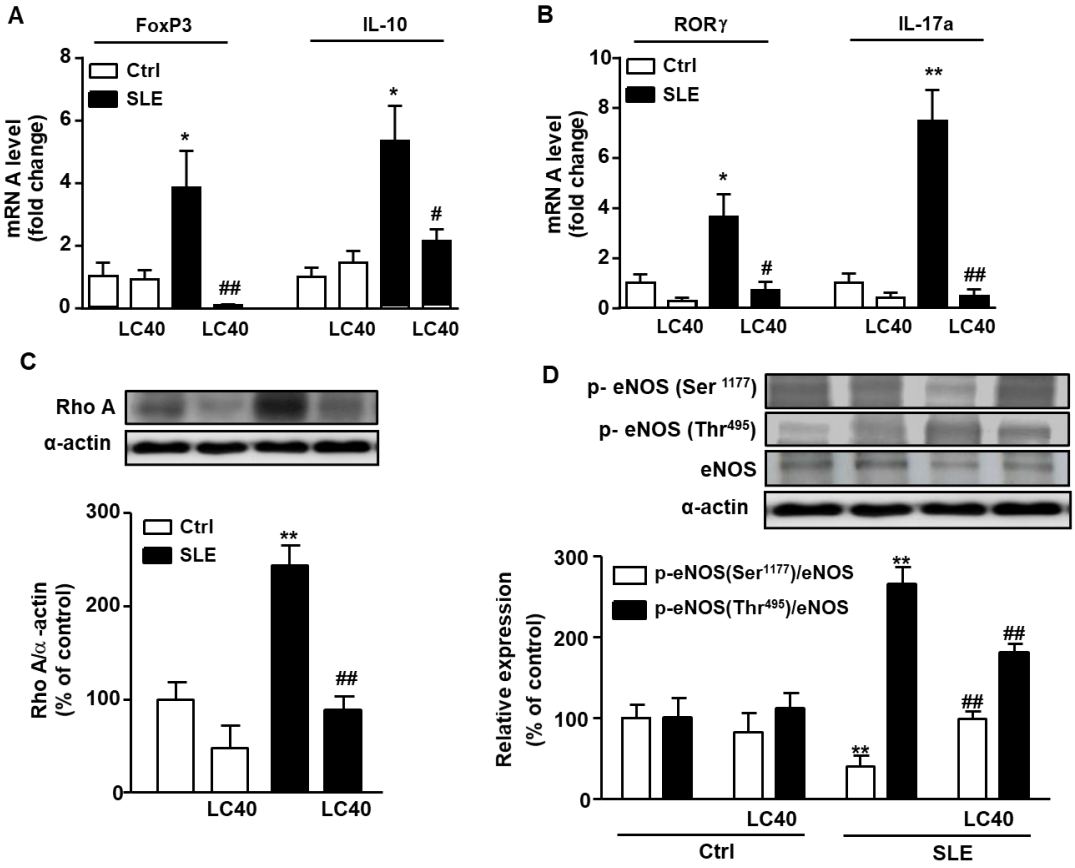

Figure 31. Effects of Lactobacillus fermentum CECT5716 (LC40) treatment on aortic T cells infiltration. *(**A**) Treg infiltration in aorta measured by FoxP3 and IL-10 mRNA levels. (**B**) Aortic Th17 infiltration measured by mRNA levels of RORγ and IL-17a. (**C**) Rho-kinase activity measured by Rho protein expression. (**D**) eNOS activity measured by Ser1177 and Thr495 eNOS phosphorylation in control (Ctrl) and systemic lupus erythematosus (SLE) mice. Values are expressed as means ± SEM (n = 4–6). *P < 0.05 and **P < 0.01 compared to the Ctrl group; #P < 0.05 and ##P < 0.01 compared to the untreated SLE group.*

Bacterial endotoxin LPS activates TLR-4, inducing cytokine expression in the vascular wall (Kim *et al*., 2005) and augmenting ROS production, primarily superoxide, which rapidly reacts with and inactivates NO in the vascular wall (Liang *et al*., 2013; Toral. *et al*., 2014). The mRNA levels of TLR-4 in aorta were significantly higher in SLE mice than in control mice. This increase was abolished by the LC40 treatment (**Fig. 32A**). Furthermore, gene expression of the pro-inflammatory cytokines IL-6, IL-1β, and TNF-α in aorta was higher in SLE mice than in control mice. Probiotic administration significantly reduced mRNA levels of these genes (**Fig. 32B**).

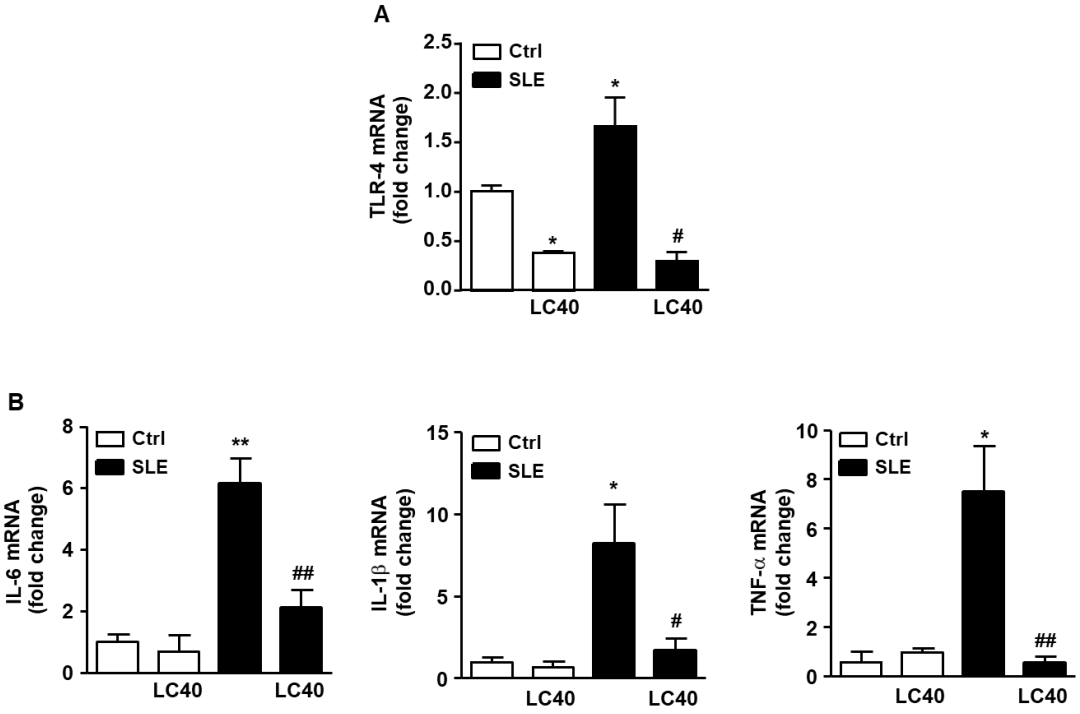

Figure 32. Effects of Lactobacillus fermentum CECT5716 (LC40) treatment on vascular inflammation. *Aortic mRNA levels of toll-like receptor (TLR)-4 (**A**), and pro-inflammatory cytokines (**B**) measured by RT-PCR in control (Ctrl) and systemic lupus erythematosus (SLE) mice. Values are expressed as means ± SEM (n = 4-6). *P< 0.05 and **P< 0.01 compared to the Ctrl group. #P< 0.05 and ##P< 0.01 compared to the untreated SLE group.*

3. Lactobacillus fermentum CECT5716 prevents renal damage in the NZBW/F1 mice model of systemic lupus erythematosus

3.1. LC40 treatment prevents renal damage

Kidney function in SLE mice was altered as evidenced by the lower urine concentration of creatinine (≈ -72%) (**Figure 33A**) and urea (≈ -83%) (**Figure 33B**) compared to control group. Interestingly, chronic LC40 consumption improves renal function since normalized both parameters. In respect to urinary albumin excretion, we found a time-dependent increase in SLE mice compared to control mice, being significant at 30 weeks old. LC40 treatment significantly prevented albumin excretion (**Figure 33C**). No significant changes in kidney function and damage were observed in control mice treated with LC40. The comparative study of renal injury in different groups is shown in representative micrographs in **Figure 34A, 34B and Table 8**. Renal lesions in control groups were absent. No glomerular, tubulointerstitial or vascular lesions were present in renal parenchyma in both Ctrl and Ctrl-LC40 groups. Extracapillary proliferation (crescent in 66.6% of mice) in moderate intensity, segmental sclerosis (88.9% of mice), and abundant immune deposits on basal membrane of tuft capillary (100% of mice) were detected in SLE group glomeruli with Masson's trichrome stain. Tubular dilatation with hyaline casts and parches of chronic inflammatory infiltrate were present in 100% of SLE group kidneys. SLE-LC40 group showed presence of lesser endocapillary proliferation, immune deposits in tuft capillary, glomerular (glomerulosclerosis, crescent) and tubulointerstitial lesions (tubular casts, inflammatory infiltrate) in comparison with untreated NZBWF1 mice. The number of nuclei per glomerular cross-section, which is a measure of glomerular cellularity and proliferation, was significantly increased for mice in SLE mice. While SLE-LC40 showed lesser glomerular proliferation than SLE-group.

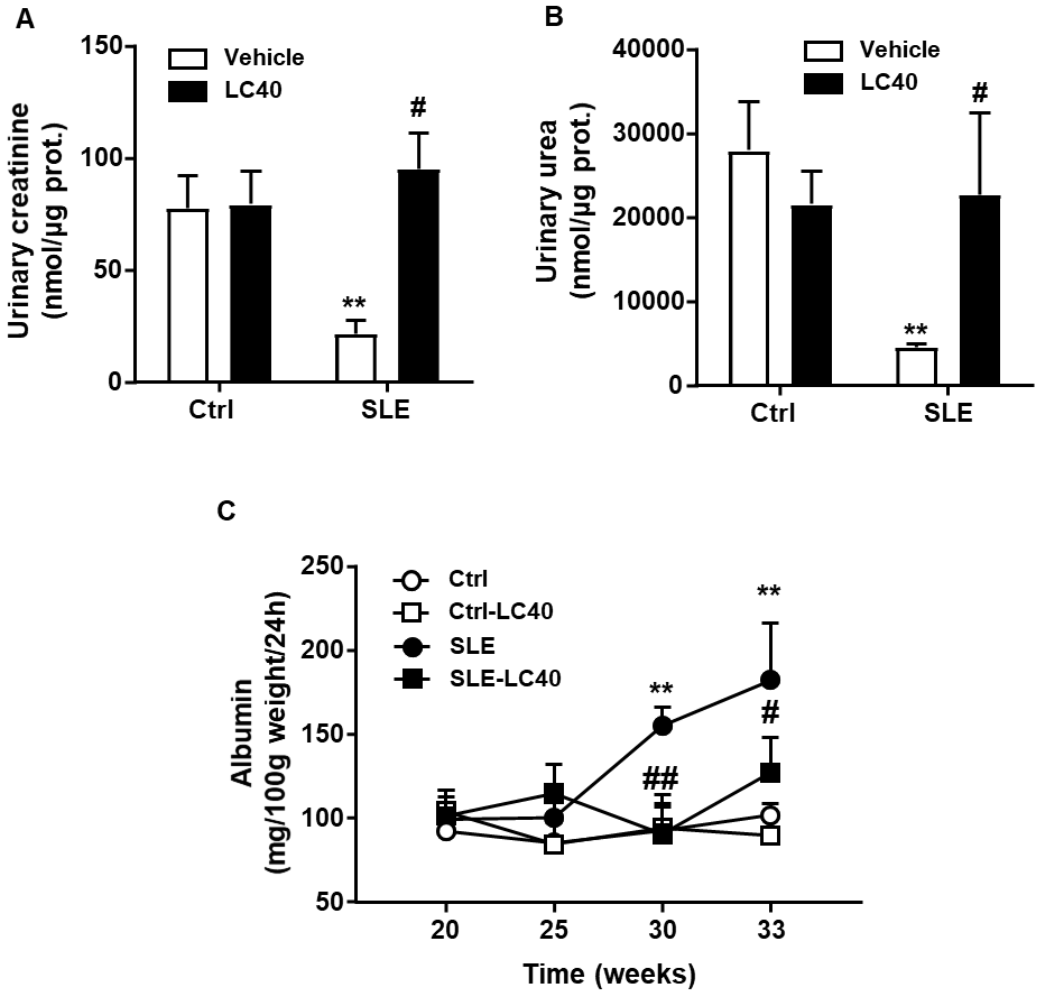

Figure 33. Effects of Lactobacillus fermentum CECT5716 (LC40) treatment on urinary parameters. (***A***) *Final creatinine and (**B**) urea concentration in urine, and (**C**) time course of albumin excretion in control (Ctrl) and systemic lupus erythematosus (SLE) mice. Values are expressed as means ± SEM (n = 5-9). **P< 0.01 compared to the Ctrl group. #P< 0.05 and ##P< 0.01 compared to the untreated SLE group.*

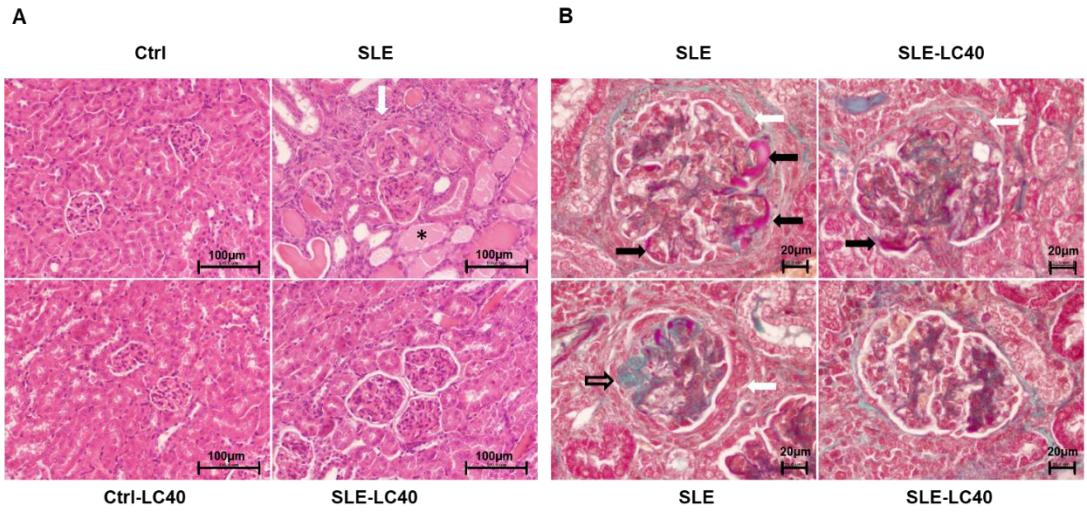

Figure 34. Effects of the Lactobacillus fermentum CECT5716 (LC40) treatment on morphological renal cortex features. *(**A**) Kidney sections in control (Ctrl) and systemic lupus erythematosus (SLE) mice untreated or treated with LC40 were stained with hematoxylin-eosin (H&E) and representative images are shown. Renal lesions in Ctrlgroups were absent. Extracapillary proliferation (white arrow) and tubular dilatation with hyaline casts (asterisk) are present in SLE mice. Bar scale: 100µm. (**B**) Kidney sections were stained with Masson's trichrome (TRIC) and glomerular representative images are shown. Note fucsinophil immune deposits in tuft capillary (black arrows), extracapillary proliferation with presence of crescents (white arrows) and mesangial sclerosis (empty arrow) in SLE mice and lesser endocapillary proliferation, immune deposits and crescents in SLE-LC40 mice. Bar scale: 20µm.*

Table 8. Effects of *Lactobacillus fermentum* CECT5716 (LC40) on renal damage.

Variables	Ctrl (n = 8)	Ctrl-LC40 (n = 5)	SLE (n = 9)	SLE-LC40 (n = 8)
Cells Nº/glomeruli	25.5±2.5	24.9±1.1	51.9±4.5**	33.3±2.3##
Glomerulosclerosis (%)	0.3±0.2	0.0±0.0	7.1±2.8*	0.6±0.5#
Crescents (%)	0.0±0.0	0.0±0.0	14.6±4.4*	2.5±2.5#
Immunocomplex (%)	1.0±0.7	3.0±2.2	37.3±9.9**	12.5±4.9#
Mesangioproliferation (%)	5.6±4.0	2.0±2.0	31.4±7.5**	13.2±4.1#
Tubular casts†	0.1±0.1	0.7±0.2	2.2±0.3**	0.9±0.2#
Inflammatory infiltrate†	0.0±0.0	0.5±0.4	1.8±0.2**	1.0±0.3#

*Values are shown as means ± SEM of 50 glomeruli without sclerosis per mouse. *P < 0.05 and **P < 0.01 compared to control (Ctrl) group; #P < 0.05 and ##P < 0.01 compared to the untreated systemic lupus erythematosus (SLE) group. Bonferroni test. †semiquantitative scale (0-3).*

3.2. LC40 treatment prevents renal oxidative stress and inflammation

NADPH oxidase activity was significantly increased in renal cortex from lupus mice as compared to control (**Figure 35A**). Chronic LC40 prevented the NADPH oxidase subunits up-regulation and the increase in NADPH oxidase activity. In addition, mRNA levels of TLR4 (**Fig. 35B**) were also increased in lupus mice, and LC40 prevented this up-regulation. Gene expression of the pro-inflammatory cytokines (**Figure 35C**), TNF-α, IL-1β, and IL-6, in renal cortex was increased in SLE mice compared to control. LC40 administration significantly reduced the mRNA levels of these genes. We also analysed the transcript levels of transcription factors, such as RORγ, FoxP3, and T-bet, which induce Th17, Tregs, Th1 populations, respectively, being indirect markers of Th17, Treg, and Th1 infiltration in the kidney. FoxP3, RORγ, and T-bet mRNA levels were increased in SLE mice, and LC40 administration restored them to the levels found in control group (**Figure 36A**). In correlation with this, the mRNA levels of the cytokines IL-10 (**Figure 36A**), mainly produced by Treg, and IL-17a, produced by Th17,

and IFNγ, released by Th1, were also higher in SLE mice as compared to control. Again, long-term LC40 administration restored the mRNA levels of these cytokines in renal cortex (**Figure 36B**). By contrast, GATA-3 mRNA level, a marker of Th2 cells, was unchanged among all experimental groups (**Figure 36A**).

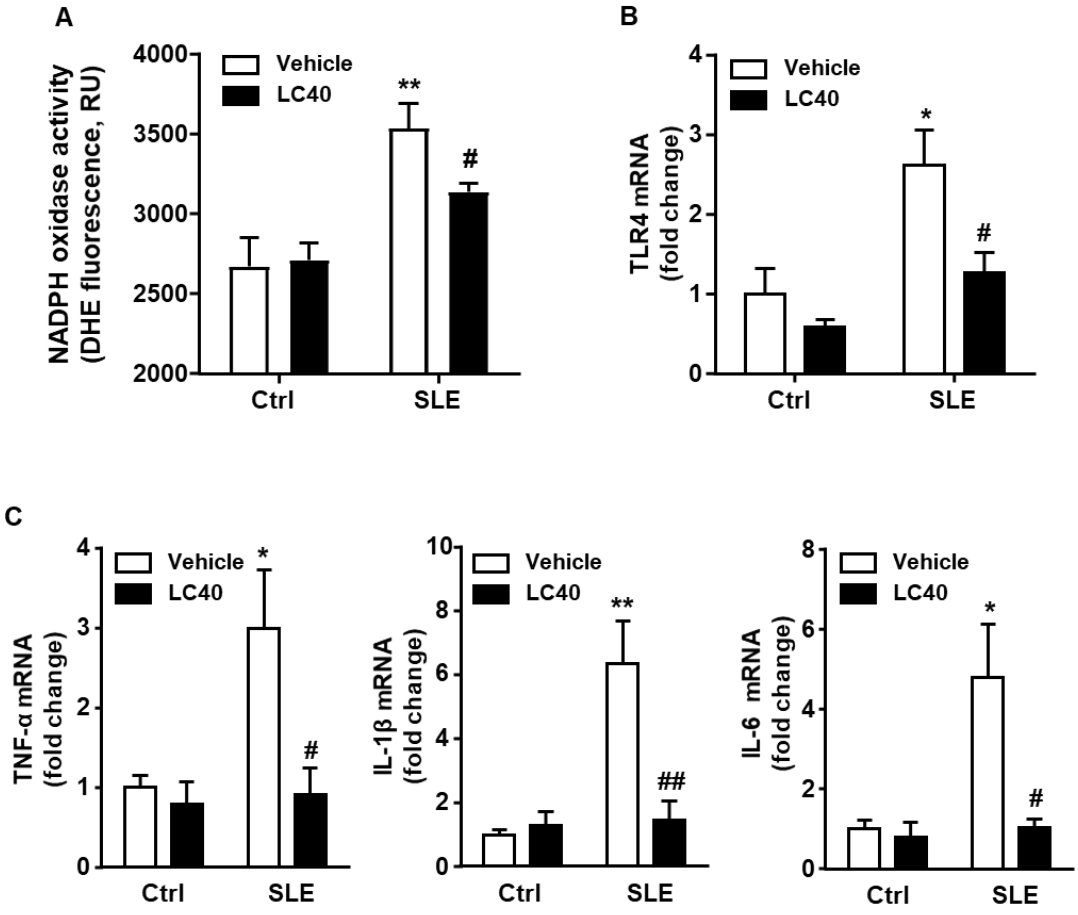

Figure 35. Effects of Lactobacillus fermentum CECT5716 (LC40) treatment on oxidative and inflammatory parameters in renal cortex. *(**A**) NADPH oxidase activity measured by dihydroethidium (DHE) fluorescence and (**B**) mRNA levels measured by RT-PCR of Toll-like receptor (TLR)-4 and (**C**) pro-inflammatory cytokines in renal cortex from control (Ctrl) and systemic lupus erythematosus (SLE) mice untreated or treated with LC40. Values are expressed as means ± SEM (n = 5-9). *P< 0.05 and **P< 0.01 compared to the Ctrl group. #P< 0.05 and ##P< 0.01 compared to the untreated SLE group.*

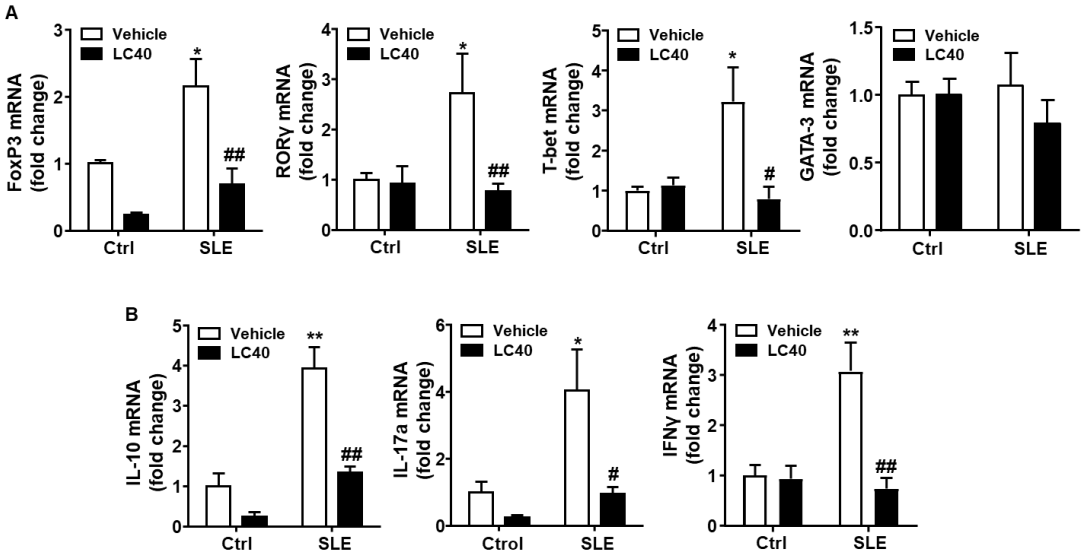

Figure 36. Effects of Lactobacillus fermentum CECT5716 (LC40) treatment on T-cells infiltration in renal cortex. *(**A**) Regulatory T(reg) cells, measured by FoxP3, T helper(h) 17, measured by RORγ, and Th1, measured by mRNA levels of T-bet, infiltration in renal cortex from control (Ctrl) and systemic lupus erythematosus (SLE) mice untreated or treated with LC40. (**B**) mRNA levels of the main interleukins (IL) produced by these T cells in all experimental groups. Values are expressed as means ± SEM (n = 5-9). *P< 0.05 and **P< 0.01 compared to the Ctrl group. #P< 0.05 and ##P< 0.01 compared to the untreated SLE group.*

4. Toll-like receptor 7-driven lupus autoimmunity induces hypertension and vascular alterations in mice.

4.1. Blood pressure, target organs damage and systemic inflammation are increased in SLE induced by TLR-7 activation

IMQ treated mice displayed a higher mortality rate (approximately 20%, **Figure 37A**) and a significantly increased weight gain when compared to the control group (final weight: 24.10 ± 0.62 g and 21.89 ± 0.54, respectively, $p<0.05$) at 8 weeks of treatment, as already shown in the original description of this model (Yokogawa *et al.*, 2014). The gonadal and mesenteric fat weight indices were found decreased in the IMQ group (**Table 9**) despite the weight gain observed, which points to the development of oedema and swelling. Additionally, the IMQ group presented a progressive raise in SBP (**Figure 37B**) and in the final mean arterial pressure (**Figure 37C**) measured by tail-cuff plethysmography and direct recordings, respectively, being approximately 20 mmHg higher in the IMQ group when compared to the Control group at the end of the experiment. No significant changes in HR were induced by IMQ treatment (**Figure 37D**). In addition, both heart weight/tibia length and left ventricular weight/tibia length were higher in IMQ-treated mice than in control mice at 8 weeks of treatment (**Table 9**), whereas renal hypertrophy and hepatomegaly were found from 4 weeks of IMQ treatment (**Table 9**).

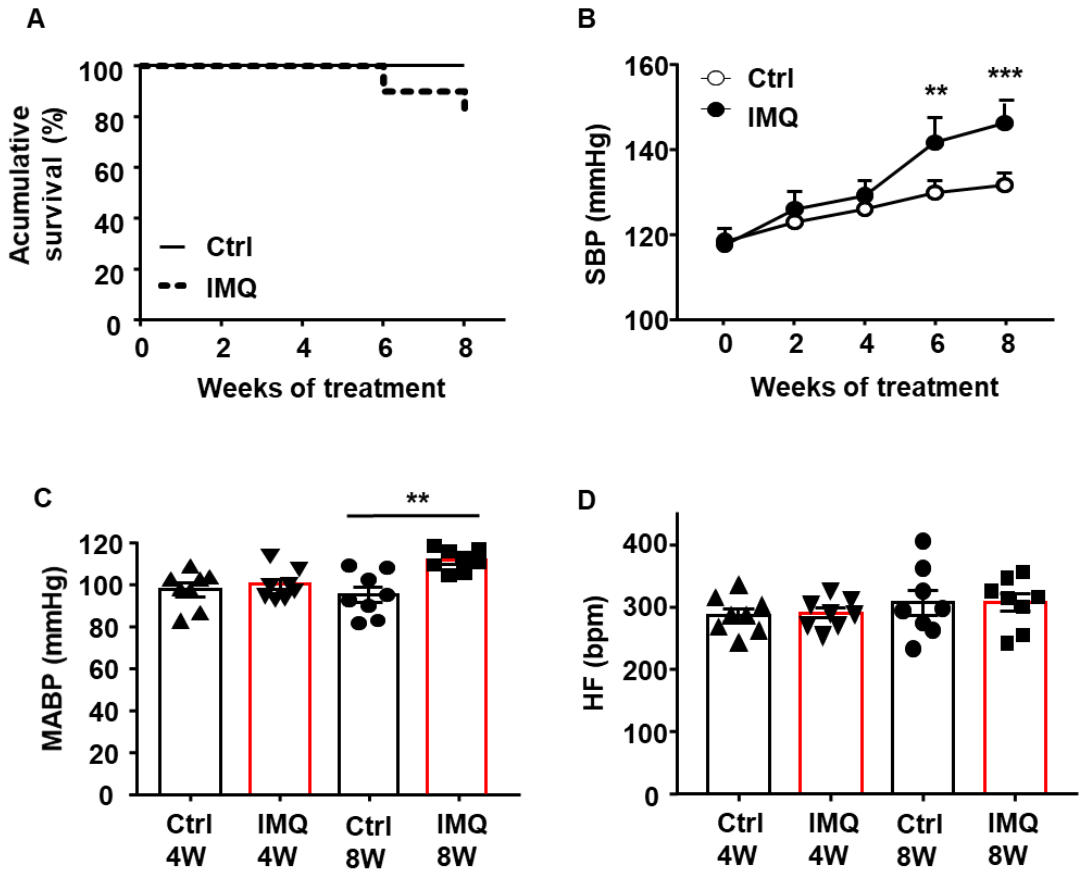

Figure 37. TLR-7 activation promotes blood pressure increase in imiquimod (IMQ)-induced autoimmunity. *(**A**) Cumulative survival rate of BALB/c mice following topical application of IMQ on their right ears three times per week for 8 weeks. (**B**) Time course of systolic blood pressure (SBP) measured by tail-cuff plethysmography was determined in control (Ctrl) and IMQ-treated mice. (**C**) Mean arterial blood pressure (MABP) and (**D**) heart rate (HR) measured by direct recording in left carotid artery at the end of the experimental period. Experimental groups: Ctrl 4 weeks (W) (n=8), Ctrl 8W (n=8), IMQ 4W (n=8), IMQ 8W (n=8). Values are represented as mean ± SEM.. **P<0.01 and ***P<0.001 compared to their respective Ctrol groups.*

Table 9. Morphological parameters.

Variables	Ctrl 4W (n=8)	IMQ 4W (n=8)	Ctrl 8W (n=8)	IMQ 8W (n=8)
BW (g)	21.54±0.61	21.75±0.64	21.89±0.54	24.10± 0.62 ** †
TL (mm	20.61±0.19	21.50±0.40	21.11±0.14	21.13± 0.30
HW/TL (mg/cm)	4.56±0.16	4.71±0.14	4.61±0.11	5.25± 0.24 * †
LVW/TL (mg/cm)	2.93±0.07	2.91±0.08	2.80±0.06	3.17± 0.12 * †
KW/TL (mg/cm)	5.36±0.06	5.89±0.21 *	5.20±0.08	6.83± 0.43 ** †
LW/TL (mg/cm)	42.35±2.49	67.15±2.29 **	39.29±1.42	86.26± 5.88 ** ††
Spleen/TL (mg/cm)	4.50±0.17	24.04±2.00 **	4.70±0.29	36.18± 3.63 ** †
Mesenteric fat/BW (%)	0.42±0.03	0.39±0.04	0.38±0.02	0.21±0.03 ** ††
Gonadal fat/BW (%)	2.04±0.18	1.89±0.18	1.80±0.16	0.89±0.07 ** ††

*Results are shown as means ± SEM. *P < 0.05 and **P < 0.01. compared to control (Ctrl) group; †P < 0.05 and ††P < 0.01 compared to imiquimod (IMQ) 4 weeks group. BW, Body weight; TL, Tibia length; HW, Heart weight; LVW, Left ventricular weight; KW, Kidney weight; LW, Liver weight.*

The IMQ model is characterized by kidney injury linked to high plasma autoantibody levels (Yokogawa *et al*., 2014; Liu *et al*., 2018). As expected, we found significant higher plasma levels of anti-dsDNA autoantibodies (**Figure 38A**) and kidney injury

(**Figure 39**) in IMQ-treated mice compared to control mice. Additionally, we found a marked splenomegaly in IMQ-treated mice (**Figure 38B**), which was associated with autoimmune disease progression. Also, a reduced clearance of apoptotic cells is associated with progressive lupus-like autoimmune disease and increased production of autoantibodies (Nagata *et al*., 2010; Sakamoto *et al*., 2016). Opsonins, such as C1q, thrombospondin-1 and milk fat globule-epidermal growth factor-8, are proteins released by macrophages enhancing the recognition and phagocytosis of apoptotic cells by macrophages. The primary source of circulating opsonins in the serum is the liver resident macrophages, Kupffer cells (Armbrust *et al*., 1997). Thereby, we investigated the opsonin expression in the livers of mice from all experimental groups. We found that activation of TLR-7 by a topical administration of IMQ reduced hepatic gene expression of opsonins only in IMQ-treated mice compared to control mice only after 8 weeks of treatment (**Figure 38C**).

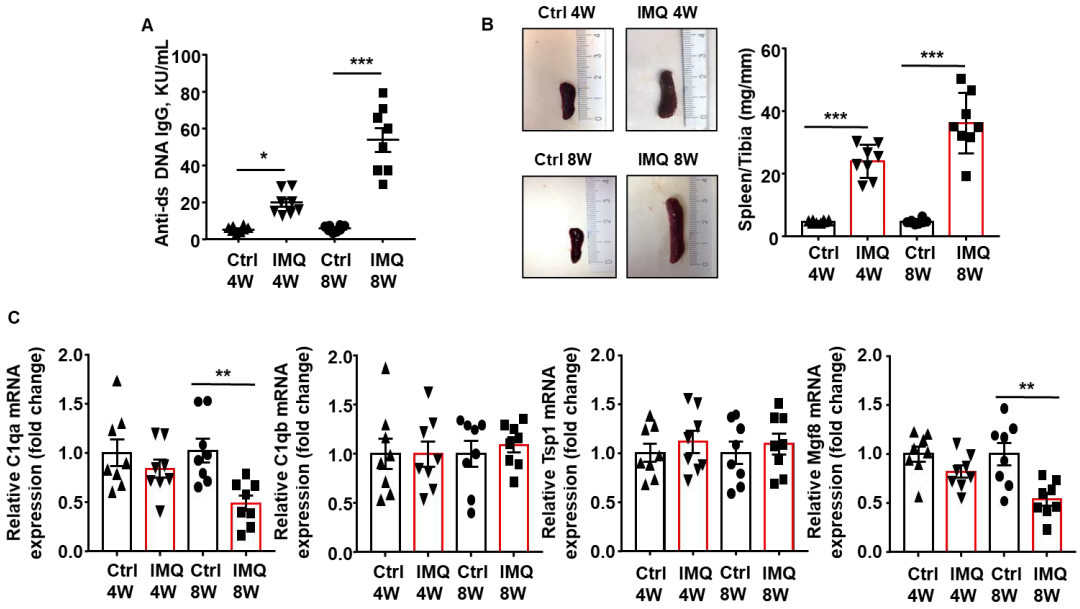

Figure 38. TLR-7 activation leads to higher levels of serum anti-double-stranded DNA (anti-dsDNA) autoantibodies, marked splenomegaly and altered clearance of apoptotic cells in imiquimod (IMQ)-treated mice. *(**A**) Circulating anti-dsDNA autoantibodies, (**B**)*

*splenomegaly, and (**C**) mRNA levels of hepatic opsonins measured by reverse transcriptase-polymerase chain reaction were assessed in Ctrl and IMQ-treated mice. Experimental groups: control (Ctrl) 4 weeks (W) (n=8), Ctrl 8W (n=8), IMQ 4W (n=8), IMQ 8W (n=8). Values are represented as means ± SEM. *P<0.05, **P<0.01 and ***P<0.001 compared to their respective Ctrl groups.*

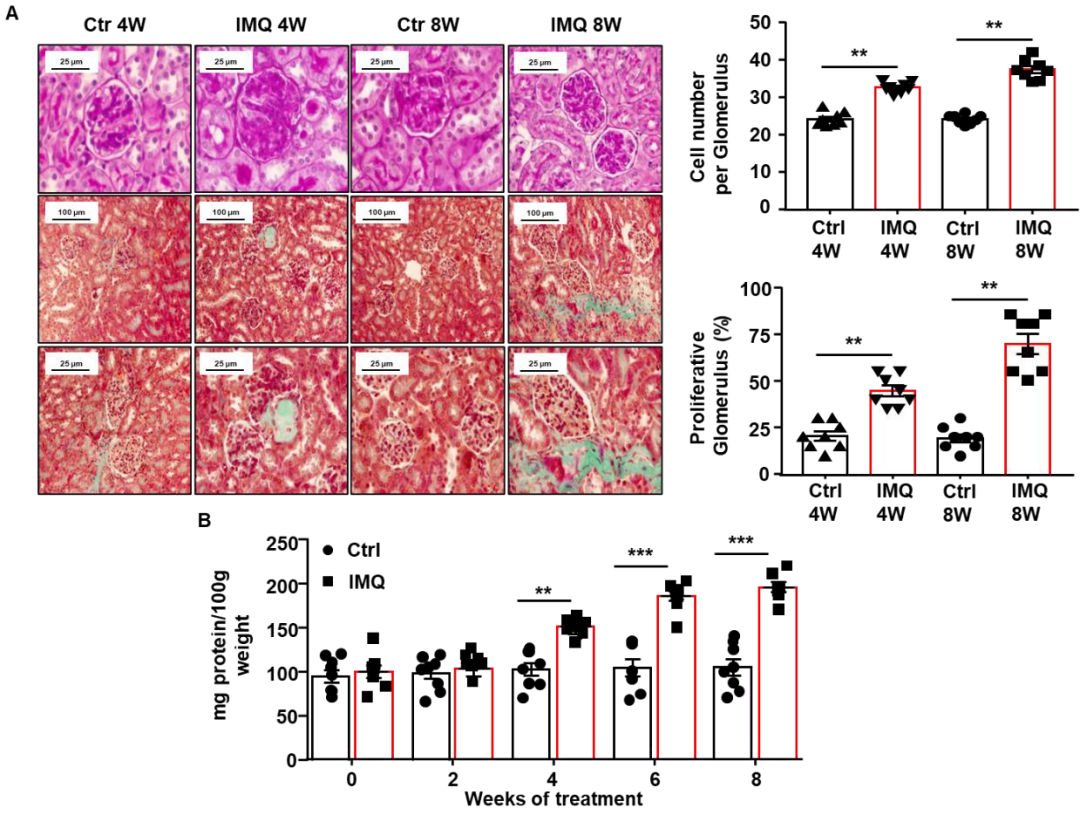

Figure 39. TLR-7 activation by topical application of imiquimod (IMQ) promotes renal injury. *(**A**) Kidney histopathology analysis. Kidney sections of control and IMQ-treated mice were stained with haematoxylin and eosin (H&E) and representative images are shown (top, original magnification: x40), and with periodic acid-Schiff and representative images are shown (intermediate and bottom, original magnifications: ×10 and x40, respectively). Beginning 4 weeks after topical IMQ treatment, histopathologic assessment of the kidneys showed proliferative glomerular lesions, enlarged, hypercellular glomeruli, an increase in the mesangial matrix, and mild peritubular mononuclear cell infiltrates. Results are shown as mean ± SEM, obtained from 8-10 separate experiments. (**B**) Urinary albumin excretion was increased in IMQ-treated mice compared with control mice after 4 weeks (W) of treatment. Experimental groups: Ctrl 4W (n=8), Ctrl 8W (n=8), IMQ 4W (n=8), IMQ 8W (n=8). Values are expressed as means ± SEM. **P<0.01 and ***P<0.001 compared to their respective Ctrl group.*

Finally, we evaluated the immunomodulatory actions of TLR-7 activation by measuring the number of total cells and the levels of B and T cells in spleens from all experimental groups. IMQ treatment led to an increase in splenocyte numbers and in the percentages of both splenic B cells and T cells from 4 weeks of IMQ treatment compared to the control group (**Figure 40A-C**). Specifically, the percentages of Th1 and Th17 cells were significantly increased only at 8 weeks of treatment, whereas percentage of Treg cells was reduced in splenocytes from all experimental groups (**Figure 40D-F**). Besides, plasma levels of IFN-α, IFN-γ, IL-21, TNF-α, IL-6, and IL-17 were also increased in IMQ-treated mice at 8 weeks compared to control group (**Figure 41**). Taken together, these results suggest that TLR-7 activation by topical application of IMQ results in systemic inflammation at 8 weeks of treatment, being these results consistent with the previously described findings (Yokogawa *et al.*, 2014; Ren *et al.*, 2016; Liu *et al.*, 2018).

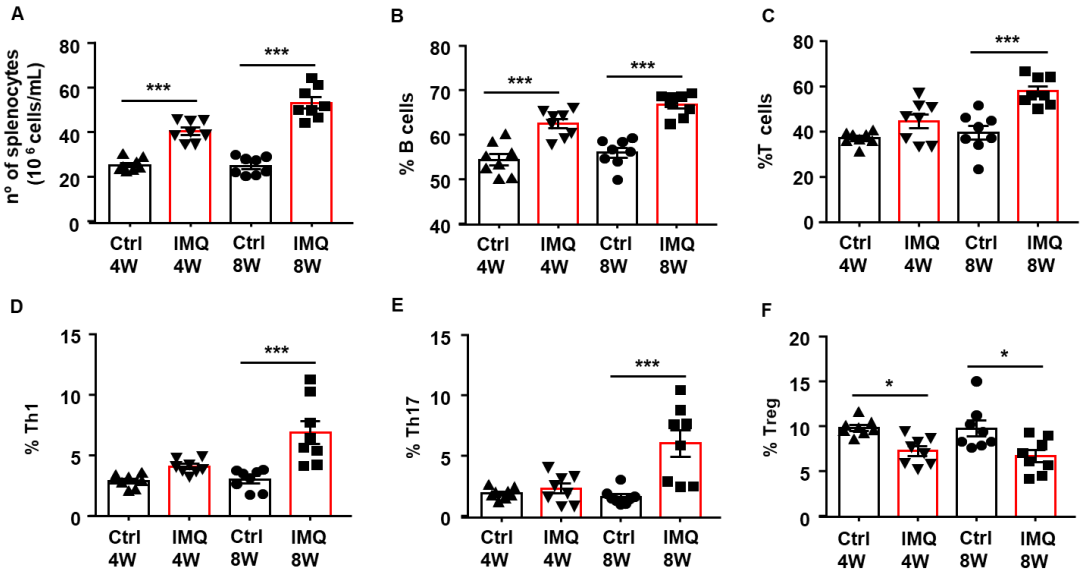

Figure 40. TLR-7 activation induces an increase in splenic B cells and T cells and promotes T cell polarization to proinflammatory phenotype. *(**A**) Number of total cells, (**B**) percentage of B cells and (**C**) percentage of T cells were measured by flow cytometry in spleens from imiquimod (IMQ)-treated mice. (**D**) Percentage of T helper (h) 1, (**E**) Th17 and*

*(**F**) regulatory T(reg) cells measured by flow cytometry were assessed in control (Ctrl) and IMQ-treated mice. Experimental groups: Ctrl 4 weeks (W) (n=8), Ctrl 8W (n=8), IMQ 4W (n=8), IMQ 8W (n=8). Values are represented as means ± SEM. *P<0.05 and ***P<0.001 compared to their respective Ctrl groups.*

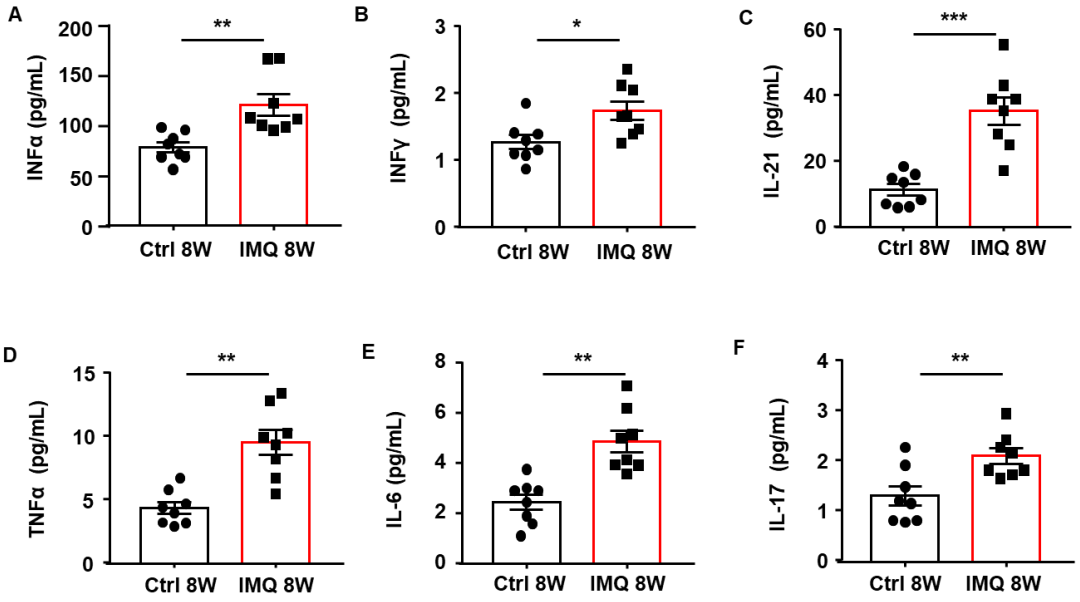

Figure 41. TLR-7 activation by topical application of imiquimod (IMQ) raises plasma levels of proinflammatory cytokines. *(**A**) Plasma levels of IFN-α, (**B**) IFN-γ, (**C**) IL-21, (**D**) TNF-α, (**E**) IL-6, and (**F**) IL-17 were measured by ELISA in control (Ctrl) and imiquimod (IMQ)-treated mice after 8 weeks (W) of treatment. Experimental groups: Control (Ctrl) 8W (n=8) and IMQ 8W (n=8). Values are expressed as means ± SEM. *P<0.05, **P<0.0,and ***P<0.001 compared to the Ctrl group.*

4.2. TLR-7 activation-induced SLE promotes vascular remodelling and endothelial dysfunction

Structural alterations in resistance arteries may be considered an important contributing factor to the pathogenesis of hypertension in humans and animal models (Schiffrin *et al.*, 2004; Briones *et al.*, 2009). Here, we found that topical administration of IMQ is associated with structural alterations in superior mesenteric arteries

characterized by a significant smaller LD and an increase in MT and M/L (≈ 40%) in BALB/c mice after 8 weeks (**Figure 42A-D**). However, non-significant changes in MCSA were found in arteries from IMQ-treated mice at any time (**Figure 42E**).

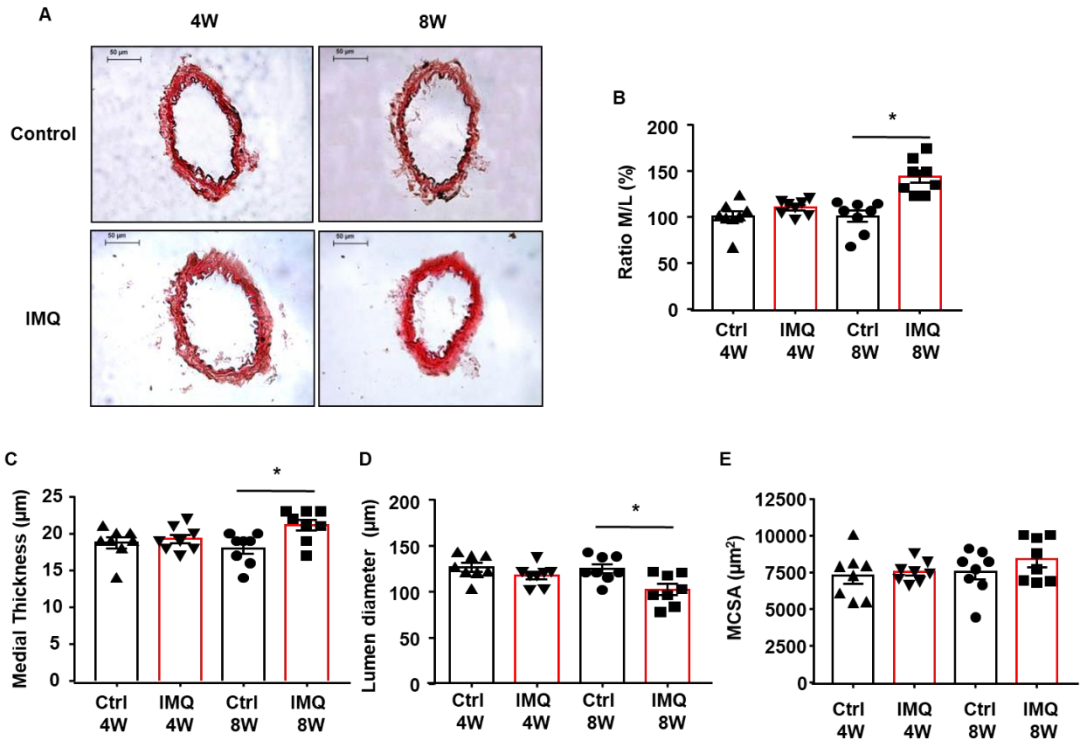

Figure 42. TLR-7 activation promotes vascular remodelling in imiquimod (IMQ)-treated mice. Effects of TLR-7 activation on structural modifications induced in superior mesenteric arteries from IMQ-treated mice. *(**A**) Representative histological sections of paraffin-embedded tissues stained with hematoxylin-eosin. Morphometric analysis of media:lumen ratio (M/L). (**B**), medial thickness (**C**), lumen diameter (**D**) and media cross-sectional area (MCSA) (**E**). Experimental groups: Control (Ctrl) 4 weeks (W) (n=8), Ctrl 8W (n=8), IMQ 4W (n=8), IMQ 8W (n=8). Values are represented as means ± SEM. *P<0.05 compared to their respective Ctrl groups.*

Similarly, SLE hypertension is known to be associated with an impaired vascular function (Ryan *et al.*, 2007; Mak *et al.*, 2017; Romero*et al.*, 2017). For that reason, we determined whether endothelial-dependent relaxation and contraction were altered in this model. We found that aorta from IMQ-treated mice showed strongly reduced endothelium-dependent vasodilator responses to Ach only after 8 weeks of topical

treatment (maximal effect, 60.35 ± 2.69% versus 79.34 ± 1.79% in the control group; P<0.001) (**Figure 43A).** The incubation for 30 minutes with the eNOS inhibitor L-NAME abolished the relaxant response induced by Ach in all experimental groups, involving NO in this relaxation (**Figure 43B**). Moreover, no differences were found in the endothelium-independent relaxant response to the NO donor sodium nitroprusside in aortic rings from both control and IMQ-treated groups, excluding changes in the sensitivity of the NO-cyclic guanosine monophosphate (cGMP) pathway in vascular smooth muscle cells (**Figure 43C**). In addition to examining endothelial-dependent relaxation, we also tested whether there are changes in vessel contractility that might contribute to endothelial dysfunction. No differences were found among all experimental groups in the contractile response induced by U46619 in both intact aortic rings and in the presence of L-NAME (**Table 10**). In addition, since endothelial-dependent relaxation was progressively impaired in IMQ-treated mice, we only evaluated whether eNOS expression was altered at 8 weeks of IMQ treatment. Aortic eNOS mRNA levels (**Figure 43D**) and protein expression (**Figure 43E**) were reduced in IMQ-treated mice compared to control mice.

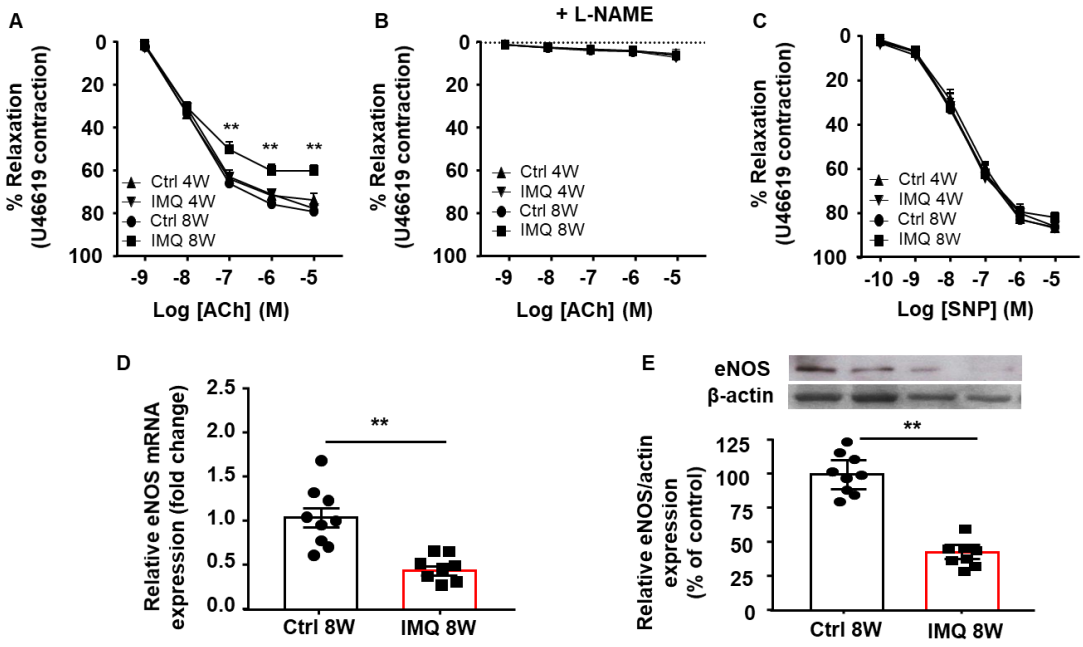

Figure 43. TLR-7 activation leads to marked impairment of endothelium-dependent vasorelaxation in imiquimod (IMQ)-treated mice. *(**A**) Vascular relaxant responses induced by acetylcholine (ACh, 1nM–10µM), in endothelium-intact aortas precontracted using U46619 (10nM) in the absence or (**B**) in the presence of the endothelial nitric oxide synthase (eNOS) inhibitor N(ω)-nitro-L-arginine methyl ester (L-NAME, 100µM). (C) Endothelium-independent relaxant responses to sodium nitroprusside (SNP, 0,1nM–10µM) in endothelium-denuded vessels precontracted using U46619 (10nM). Relaxant responses to ACh and sodium SNP were expressed as a percentage of precontraction induced by U46619. (**D**) mRNA expression and (**E**) protein expression of eNOS in aorta homogenates from all experimental groups. Experimental groups: Control (Ctrl) 4 weeks (W) (n=8), Ctrl 8W (n=8), IMQ 4W (n=8), IMQ 8W (n=8). Values are represented as means ± SEM. **P<0.01 compared to their respective Ctrl groups.*

Table 10. Maximal contractile response to U46619 in intact aortic rings in the presence of physiological salt solution (PSS).

Experimental group	N	PSS (mN)	L-NAME (mN)	Apo (mN)
Control 4W	8	10.83±0.72	12.08±0.69	10.93±0.87
IMQ 4W	8	10.55±0.26	11.50±0.64	11.10±0.39
Control 8W	8	11.27±0.38	12.32±0.43	11.74±0.37
IMQ 8W	8	11.01±0.57	12.29±0.58	12.05±0.68

N(ω)-nitro-L-arginine methyl ester (L-NAME, 100μM) or apocynin (Apo, 10μM). Values are expressed as means ± SEM. No differences were found among all experimental groups.

Finally, we also found that these changes in vascular structure and function are associated with a marked increase in vascular expression of TLR-7 mRNA in aorta and mesenteric arteries from IMQ-treated mice, whereas vascular TLR-9 mRNA expression was unaffected (**Figure 44**).

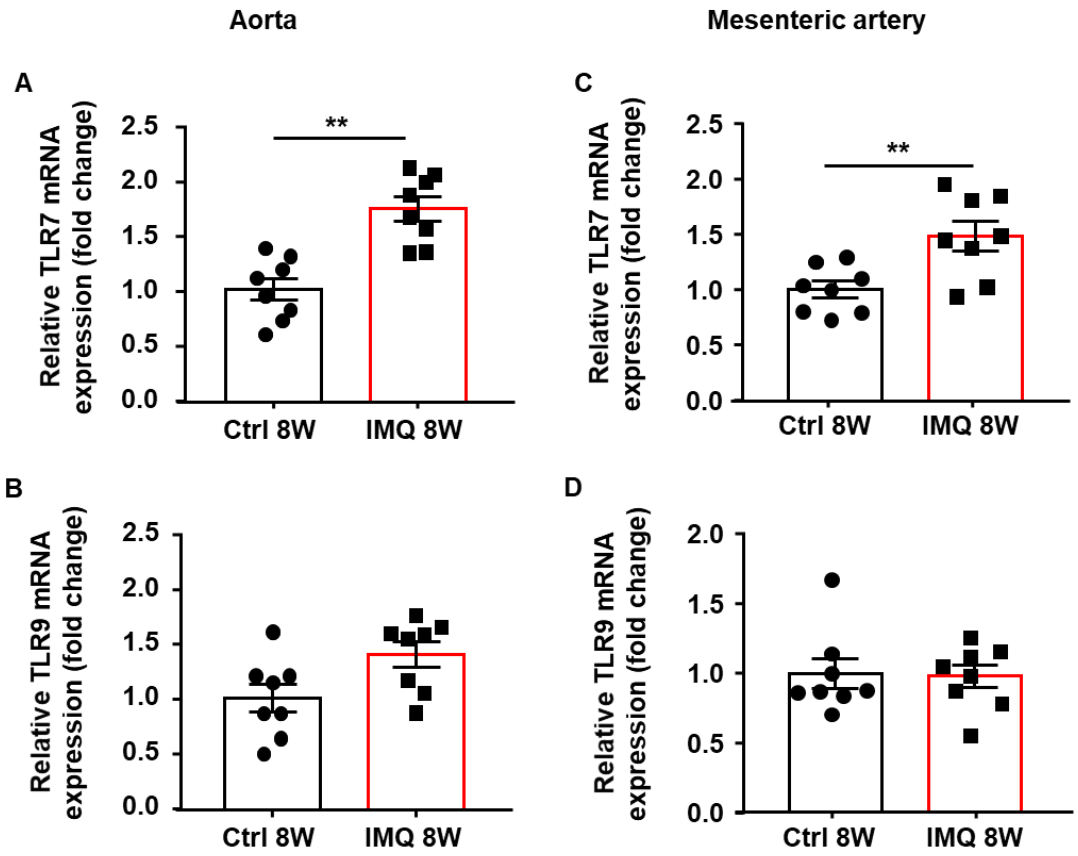

Figure 44. Increases in vascular TLR-7 mRNA expression were found after TLR-7 activation by topical application of imiquimod (IMQ). *(A, C) Aortic and mesenteric arteries TLR-7 mRNA and (B, D)TLR-9 mRNA levels measured by reverse transcriptase-polymerase chain reaction were assessed in control (Ctrl) and IMQ-treated mice after 8 weeks of treatment. Experimental groups: Ctrl 8W (n=8), IMQ 8W (n=8). Values are expressed as means ± SEM. **P<0.01 compared to the Ctrl group.*

4.3. Vascular oxidative stress and inflammation are increased in SLE induced by TLR-7 activation.

ROS, particularly O_2^-, play an important role in vascular tone and structure, contributing to pathological mechanisms related to endothelial dysfunction, arterial remodelling and vascular inflammation (Garcia-Redondo. *et al.*, 2016). Our results showed that aortic rings from IMQ-treated mice display a marked increase in red ethidium fluorescence staining of vascular wall compared to the control group (**Figure**

45A), suggesting an increased vascular ROS production. Moreover, the activity of the NADPH oxidase, considered the major source of O_2^- in the vascular wall, was also markedly increased in aorta from IMQ-treated mice at 8 weeks of treatment compared to the control mice (**Figure 45B**), which was correlated with significant mRNA increase of its catalytic subunits NOX2, p22phox and p47phox (**Figure 45C**). Likewise, the effects of the non-selective NADPH oxidase inhibitor apocynin in endothelium-dependent relaxation to Ach were analysed to evaluate the role of NADPH oxidase-driven ROS production in the impaired relaxation to ACh in aorta from IMQ-treated mice. No significant differences were found between groups after incubation with apocynin, suggesting that an increased NADPH oxidase activity is involved, at least in part, in the endothelial dysfunction found in aorta from IMQ-treated mice (**Figure 45D**).

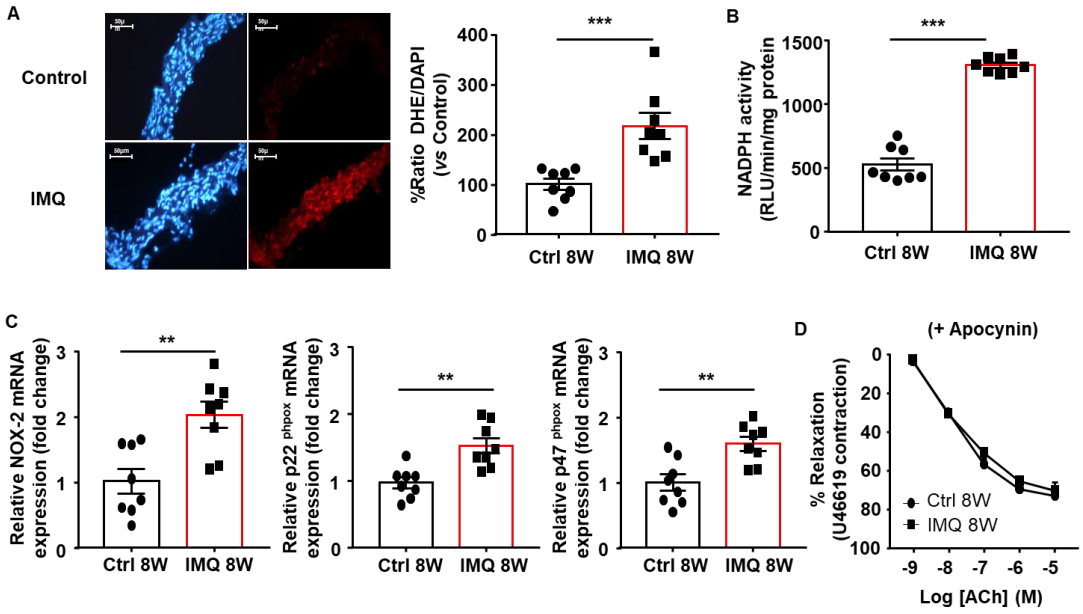

Figure 45. TLR-7 activation promotes a significant increase in vascular reactive oxygen species and NADPH oxidase activity in aorta from imiquimod (IMQ)-treated mice. *(**A**) Representative pictures of arteries incubated in the presence of dihydroethidium (DHE), which produces a red fluorescence when oxidized to ethidium by O_2^-, and the nuclear stain 4,6-diamidino-2-phenylindoledichlorohydrate (DAPI), which produces a blue fluorescence (magnification X400), and averaged values of the red ethidium fluorescence normalized to the blue DAPI fluorescence, Mean ± SEM (n= 8). (**B**) NADPH oxidase activity measured by lucigenin-enhanced chemiluminescence. (**C**) mRNA expression of the NADPH*

*oxidase subunits NOX-2, p22phox and p47phox in aorta homogenates from all experimental groups. (**D**) Endothelium-dependent vasodilator responses to acetylcholine (ACh) in intact aortic rings precontracted using U46619 (10 nM) in the presence of apocynin (10 μM). Experimental groups: Control (Ctrl) 8 weeks (W) (n=8), IMQ 8W (n=8). Values are represented as means ± SEM. **P<0.01 and ***P<0.001 compared to the Ctrl group.*

Additionally, we measured the activity of the NADPH oxidase and the mRNA expression of its catalytic subunits in mesenteric arteries to determine the role of NADPH oxidase-derived ROS on vascular remodelling. A significant increased NADPH oxidase activity and NOX2, p22phox and p47phox mRNA overexpression were found in mesenteric arteries homogenates from IMQ-treated mice compared to the control group (**Figure 46**). Incubation with PEG-SOD or Tiron for 30 min abolished this increased NADPH oxidase activity, involving O_2^- as the main ROS contributing to the vascular remodelling in these mice.

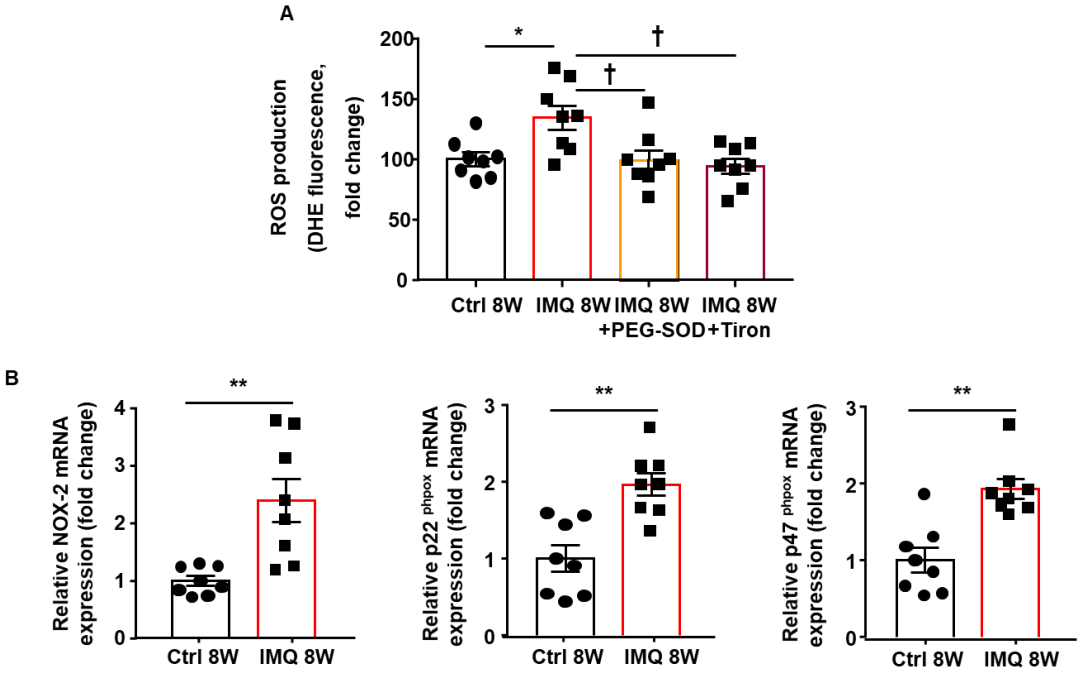

Figure 46. TLR-7 activation promotes a significant increase in NADPH oxidase activity in mesenteric arteries from imiquimod (IMQ)-treated mice. *(**A**) NADPH-stimulated ROS production, measured by dihydroethidium (DHE) fluorescence in a microplate reader, in*

*homogenates of mesenteric arteries from control (Ctrl) or IMQ-treated mice incubated with polyethylene glycol-conjugated superoxide dismutase (PEG-SOD) (250U/ml) or Tiron (10 μM). (**B**) mRNA expression of NADPH oxidase subunits NOX-2, p22phox and p47phox in mesenteric arteries homogenates from Ctrl and IMQ-treated mice.. Experimental groups: Ctrl 8W (n=8), IMQ 8W (n=8). Values are expressed as means ± SEM. *P<0.05 and **P<0.01 compared to the Ctrl group; †P<0.05 compared to the IMQ-treated group.*

Furthermore, given the key role played by proinflammatory cytokines and chemokines in the pathogenesis of vascular remodelling and endothelial dysfunction in SLE (Sun *et al*., 2013; Tselios *et al*., 2016), we also analysed the transcript level of vascular adhesion molecules and proinflammatory cytokines in aorta and mesenteric arteries homogenates from control and IMQ-treated mice. We found a higher mRNA expression of VCAM-1 and the proinflammatory cytokines IFN-α, IFN-γ, IL-1β, IL-6 and IL-17, whereas mRNA expression of IL-10 and TFG-β were reduced in aorta (**Figure 47**) and mesenteric artery (**Figure 47**) homogenates from IMQ-treated mice compared to control mice. These results are correlated with the increased systemic inflammation and the changes in splenic lymphoid cell populations induced by IMQ described above.

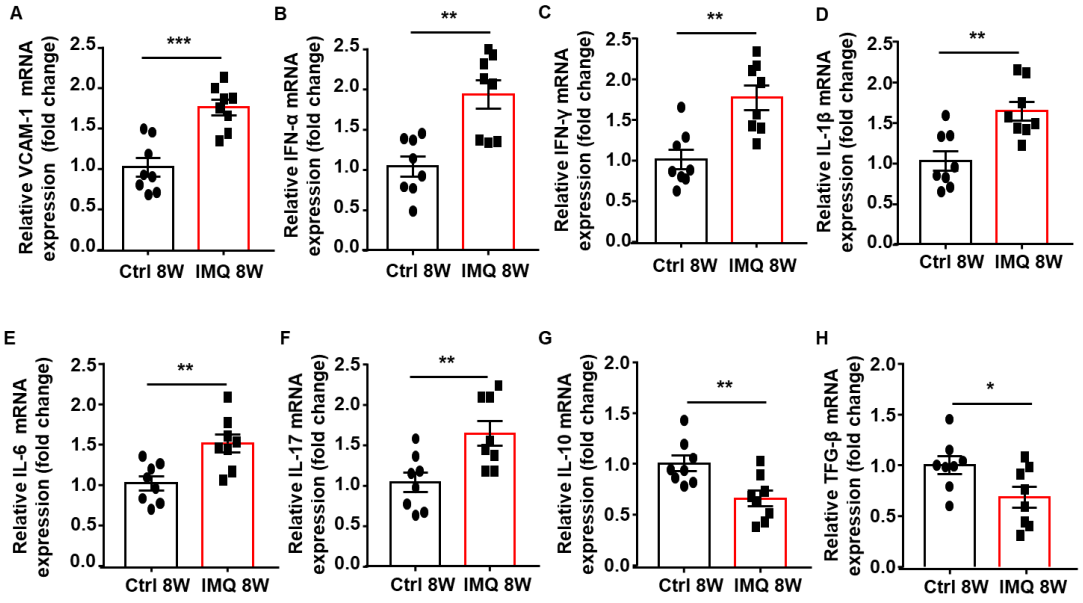

Figure 47. TLR-7 activation promotes a higher gene expression of vascular adhesion molecules and proinflammatory cytokines in aorta from imiquimod (IMQ)-treated mice. *(**A**) mRNA expression of vascular cell adhesion molecule-1*

*(VCAM-1), proinflammatory cytokines (**B**) IFN-α, (**C**) IFN-γ, (**D**) IL-1β, (**E**) IL-6 and (**F**) IL-17, and (**G**) anti-inflammatory cytokine IL-10 and (**H**) TFG-β in aorta homogenates from IMQ-treated mice at 8 weeks of treatment (8W). Experimental groups: Control (Ctrl) 8W (n=8), IMQ 8W (n=8). Values are represented as means ± SEM. *P<0.05, **P<0.01 and ***P<0.001 compared to the Ctrl group.*

4.4. Role of ROS in cardiovascular alterations induced by TLR-7 activation

Antioxidant treatment prevented the raise of SBP (**Figure 48A**), and the vascular remodelling, reducing M/L ratio, MT, and MCSA, and increasing LD in mesenteric arteries from IMQ-treated mice (**Figure 48B-F**). In addition, both the impaired endothelium-dependent relaxation to Ach (**Figure 48G**) and the higher NADPH oxidase activity (**Figure 48H**) found in aorta from IMQ-treated mice, were also improved by antioxidant treatment.

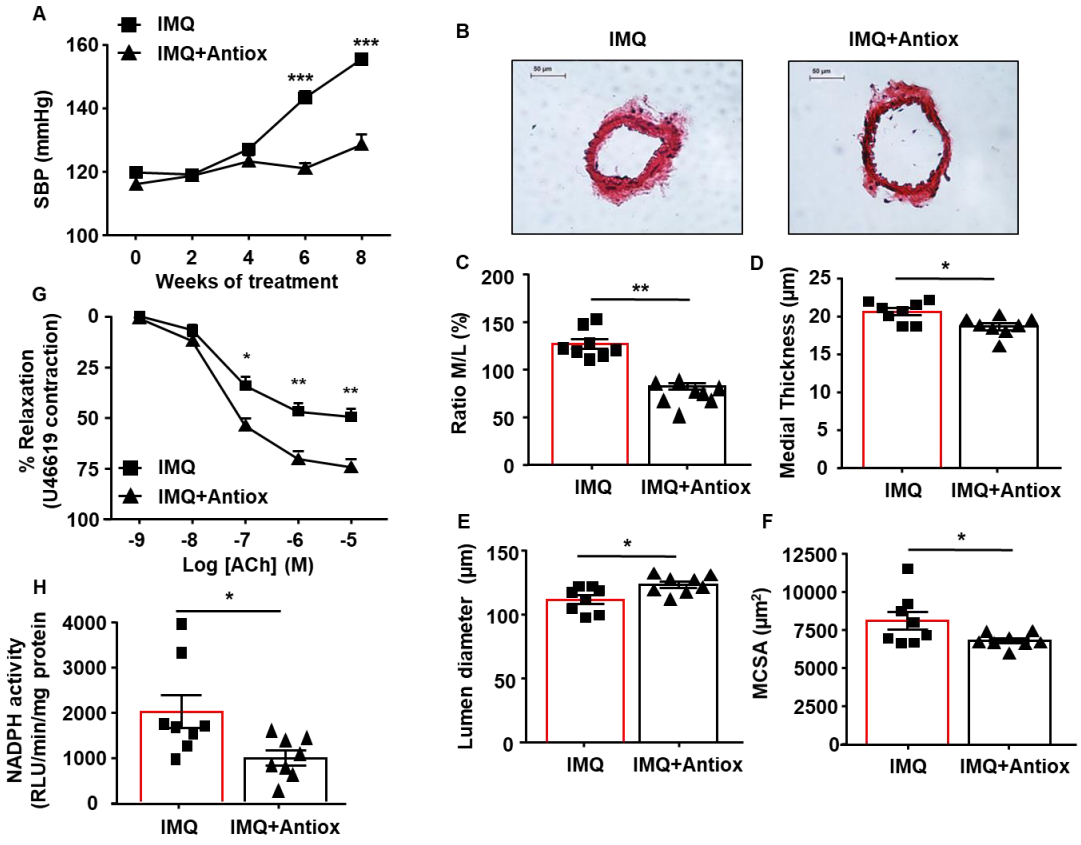

Figure 48. Antioxidant treatment prevents hypertension, vascular remodelling, endothelial dysfunction and increased NADPH oxidase activity induced by TLR-7 activation in imiquimod (IMQ)-treated mice. *Effects of chronic antioxidant (Antiox; tempol+apocynin) treatment on (**A**) time course of systolic blood pressure (SBP) measured by tail-cuff plethysmography, and structural modifications induced in superior mesenteric arteries: (**B**) Representative histological sections of paraffin-embedded tissues stained with hematoxylin-eosin, morphometric analysis of media:lumen ratio (M/L) (**C**), medial thickness (**D**), lumen diameter (**E**) and media cross-sectional area (MCSA) (**F**). Effects of chronic antioxidant (Antiox; tempol+apocynin) treatment on (**C**) vascular endothelium-dependent vasorelaxation induced by acetylcholine (ACh, 1nM–10µM) in endothelium-intact aortas precontracted using U46619 (10nM), and (**D**) NADPH oxidase activity measured by lucigenin-enhanced chemiluminescence in aorta from IMQ-treated mice. Experimental groups: IMQ (n=8) and IMQ+Antiox (n=8).. Values are represented as means ± SEM. *P<0.05, **P<0.01 and ***P<0.001 compared to the IMQ group.*

4.5. Involvement of IL-17 in hypertension and vascular dysfunction induced by TLR-7 activation

To further analyse the participation of IL-17 in the hypertensive effects of IMQ, we administered nIL-17a to hypertensive mice. Treatment of these mice with nIL-17 significantly reduced SBP (**Figure 49A**) as well as improved both aortic endothelium-dependent relaxation to acetylcholine (**Figure 49B**) and the activity of NADPH oxidase (**Figure 49C**).

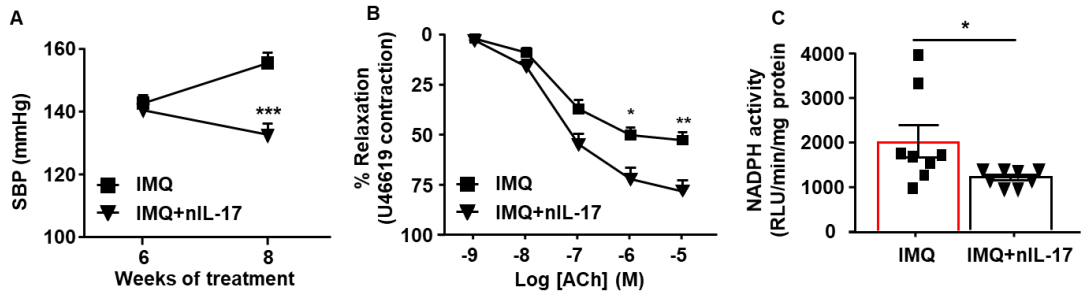

Figure 49. Role of IL-17a in hypertension, endothelial dysfunction and increased NADPH oxidase activity induced by TLR-7 activation in imiquimod (IMQ)-treated mice. *Effects of a neutralising agent against IL-17a (nIL-17) (10µg/mouse) or the isotype control (10µg/mouse, start of nIL-17 administration) on (**A**) time course of systolic blood pressure (SBP) measured by tail-cuff plethysmography, (**B**) vascular endothelium-dependent vasorelaxation induced by acetylcholine (ACh), (1nM–10µM) in endothelium-intact aortas precontracted using U46619 (10nM), and (**C**) NADPH oxidase activity measured by lucigenin-enhanced chemiluminescence in aorta from IMQ-treated mice. nIL-17antibody or the isotype control were intraperitoneally injected from the sixth week of imiquimod treatment every three days until the end of the experiment. Experimental groups: IMQ (n=8) and IMQ+nIL-17 (n=8). Values are represented as means ± SEM. *P<0.05, **P<0.01 and ***P<0.001 compared to the IMQ group.*

5. Probiotics prevent hypertension in a murine model of SLE induced by TLR-7 activation

5.1. Probiotics improve intestinal integrity without preventing gut dysbiosis in SLE mice

To investigate whether the overactivation of the TLR-7 pathway is linked to the presence of gut dysbiosis, we analysed faecal DNA isolated from all experimental mice groups. The composition of the bacterial communities was evaluated, calculating major ecological parameters, including Shannon's diversity, Simpson's, Chao's richness, Pielou's evenness, and the number of observed species. IMQ-treated animals display a significant reduction in α-diversity measured by the number of species, without significant changes in the other parameters. Probiotic treatments did not alter microbial richness, diversity, and evenness (**Figure 50A**). Similarly, when we studied the phyla composition, *Firmicutes* and *Bacteroidetes* were the most abundant phyla, and with smaller proportions of *Tenericutes*, *Cyanobacteria*, and *Proteobacteria* in mouse faeces. The proportion of bacteria from the phylum *Firmicutes* was significantly lower in IMQ than in Ctrl. Moreover, bacteria from the phylum *Bacteroidetes* were increased in the IMQ group. Probiotics tend to reduce *Bacteroidetes* and increase *Firmicutes* but these changes were not statistically significant (**Figure 50B, Table 11**). The F/B ratio, a marker of dysbiosis, tended ($P = 0.073$) to be lowered in IMQ mice, and was unchanged by LC40 and BFM treatments (**Figure 50C**). In addition, the short chain fatty acids (SCFAs) producing bacteria were also analysed. The level of acetate-producing bacteria was found elevated in the IMQ group, but neither of the probiotics restored it (**Figure 50D**).

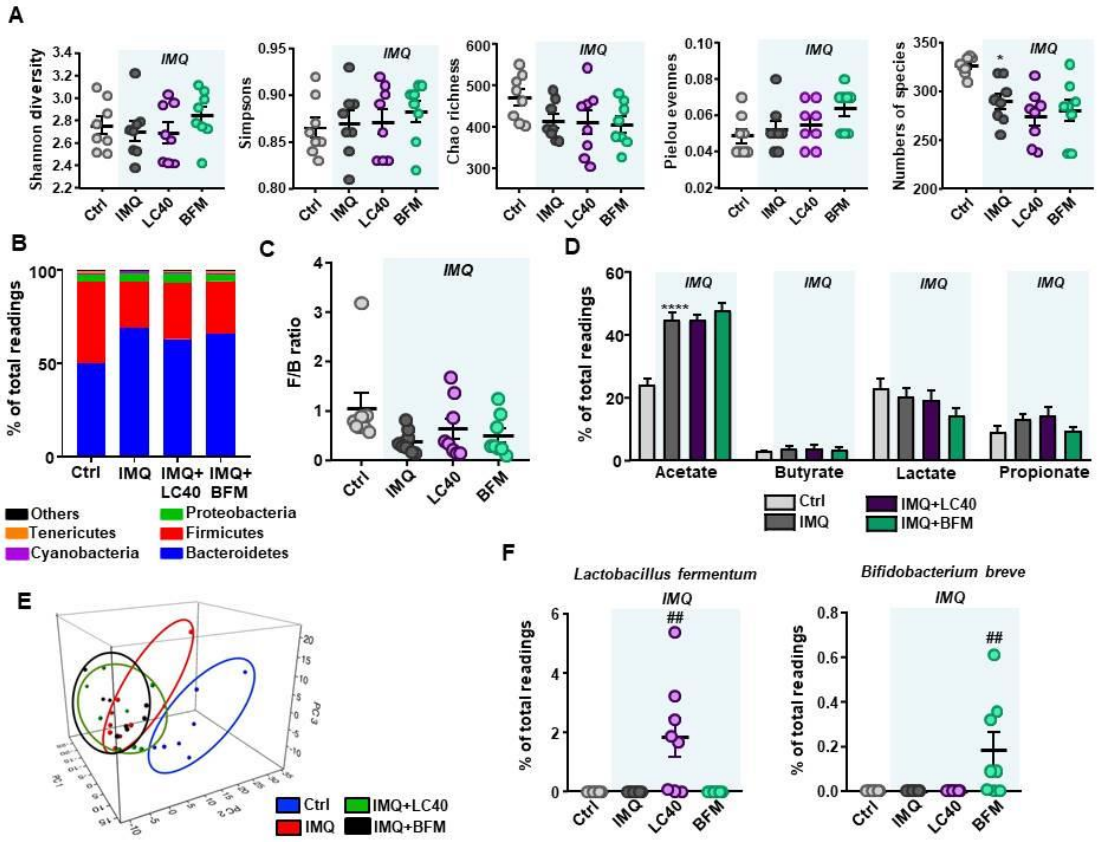

Figure 50. Effects of probiotic treatments on phyla changes in the microecological parameters and gut microbiota composition. *(**A**) Bacterial 16S ribosomal DNA were amplified and sequenced to evaluate faecal diversity, richness, evenness and numbers of species. (**B**)Phylum breakdown of the 6 most abundant bacterial communities in the faecal samples from all experimental groups. (**C**) The Firmicutes/Bacteroidetes (F/B) ratio was calculated as a biomarker of gut dysbiosis. (**D**) Relative proportions of acetate-, butyrate-, lactate-, and propionate-producing bacteria. (**E**) Principal coordinate analysis. (**F**) Bacterial species Lactobacillus fermentum and Bifidobacterium breve in the gut microbiota in control (Ctrl) and imiquimod (IMQ)-treated groups. Values are expressed as means ± SEM (n = 8). *P< 0.05 and ****P< 0.0001 compared to the Ctrl group; ##P< 0.01 compared to the untreated IMQ group. LC40, Lactobacillus fermentum CECT5716; BFM, Bifidobacterium breve CECT7263.*

Table 11. Phylum breakdown of the 6 most abundant bacterial communities in the fecal samples from all experimental groups.

	Tenericutes	*Cyanobacteria*	*Proteobacteria*	*Bacteroides*	*Firmicutes*	*Others*
Ctrl	**1.5±0.2**	**0.5±0.1**	**3.6±0.3**	**49.9±4.3**	**44.0±4.5**	**0.6±0.0**
IMQ	**0.3±0.1**	**1.0±0.1**	**4.4±0.3**	**69.0±3.9******	**24.9±3.9******	**0.5±0.1**
IMQ+LC40	**0.4±0.2**	**0.9±0.1**	**4.6±0.8**	**63.0±7.4**	**30.4±6.8**	**0.8±0.2**
IMQ+BFM	**0.9±0.4**	**0.7±0.1**	**3.7±0.3**	**66.0±5.9**	**28.0±5.5**	**0.7±0.1**

*Ctrl, control; IMQ, imiquimod; LC40, Lactobacillus fermentum CECT5716; BFM, Bifidobacterium breve CECT7263. Values are expressed as means ± SEM (n = 8). ****P< 0.0001 compared with the control (Ctrl) group.*

The three-dimensional principal component analysis of the bacterial taxa in faecal samples showed perfect clustering among groups (Ctrl and IMQ). The clusters corresponding to LC40 and BFM were more similar to IMQ (**Figure 50E**). **Figure 51** shows the bacterial taxa (class, order, family, and genus) that were altered by TLR-7 activation, according to our LEfSe analysis. Prominent changes in bacterial taxa occurred at the end of the treatment, where the relative abundance of 29 taxa was increased (green) and 69 taxa were decreased (red), when compared with the control group. All of these shifts in microbiota composition were still present in both probiotic-treated groups. In fact, when studying the graphical analysis of beta-diversity through the PCA, we observed that, while there was a great difference between the Ctrl and IMQ groups, IMQ-LC40 and IMQ-BFM mostly overlapped with IMQ (**Figure 50E**). Despite probiotics seeming unable to prevent or reverse the changes experimented by the IMQ microbiota, LC40 and BFM were detected in the faecal samples of animals treated respectively, demonstrating that both microorganisms were able to colonise their respective hosts (**Figure 50F**).

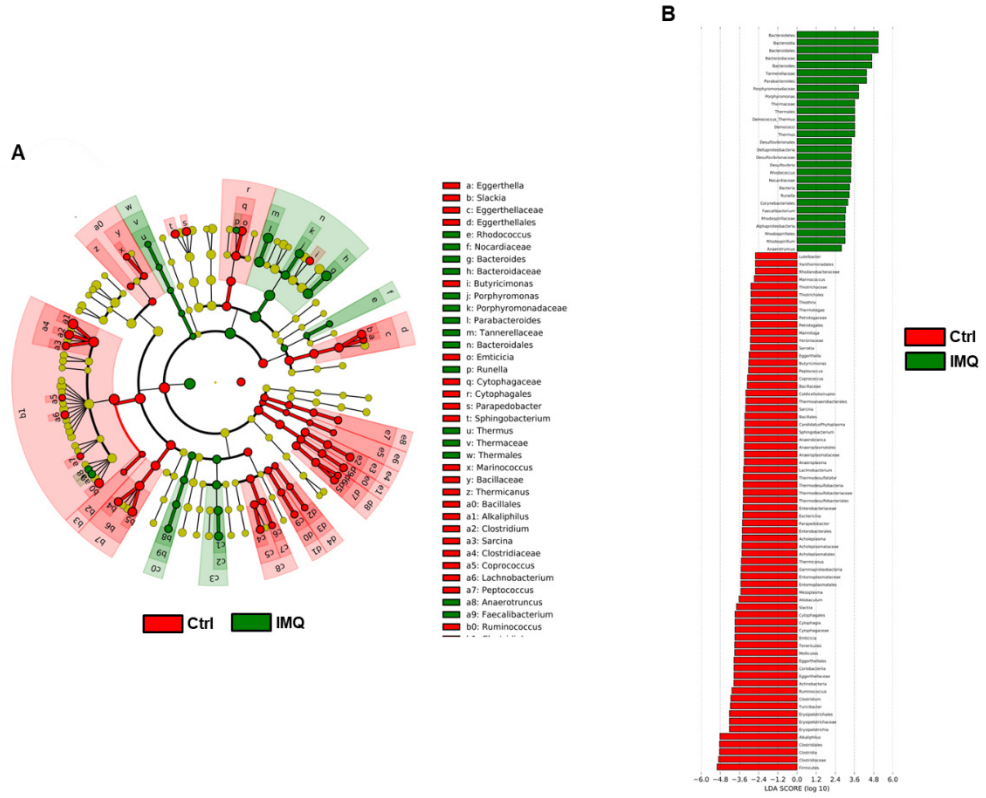

Figure 51. Effects of probiotic treatments on changes in the gut microbiota composition. *(**A**) Comparisons of microbiome changes in control (Ctrl) versus imiquimod (IMQ) mice. (**B**) Linear discriminant analysis effects size (LEfSe) identified significantly different bacterial taxa enriched in each cohort at LDA Score > 2, p<0.05 (red bars Ctrl enriched, green bars IMQ enriched,. Cladograms show the significantly enriched taxa, the taxa are identified in the key to the right of each pane. Larger the circles greater the difference in abundance between the groups. n =8 mice per treatment group in each comparison.*

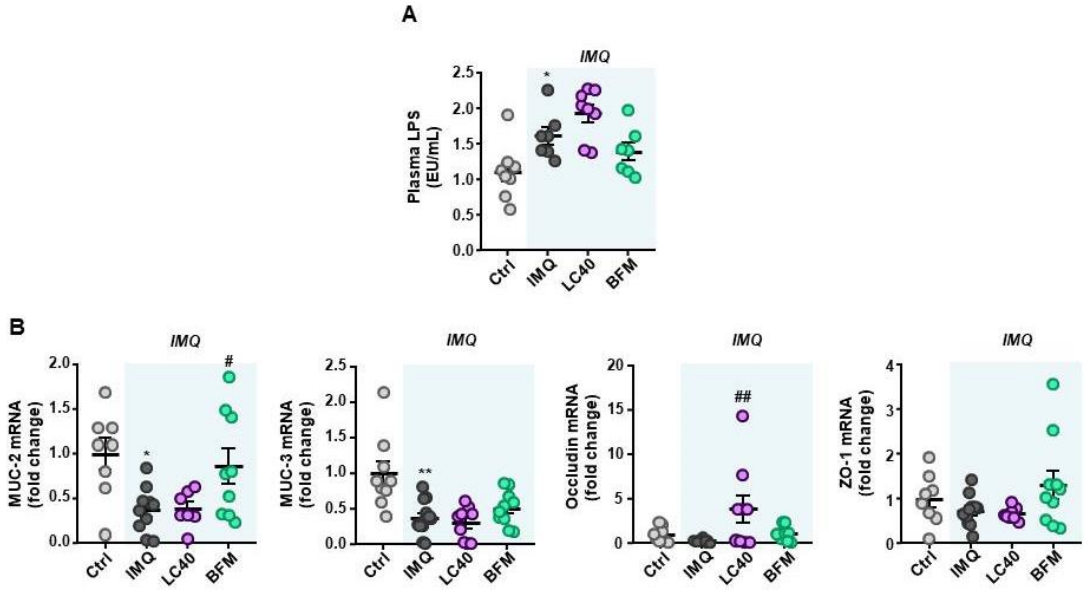

Figure 52. Effects of probiotic treatments on epithelial integrity markers. *(**A**) Plasma endotoxin concentrations (EU/mL, endotoxin units/mL. (**B**) Colonic mRNA levels of mucin (MUC)-2, MUC-3, Occludin, and zonula occludens protein (ZO)-1 in control (Ctrl) and imiquimod (IMQ)-treated groups. Values are expressed as means ± SEM (n = 8-12). *P< 0.05 and **P< 0.01 compared to the Ctrl group; #P< 0.05 and ##P< 0.01 compared to the untreated IMQ group. LC40, Lactobacillus fermentum CECT5716; BFM, Bifidobacterium breve CECT7263.*

On the other hand, we measured endotoxin levels in plasma, and found them to be significantly higher in IMQ mice compared with the control group. However, the long-term treatment with both probiotics was unable to prevent endotoxemia in the IMQ group (**Figure 52A**). These results suggest that intestinal permeability is increased in this induced mouse model of lupus and allow bacterial components (e.g., LPS) to enter the blood stream. Because of this, we tested the integrity of the gut barrier and we found that the treatment with LC40 significantly increased the colonic mRNA expression of barrier-forming junction transcripts (occludin), whereas BFM increased mucin-2 (MUC-2) (**Figure 52B**).

5.2. Probiotics attenuate lupus disease activity and modulate the immune response

We measured lupus disease activity by plasma levels of autoantibodies and we found they significantly increase in IMQ mice compared with control group (**Figure 53A**), as previously reported (Yokogawa *et al*., 2014; Liu *et al*., 2018;). Both LC40 and BMF significantly reduced the levels of anti-dsDNA antibodies in IMQ mice. As expected, we found a marked splenomegaly in IMQ-treated mice (**Table 12**), which was associated with autoimmune disease progression (Wofsy *et al*., 1988). Besides, we observed in the IMQ group localized signs of inflammation, such as hepatomegaly, or a reduced colon weight/colon length ratio indicating an immune response in this direction (**Table 12**). Neither LC40 nor BFM were able to prevent this. SLE is a prototypical autoimmune disease characterized by a type I IFN signature (Crow. *et al*., 2014). In fact, higher plasma levels of IFN-α were found in IMQ mice when compared with control. Probiotic treatments were unable to change this parameter (**Figure 53B**).

Table 12. Morphological parameters of all experimental groups.

Variables	Ctrl (n = 8)	IMQ (n = 12)	IMQ LC40 (n = 9)	IMQ BFM26 (n = 10)
BW (g)	21.45± 0.4	20.68± 0.6	19.51 ± 2.3	21.08 ± 0.7
HW/TL (mg/cm)	5.39 ± 0.2	5.40 ± 0.2	5.37 ± 0.1	5.43± 0.1
LVW/TL (mg/cm)	3.66 ± 0.1	3.59± 0.1	3.52 ± 0.2	3.53 ± 0.1
KW/TL (mg/cm)	6.1 ± 0.2	7.34 ± 0.2**	6.98 ± 0.1	6.77 ± 0.4
LW/TL (mg/cm)	53.77 ± 2.4	61.34 ± 4.2	67.58 ± 4.4	66.21 ± 3.7
SW/TL (mg/cm)	4.37 ± 0.4	25.35 ± 2.3**	30.77 ± 2.2	22.14 ± 3.5
CW/CL (mg/cm)	21.53 ± 1.1	16.94 ± 0.07**	17.34 ± 0.9	17.14 ± 0.9

*BW, Body weight; HW, Heart weight; KW, IMQ, imiquimod; Kidney weight; LVW, Left ventricular weight; LW, Liver weight; SW, Spleen weight; TL, Tibia length; CW, Colon weight; CL, Colon length. Values are shown as mean ± SEM. All parameters were assessed in mice treated with vehicle or Lactobacillus fermentum CECT5716 (LC40) or Bifidobacterium breve CECT7263 (BFM). **P < 0.01 compared to the control (Ctrl) group.*

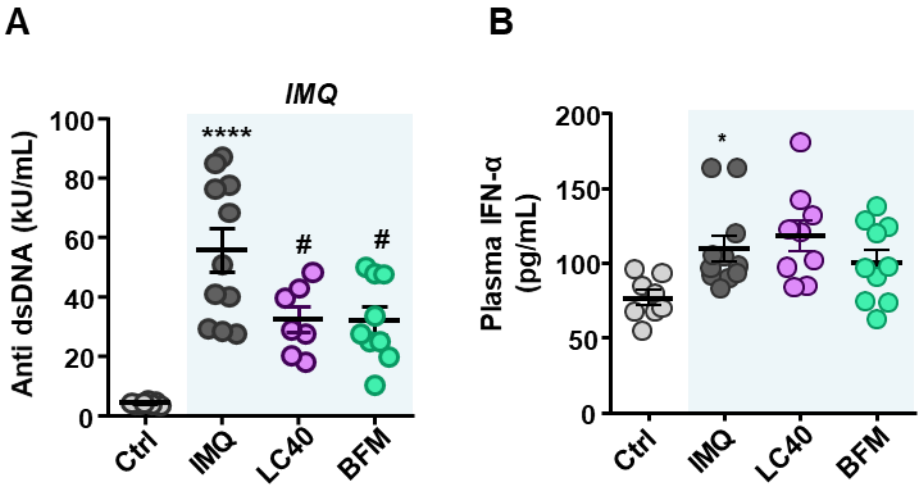

Figure 53. Effects of probiotic treatments on systemic lupus erythematosus activity. ***(A)*** *Circulating anti-double-stranded DNA autoantibodies (presented as antibody activity index; and interferon (IFN)-α plasma levels measured by ELISA in control (Ctrl) and imiquimod (IMQ)-treated groups. Values are expressed as means ± SEM (n = 8-12). *P< 0.05and ****P< 0.0001 compared to the Ctrl group; #P< 0.05 compared to the untreated IMQ group. LC40, Lactobacillus fermentum CECT5716; BFM, Bifidobacterium breve CECT7263.*

TLR-7 activation is associated with an imbalance of T cells and increased B cells, as seen in the previous experiment. In order to determine the immunomodulatory actions of the probiotics, we measured the levels of B and T cells in spleen and MLNs from all experimental groups. The percentage of T cells was higher in both organs from IMQ mice than in those of the control group (**Figure 54A, B**). Splenic B cells levels were significantly decreased with probiotics in the IMQ group (**Figure 54A**). As expected, the percentages of Th17 cells were increased in both organs from IMQ mice (**Figures 55 and 56**), while Th1 cells were also increased in spleens from IMQ group (**Figure 56**). On the other hand, IMQ treatment led to a reduction in the percentage of Treg cells in MLNs (**Figure 55**) and spleens (**Figure 56**). Again, both probiotics reduced Th17 in MLNs, however, only in the LC40-treated group Treg were elevated (**Figure 55**). No significant effects of both probiotics were found in the population of Treg, Th17 and Th1 in spleen (**Figure 56**).

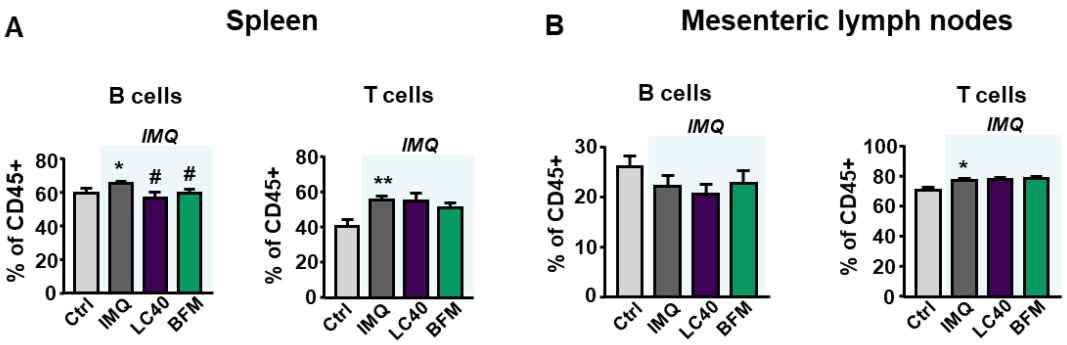

Figure 54. Effects of probiotic treatments on percentage of B and Tcells in spleen and mesenteric lymph nodes. *(**A**) Total B and T lymphocytes in spleen and (**B**) mesenteric lymphoid nodes in the control (Ctrl) and imiquimod (IMQ)-treated groups. Values are expressed as mean ± SEM (n = 8-12). *P< 0.05 and **P< 0.01 compared to the Ctrl group. #P< 0.05 compared to the untreated IMQ group LC40, Lactobacillus fermentum CECT5716; BFM, Bifidobacterium breve CECT7263.*

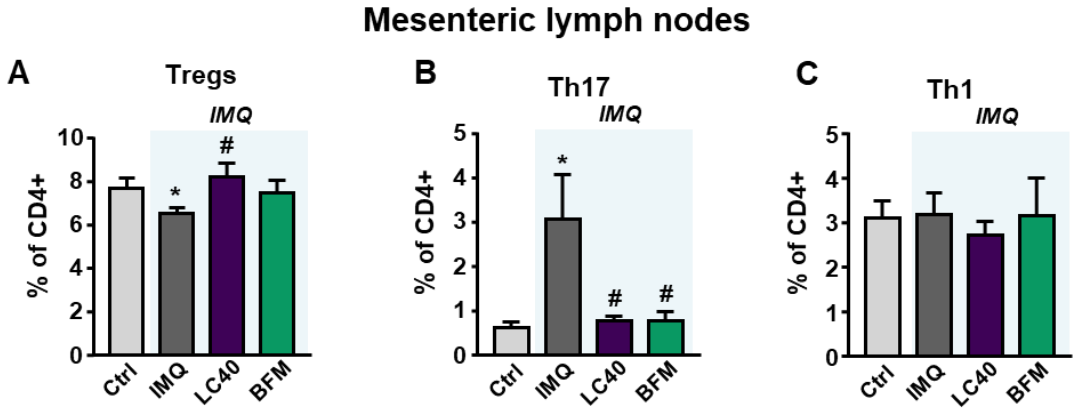

Figure 55. Effects of probiotic treatments on T-cell polarization in mesenteric lymph nodes. *(**A**) Regulatory T(reg), (**B**) T helper (h) 17, and (**C**) Th1 cells measured in mesenteric lymphoid nodes in the control (Ctrl) and imiquimod (IMQ)-treaded groups. Values are expressed as mean ± SEM (n = 8-12). *P< 0.05 compared to the Ctrl group; #P< 0.05 compared to the untreated IMQ group. LC40, Lactobacillus fermentum CECT5716; BFM, Bifidobacterium breve CECT7263.*

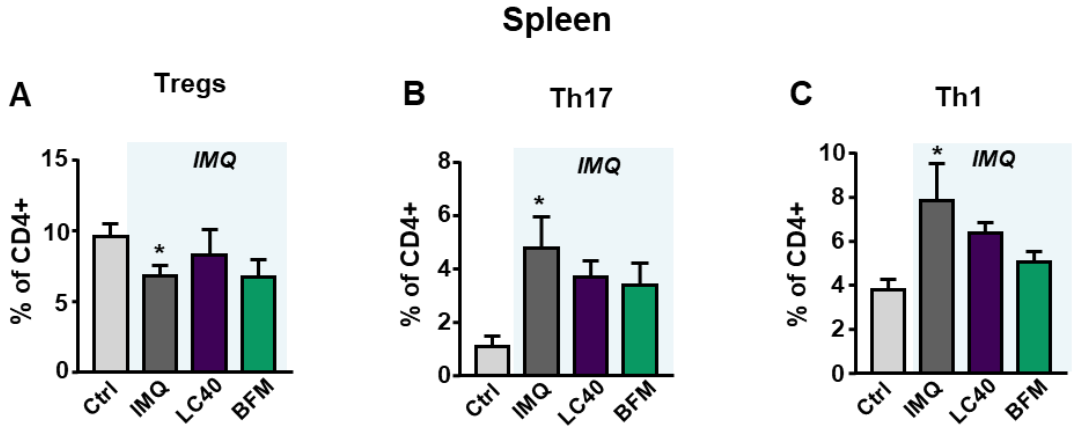

Figure 56. Effects of probiotic treatments on T cell polarization in spleens. *(**A**) Regulatory T(reg), (**B**) T helper (h) 17, and (**C**) Th1 cells measured in spleens in the control (Ctrl) and imiquimod (IMQ)-treated groups. Vaues are expressed as mean ± SEM (n = 8-12). *P< 0.05 compared to the Ctrl group. LC40, Lactobacillus fermentum CECT5716; BFM, Bifidobacterium breve CECT7263.*

5.3. Probiotics prevent endothelial dysfunction, oxidative stress and hypertension

The treatment of IMQ mice with both probiotics showed an increase in the acetylcholine-induced vasorelaxation when compared with the IMQ group (**Figure 57A**). In all experimental groups, the acetylcholine-induced relaxation was fully inhibited by the eNOS inhibitor L-NAME (**Figure 58A**), showing that this vessel relaxation induced by acetylcholine was completely dependent on NO derived from endothelium. In addition, the endothelium-independent vasodilator responses to nitroprusside, which directly activates soluble guanylyl cyclase in vascular smooth muscle, were not different among groups (**Figure 58B**), showing no change in the signalling of NO in the vascular smooth muscle. Moreover, no significant changes in eNOS gene expression in aorta from all experimental groups were observed (**Figure 58C**).

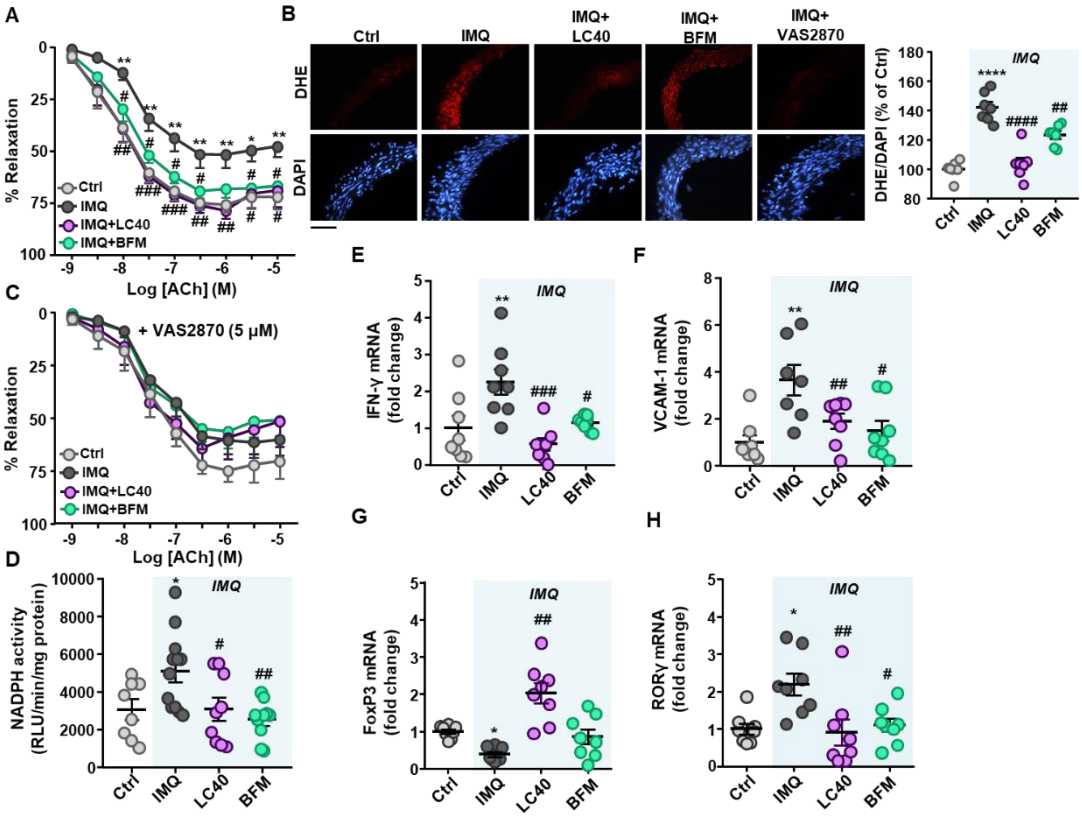

Figure 57. Effects of probiotic treatments on endothelial function and vascular oxidative stress-inflammation. *(**A**) Vascular relaxant responses induced by acetylcholine (Ach), in endothelium-intact aortae pre-contracted by U46619 (10 nM) in the absence and (**C**) in the presence of the specific NADPH oxidase inhibitor VAS2870 (5 µM) in control (Ctrl) and imiquimod (IMQ)-treated groups. (**B**) Top pictures show arteries incubated in the presence of dihydroethidium (DHE), which produces a red fluorescence when oxidised to ethidium by ROS. Bottom pictures show blue fluorescence of the nuclear stain 4,6-diamidino-2-phenylindole dichlorohydrate (DAPI; x 400 magnification). Averaged values, mean ± SEM (n= 6-9 rings from different mice) of the red ethidium fluorescence normalized to the blue DAPI fluorescence. (**D**) NADPH oxidase activity measured by lucigenin-enhanced chemiluminescence. Aortic expression of (**E**) pro-inflammatory cytokine, interferon (IFN)-γ, (**F**) vascular cell adhesion molecule-1 (VCAM-1), (**G**) Forkhead box P3 (FoxP3) and (**H**) the RAR-related orphan receptor gamma (RORγ) at the level of mRNA by RT-PCR. Values are expressed as means ± SEM (n = 8-12). *P< 0.05, **P< 0.01and ****P< 0.0001 compared to the Ctrl group. #P< 0.05, ##P< 0.01, ###P< 0.001 and ####P< 0.0001 compared to the untreated IMQ group. LC40, Lactobacillus fermentum CECT5716; BFM, Bifidobacterium breve CECT7263.*

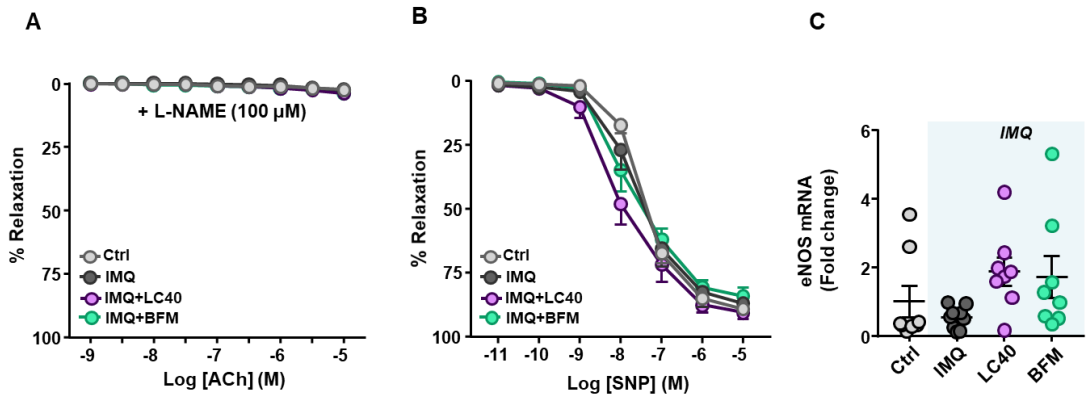

Figure 58. Effects of probiotic treatments on vascular nitric oxide pathway. (A) *Vascular relaxant responses induced by acetylcholine (ACh), in endothelium-intact aortae pre-contracted by U46619 (10 nM) in the presence of NG-nitro-L-arginine methyl (L-NAME. (**B**) Endothelium-independent vasodilator responses to sodium nitroprusside (SNP in endothelium-denuded aorta pre-contracted by U46619 (10 nM) in control (Ctrl) and imiquimod (IMQ)-treated groups. (**C**) eNOS expression levels of mRNA measured by RT-PCR. Values are expressed as means ± SEM (n = 6-9). LC40, Lactobacillus fermentum CECT5716; BFM, Bifidobacterium breve CECT7263.*

Since, as seen before, ROS production from the NADPH oxidase is a crucial element in endothelial dysfunction in IMQ-treated mice, both ethidium red fluorescence and NADPH oxidase activity were analysed in aorta from all experimental groups. Positive red nuclei were observed in adventitial, medial and endothelial cells from sections of aorta incubated with DHE (**Figure 57B**). Aortic rings from the IMQ group showed a marked staining in adventitial, medial and endothelial cells, which was higher than in control mice, which was almost suppressed by the selective NADPH oxidase inhibitor VAS2870. These effects were prevented by the LC40 and BFM treatments (**Figure 57B**). On the other hand, we tested endothelium-dependent relaxation to acetylcholine in the presence of VAS2870. No significant differences among groups were observed after incubation with VAS2870, showing the critical role of increased NADPH oxidase in the endothelial dysfunction found in aorta from IMQ-treated mice (**Figure 57C**). In addition, NADPH oxidase activity was increased in aortic rings from lupus mice when compared with control mice. Chronic administration of both probiotics reduced significantly the increased NADPH oxidase activity in IMQ mice (**Figure 57D**).

To determine whether proinflammatory cytokines play a key role in the pathogenesis of vascular remodelling and endothelial dysfunction in SLE, we measured the mRNA level of proinflammatory cytokines and vascular adhesion molecules and in aorta from all experimental groups. Again, both probiotics reduced the expression of IFN-γ (cytokines released by Th1) (**Figure 57E**) and the vascular cell adhesion molecule-1 (VCAM-1) (**Figure 57F**), which were found elevated in the IMQ model. In addition, we also analysed the transcript levels of transcription factors, such as RORγ and FoxP3, which induce the maturation of Th17 and Tregs populations, respectively. The mRNA levels of these transcription factors in lymphocytes were measured as indirect markers of Treg and Th17 cells. FoxP3 and RORγ mRNA levels were reduced and increased, respectively, in IMQ group, and LC40 administration increased the levels of Treg found in aorta from IMQ group (**Figure 57G**), whereas both LC40 and BFM reduced Th17 infiltration in aorta (**Figure 57H**).

Finally, analysing the evolution of SBP, we observed the already stablished hypertension in the IMQ group, which was prevented by both probiotics (**Figure 59**). Anatomical analysis revealed that a kidney weight/tibia length index was higher in IMQ-treated mice than in control mice. However, long-term administration of probiotics was without effect on renal hypertrophy found in IMQ mice (**Table12**).

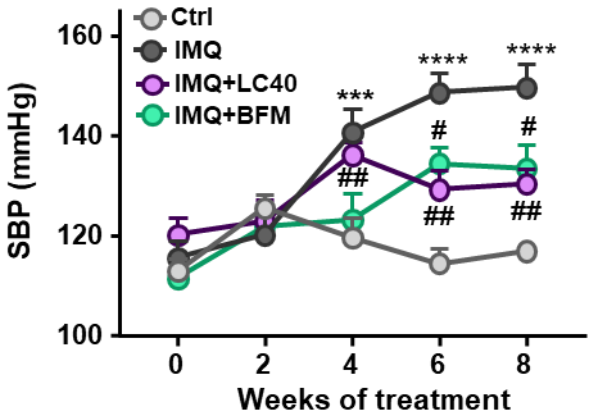

Figure 59. Effects of the probiotics on the evolution of blood pressure. *Systolic blood pressure (SBP) was measured by tail-cuff plethysmography in control (Ctrl) and imiquimod (IMQ)-treated groups. Values are expressed as means ± SEM (n = 8-12). ***P< 0.001 and ****P< 0.0001 compared to the Ctrl group. #P< 0.05 and ##P< 0.01compared to the untreated IMQ group. LC40, Lactobacillus fermentum CECT5716; BFM, Bifidobacterium breve CECT7263.*

DISCUSSION

DISCUSSION

1. Gut microbiota is involved in the development of hypertension in a mouse model of systemic lupus erythematosus

Interactions of gut microbiota and host genetics play important roles in the development of autoimmune diseases, such as SLE. We have demonstrated for the first time that gut microbiota is involved in the regulation of endothelial function and BP in female NZBW/F1 mice. This is mainly supported by the improvement of endothelial dysfunction, vascular oxidative stress, and the inhibition of SBP increase induced by an important reduction of faecal biomass induced by chronic vancomycin or MIX treatments. In addition, morphological alterations of target organs of hypertension, such as left ventricle or kidney, was also prevented.

Previous studies have described that the oral administration of antibiotics ameliorates BP in angiotensin II-induced hypertension and in spontaneously hypertensive rats (Yang *et al*., 2015), and a treatment based on the combination of antibiotics was able to reduce the blood pressure in a resistant hypertensive patient (Qi *et al*., 2015). However, a quadruple antibiotic treatment increased BP of healthy rats (Yan *et al*., 2020). These data indicated that the effect of antibiotics on BP should be closely related to the composition of intestinal flora. In the present Thesis, MIX or vancomycin administered to mice with genetic background of SLE prevented in the same extension the raise of BP, suggesting that vancomycin-sensitive bacteria were the main responsible for blood pressure increase. It is interesting to note that the PCA of gut microbiota, as assessed by 16S rRNA sequencing of the V3-V4 region of gut microbiota, from normotensive (at 26 weeks of age) NZBW/F1 mice and control mice showed clear differences in the microbial communities, suggesting that these changes could be involved in the increased protein excretion found in SLE mice at 26 weeks. This dysbiotic microbiota, characterized by an increased F/B ratio, might induce changes in the host addressed to start the increase in BP. In contrast to genetic

hypertension, such as spontaneously hypertensive rats (Yang *et al*., 2015; Robles-Vera *et al*., 2020a, b), and human hypertension (Yang *et al*., 2015; Li *et al*., 2017), the dynamics of gut microbiota during the development of hypertension associated with lupus progression in female NZBW/F1 mice was characterized by no significant changes in ecological parameters (ex., lower Simpson's diversity), in the F/B ratio, and in the proportion in SCFA-producing bacteria. SCFA are among the main classes of bacterial metabolic products involved in the bacteria and host interaction, to regulate BP (Pluznick *et al*., 2013). However, no significant differences were observed in acetate-, butyrate-, or propionate-producing bacteria populations between gut microbiota from control and SLE mice (not shown), suggesting that these SCFAs are not involved in the initiation of hypertension. However, increased percentage of vancomycin-sensitive bacteria, such as *Parabacteroides*, *Pedobacter*, *Olivibacter* and *Clostridium* were positively linked to in high blood pressure in SLE mice. Surprisingly, *Clostridium* correlates negatively with blood pressure in chinese patients (Zeng. *et al*., 2019), and suppresses systemic inflammatory responses. (Van den Abbeele *et al*., 2013). However, *Clostridium* XI and *Clostridium* XIVa express the bacterial enzyme baiE (Ridlon *et al*., 2006), involved in 7-α-dehydroxylation of taurocholic acid and cholic acid to the production of inflammatory bile acids (taurodeoxycholic acid and deoxycholic acid), which have been implicated in the impaired glucose metabolisms in mice on a high fat diet (Fujisaka *et a*l., 2016). Moreover, bile acid metabolites control Th17 and Treg cell differentiation (Hang *et al*., 2019), which have been described to be involved in BP regulation. Meanwhile, *Parabacteroides* produced metabolites to promote Treg cells generation (Arpaia *et al*., 2013), which is in agreement with our results in MLNs and spleen. Interestingly, vancomycin increased *Lactobacillaceae* and *Lactobacillus* proportion in faeces, as compared to untreated-SLE. *Lactobacillus* spp. could inhibit inflammation and decrease BP through its indole metabolites, which reduced the Th17 population in gut lymphoid organs (Wilck *et at*., 2017). However, we did not measure the contents of indole metabolites in faeces. Furthermore, in faeces from hypertensive SLE the proportion of *Lactobacillus* was similar to normotensive control, and MIX treatment did not change it, despite reduced BP. This suggests that the effect of the gut microbiota on SLE hypertension is not the consequence of the

change in the proportion of specific bacteria, but rather to a positive effect on the whole microbiota.

The transplantation of intestinal microbiota from hypertensive SLE mice to recipient normotensive mice without genetic background of SLE disturbs the intestinal microbiota balance, possibly increasing the harmful bacteria with prohypertensive effect, resulting in BP elevation. These results implied that the abnormal gut microbiota plays a key role in the development of hypertension and are one of the causes of SLE hypertension, rather than being the result and accompanying phenomena of lupus progression. However, the harmful bacteria involved in BP elevation were not evaluated in the present study, because we did not analyse the composition of gut microbiota after the FMT.

Several studies using female NZBW/F1 mice have demonstrated that multiple factors contribute to the pathogenesis of hypertension, including the inflammatory cytokines, and oxidative stress, as well as B-cell hyperactivity and autoantibody production (Taylor and Ryan, 2017). These mediators, that contribute to local inflammation and the subsequent renal and vascular dysfunction, are likely downstream of the initial immune system dysregulation. In agreement with this data, we found in hypertensive SLE mice increased plasma levels of proinflammatory cytokines (IL-6, IL-17a, and IFN-γ), vascular oxidative stress, increased circulating B, and plasma anti-ds-DNA. Interestingly, both vancomycin and MIX reduced plasma levels of these cytokines and vascular ROS content, involving these mediators in the pro-hypertensive effects of microbiota in SLE mice. In our experiments, B cell populations were higher in MLNs and spleen in SLE mice as compared to control, but neither vancomycin nor MIX treatments reduced B cell generation and circulating B cells, ruling out the involvement of B cells in the blood pressure regulation induced by microbiota. Furthermore, stool transplantation from SLE mice to control mice did increase the proportion of B cells in MLNs. A direct role of autoantibodies in humans was shown in patients with refractory hypertension, in which immunoadsorption of autoantibodies to the α1-adrenergic receptor was sufficient to lower mean arterial pressure (Wenzel *et al.*, 2008). Anti-ds-DNA production is regulated by microbiota in

female NZBW/F1 mice, since we showed that the MIX treatment reduced plasma level of this autoantibody. However, in the present study the pathogenic role of anti-ds-DNA, as mediator of BP increase induced by microbiota, was not sufficiently supported. First, vancomycin reduced faecal mass and BP but did not modified plasma anti-ds-DNA. Second, stool transplantation from hypertensive mice to control increased BP but did not increased circulating anti-ds-DNA. It is interesting to note that mortality, lupus-related autoantibodies, and autoimmune manifestations were relieved in (NZW x BXSB)F1 hybrid mice after oral administration of vancomycin, due to reduced translocation of a gut pathobiont, *Enterococcus gallinarum*, to the liver and other systemic tissues to trigger an autoimmune response (Manfredo-Viera *et al*., 2018). However, we did not find any differences in *E. gallinarum* contents in faeces among all experimental groups, and no translocations to the liver were detected by PCR analysis in untreated SLE mice (not shown). In addition, the antibiotic treatment given after disease onset in MRL/lpr mice ameliorated lupus-like symptoms, reducing the size of lymphoid organs, decreasing the level of circulating autoantibodies, and attenuating lupus nephritis (Mu. *et al*., 2017b). These data suggest that different genetic backgrounds predispose to autoimmunity in different lupus-prone mice.

Hypertension is often associated with impaired endothelial function, but whether this is causative in the progression of hypertension is difficult to prove. Recently, we have shown an impaired aortic endothelium-dependent relaxation response to acetylcholine in NZBW/F1 mice (Gómez-Guzmán *et al*., 2014; Romero *et al*., 2017) and a reduction in NO production induced by plasma from SLE patients with active nephritis in human endothelial cells (Toral *et al*., 2017). Increased NADPH oxidase-driven ROS production has been involved in both endothelial dysfunction and the raise of blood pressure in female NZBW/F1 mice (Gómez-Guzmán *et al*., 2014). Agreeing with this information, in the present study we also found reduced acetylcholine induced relaxation and increased NADPH oxidase activity in aorta from hypertensive SLE mice as compared to normotensive control mice. Interestingly, chronic antibiotic treatments prevented the altered responses to acetylcholine and the higher NADPH oxidase activity, involving gut microbiota in oxidative stress and endothelial function regulation.

Additionally, stool transfer of dysbiotic microbiota from SLE to control mice impaired acetylcholine relaxation and increased NADPH oxidase activity. NADPH oxidase-driven ROS production is a key event in endothelial dysfunction induced by dysbiotic microbiota because incubation with the selective NADPH oxidase inhibitor VAS2870 suppressed the impairment of aortic endothelium-dependent relaxation to acetylcholine. Circulating pro-inflammatory cytokines or those produced locally in vascular tissues, as consequence of inflammatory cells infiltration, regulate NADPH oxidase activity (Kelleyand Wüthrich, 1999; Ryan, 2013). Antibiotic treatments reduced Th17 differentiation in MLNs, circulating Th17, and Th17 infiltration in aorta. The pro-inflammatory cytokine IL-17 causes Rho-kinase-mediated endothelial dysfunction in the vascular wall by increasing ROS generation by NADPH oxidase activation (Dhillion *et al*., 2012). In fact, the Rho-kinase inhibitor Y27632 restored acetylcholine relaxation to levels similar to those induced by the antibiotic, suggesting that IL-17-Rho-kinase-pathway is controlled by gut microbiota in NZBW/F1 mice. In agreement with this, FMT from SLE to control mice increased Th17 populations in MLNs, and Th17 infiltration in aorta. Moreover, the IL-17 neutralization improved acetylcholine relaxation in control mice with SLE microbiota, showing that regulation of naïve T cells differentiation towards Th17 in secondary lymph organs at the gut, with the subsequent Th17 infiltration in vascular tissues is a key mechanism in the endothelial dysfunction induced by SLE microbiota. However, if these changes in T cells polarization were related to changes in bile acids profile or indole metabolites induced by gut microbiota are unknown.

In the vasculature, the activation of TLR-4 by the bacterial products, such as LPS, results in increased NADPH oxidase dependent O_2^- production and inflammation (Liang *et al*., 2013). We also found higher circulating levels of LPS in SLE mice, despite no change in the capacity of gut microbiome to synthetize and export LPS and no increased gut permeability. Paradoxically, vancomycin, which reduced gut permeability, or MIX, which inhibited the synthesis and export of LPS, were unable to reduce endotoxemia. This data could be related to the increased relative abundance of LPS-containing Gram-negative bacteria (*Proteobacteria*), induced by vancomycin and MIX

treatments. Further studies are required to explain endotoxemia regulation in SLE mice. Interestingly, our results suggest that higher plasma LPS levels are not a key event in endothelial dysfunction and blood pressure regulation induced by dysbiotic microbiota in NZBW/F1 mice.

2. *Lactobacillus fermentum* CECT5716 is a novel alternative for the prevention of vascular disorders in a genetic mouse model of systemic lupus erythematosus

We have demonstrated for the first time that chronic oral administration of the probiotic LC40 can improve the cardiovascular complications occurring in an experimental model of SLE with hypertension. The protective effects of LC40 are the following: (a) a markedly attenuated lupus disease progression as evidenced by a decrease in splenomegaly, B cells accumulation, and plasma anti-dsDNA; (b) a significant decrease in SBP and heart and kidney hypertrophy; (c) a restoration of endothelial function associated with lower vascular Th17 infiltration; and (d) an improvement in gut dysbiosis linked to increased colonic integrity and reduced endotoxemia. Herein, we suggest the important role of gut microbiota manipulation in preventing cardiovascular alterations associated with SLE.

Our results in gut microbiota composition are consistent with the relative higher abundance of a group of Lactobacilli found in the gut microbiota of NZBW/F1 mice associated with deteriorated disease (Luo *et al*., 2018). However, these authors did not compare the faecal microbiota between NZBW/F1 mice and a control mouse strain. In our experimental conditions, LC40 treatment increased significantly *Bifidobacterium* and *Parabacteroides*, and reduced significantly *Lachnospira* and *Blautia*. Importantly, treatments improving lupus symptoms in lupus lpr mice restored gut colonization of *Lactobacillus* spp. and decreased that of *Lachnospiraceae* (Mu. *et al*., 2017a, 2017b).

In lpr mice a leaky gut has been described (Mu *et al*., 2017a), characterized by decreased expression of tight junction proteins, increased permeability and increased

plasma LPS levels. LPS accelerates lupus progression in several lupus-prone mouse models, including NZBW/F1 mice, enhancing polyclonal B-cell activation, plasma anti-dsDNA antibodies, and renal failure (Cavallo and Granholm, 1990; Granholm and Cavallo, 1994). A leaky gut may allow the translocation of Gram-negative bacteria across the intestinal epithelium, leading to an increase in LPS, a cell wall component of Gram-negative bacteria, into the circulation. Our data showed that the intestinal epithelium is compromised in lupus mice and that LC40 treatment can restore mucosal barrier integrity. In addition, the effect of LC40 on gut barrier function may also be attributed to the increase of MUC-2, a mucin protein that functions primarily to protect the intestinal epithelium (Mack *et al*., 1999). Interestingly, the LC40 treatment decreased LPS plasma levels. Consistently with previous data obtained from lpr mice treated with *Lactobacillus* (Mu *et al*., 2017a), we have shown that the administration of *L. fermentum* to SLE mice was associated with a significant increase in the colonic expression of IAP, which has been reported to support growth of Gram-positive bacteria (Kaliannan *et al*., 2015), and might explain the increase of Bifidobacterium in SLE treated mice. Bifidobacterium can also promote gut epithelial integrity by strengthening tight junctions (Yang *et al*., 2015). In conjunction, these results suggest that LC40 can restore intestinal mucosal barrier function, which is compromised in lupus mice.

Furthermore, humoral immune system activation plays a central role in the pathogenesis of SLE as pointed out by evidence suggesting that the number of B cells, which differentiate into antibody-producing plasma cells, is increased in SLE (Dar *et al*., 1988). IL-21 drives B cell maturation and autoantibody production in rodent models of lupus (Spolski *et al*., 2014). Accordingly, we found a higher number of B cells in both secondary lymphoid organs and a higher plasma level of IL-21 in SLE mice than in the control group. These changes were counteracted after LC40 treatment in SLE mice, that is, this probiotic treatment attenuated the size of the B cell population in mesenteric lymph nodes. Furthermore, IL-18 inhibits B cell antibody production (Lauwerys *et al*., 1998), and abnormal activation of B cells might be related to IL-18 down-regulation found in colon of SLE mice. Therefore, the increased IL-18 expression

found in colonic samples of the SLE-LC40 group compared to the values found in SLE mice might also account for the reduction of B cell activity in mesenteric lymph nodes, leading to lower plasma anti-dsDNA levels in the SLE-LC40 group than in the SLE group. Moreover, despite the elevated proportion of Treg cells in aged lupus mice, these cells are ultimately unable to control cumulative impact of multiple genetic elements driving lymphocyte activation and autoreactivity (Zhang *et al*., 2015). The reduction induced by LC40 in Treg cell counts might also decrease these processes, leading to a decrease in autoantibodies. The administration of a mouse anti-CD20 antibody (the equivalent of rituximab in humans) to deplete B cells markedly attenuates autoantibody production and prevents the development of hypertension in female NZBW/F1 mice (Mathis *et al*., 2014). Overall, reduced anti-dsDNA levels, mediated by B cells depletion and lower activation, might be involved in the antihypertensive effects of LC40 consumption. Moreover, an imbalance between anti-inflammatory Treg and pro-inflammatory Th17 cells is widely recognized as a cause in the establishment of both human SLE and murine lupus (Alunno *et al*., 2012). A lower Th17 count induced by LC40 might be related to an increase in IL-18 production from colonic tissue, an important cytokine for limiting colonic Th17 cell differentiation in mesenteric lymph nodes (Harrison *et al*., 2015).

Hypertension is often associated with impaired endothelial function, but whether this is causative in the progression of hypertension is difficult to prove. Recently, we have shown an impaired aortic endothelium-dependent relaxation response to acetylcholine in NZBW/F1 mice (Gómez-Guzmán *et al*., 2014; Romero *et al*., 2017) and a reduction in NO production induced by plasma from SLE patients with active nephritis in human endothelial cells (Toral *et al*., 2017). In consistency with this information, our data showed that chronic probiotic administration prevented the altered responses to acetylcholine observed in aortas from SLE mice, and improved the reduced eNOS phosphorylation at the activation site Ser1177. Interestingly, the improvement in acetylcholine relaxation induced by LC40 in SLE mice was suppressed by L-NAME, indicating a protective role in NO bioactivity.

A crucial mechanism of endothelial dysfunction involves the vascular production of ROS, particularly O_2^-, which reacts rapidly with NO and inactivates it (Tschudi *et al*., 1996). Herein, we found that ROS levels are increased in aortas from SLE mice and that LC40 decreased ROS content. The activity of the NADPH oxidase, considered the major source of O_2^- in the vascular wall, was markedly increased in SLE mice. NADPH oxidase-driven ROS production is a key event in endothelial dysfunction in SLE because incubation with the selective NADPH oxidase inhibitor VAS2870 increased the aortic endothelium-dependent relaxation to acetylcholine in SLE mice up to similar levels found in control mice. The probiotic treatment inhibited the upregulation of NADPH oxidase subunits and its activity in SLE mice. All the results suggest that the reduction of ROS levels in the vascular wall, and the subsequent prevention of NO inactivation, constitute a pivotal mechanism involved in the LC40 protective effects on endothelial function in SLE disease. Increased ROS production has also been involved in the raise of BP in female NZBW/F1 mice, since chronic treatment with a mixture of antioxidants decreased BP (Gómez-Guzmán *et al*., 2014).

Another remarkable event involved in BP regulation is T cell infiltration in vascular tissues (Ryan, 2013). In fact, preventing T-cell polarization in mesenteric lymph nodes by LC40 administration reduced Th17 accumulation in aorta and improved endothelial dysfunction. The pro-inflammatory cytokine IL-17 causes Rho-kinase-mediated endothelial dysfunction in the vascular wall by increasing the phosphorylation of the inhibitory eNOS residue Thr495 (Talaat *et al*., 2015). In addition, IL17 promotes ROS generation by NADPH oxidase activation (Dhillion, P. et al. 2012). We found lower IL17 mRNA levels in aortas from the SLE-LC40 group compared to SLE group, associated to a reduced Rho expression, Thr495 eNOS phosphorylation, and NADPH oxidase activity, which might be involved in the protective effect of LC40 administration in endothelial dysfunction. However, we did not test if there is a mechanistic link between vascular IL-17 levels and both transcriptional and function changes found in SLE mice in the vascular wall.

Furthermore, the immune system is intimately associated with TLR signals, which are involved in the pathogenesis of SLE (Ma *et al*., 2015). Our findings revealed

that aortic mRNA levels of TLR-4 were higher in NZBW/F1 mice compared to control mice. In the vasculature, the activation of TLR-4 by bacterial products, such as LPS, results in increased NADPH oxidase dependent O_2^- production and inflammation (Liang *et al*., 2013). Probiotic administration reduced plasma LPS levels with the subsequent reduction in the mRNA levels of TLR-4 and, consequently, improvement of vascular oxidative stress and inflammation in SLE. Moreover, inflammatory responses in the endothelium induced by circulating autoantibodies and other inflammatory mediators are known to contribute to the pathogenesis of endothelial dysfunction (Toral *et al*., 2017), and numerous studies have related the release of cytokines to the progression of SLE (Kelley and Wüthrich, 1999). Therefore, we found increased plasma levels of pro-inflammatory cytokines TNF-α, IFN-γ, IL-17a, and IL-21 in SLE mice. The LC40 treatment decreased the number of Th1 cells, as well as IFN-γ and IL-21 levels in plasma; therefore, their deleterious effects on the vasculature were decreased. One important limitation of our study is that we have not followed the evolution of the immunological, vascular and BP improvements induced by LC40, and it is not clear whether vascular and immunological benefits are secondary to decreased BP or are early events involved in BP control.

3. *Lactobacillus fermentum* CECT5716 prevents renal damage in the NZBW/F1 mice model of systemic lupus erythematosus

In the present study we have demonstrated for the first time that chronic oral administration of the probiotic LC40 in NZBW/F1 mice profoundly improves renal damage as indicated by lower endocapillary proliferation, immune deposits in tuft capillary, glomerulosclerosis, and tubulointerstitial lesions. In addition, this probiotic improved renal function, since it increased the urinary creatinine and urea excretion, and delayed the onset of albuminuria and high BP. These changes appeared dependent of both reduced circulating anti-dsDNA and LPS levels. Taken together, our

data indicate that diet supplementation with the probiotic LC40 may provide a novel therapeutic strategy to prevent renal injury and hypertension in SLE.

LN is a chronic inflammatory disease of the kidneys that is fatal if not resolved (Alperovich*et al*., 2007). One of the hallmarks of SLE is the presence of anti-dsDNA, which results in the formation of autoantibody-autoantigen complexes and their subsequent deposition in the kidney and other tissues, which has been tightly linked to the development of fatal LN (Swaak *et al*., 1990; Zhao*et al*., 2005). We found increased immunocomplexes deposition in the kidney associated with higher circulating levels of anti-dsDNA in SLE mice. Interestingly, LC40 consumption reduced both the plasma levels of this nuclear autoantibody and the subsequent immunocomplexes deposition. We previously demonstrated that LC40 was able to reduce B cells populations in mesenteric lymph nodes of NZBW/F1 mice, which differentiate into antibody-producing plasma cells. In addition, LC40 also reduced Treg cell counts, which drive lymphocyte activation and autoreactivity, leading to a decrease in autoantibodies that are critical for the formation of immunocomplexes.

Recently, it has been demonstrated that anti-dsDNA antibodies also contribute to inflammatory processes in the tubulointerstitium in LN through their binding to proximal renal tubular epithelial cells and induction of pro-inflammatory mediators (Yung *et al*., 2017). Moreover, in proteinuric kidney diseases, such as SLE, excessive albumin is filtered from glomeruli and reabsorbed into proximal tubular cells. This causes an inflammatory vicious cycle via secretion of pro-inflammatory cytokines, and subsequent infiltration of inflammatory cells, which secrete TNF-α (Abbate *et al*., 2006). We also found increased albumin excretion in SLE mice aged > 30 weeks-old, which was reduced by concomitant LC40 supplementation. This effect was also associated with lower inflammatory infiltrates, and lower pro-inflammatory cytokines accumulation (TNF-α, IL-1β and IL-6). In addition, we also described in LC40-treated mice a reduced expression of RORγ, a Th17 marker, and T-bet, a Th1 marker, that might also contribute to reduce kidney inflammation. This lower Th17 and Th1 infiltration in the kidney is consistent with our previous data showing that microbiota modulation with LC40 reduced Th17 and Th1 population in mesenteric lymph nodes from NZBW/F1

mice. Th17 cells, by producing IL-17, are considered to play a central role in the development of glomerular and tubulointerstitial tissue damage, loss of renal function, and albuminuria (Krebs *et al*., 2017). Thus, the lower IL17 mRNA levels found in renal cortex from SLE mice treated with LC40 might also reduce kidney inflammation. However, the contribution of this mechanism to kidney protection induced by LC40 are unclear, since IL-17 deficiency did not affect the course of lupus nephritis in lpr mice or NZB/NZW mice (Schmidt *et al*., 2015). However, anti-IFN-γ treatment attenuated the severity of LN, suggesting a predominance of the Th1/IFN-γ pathway in kidney damage progression in these models of SLE (Schmidt *et al*., 2015). Thus, suppression of inflammation caused by all these factors should serve as an important mechanism through which to protect proximal tubular cells and maintain renal function in SLE kidneys. In fact, we also observed increased urinary creatinine and urea excretion in mice treated with LC40, showing renal function improvement.

Renal inflammation, also directly affects kidney processes that may promote increases in blood pressure. In fact, blockade of TNF-α with etanercept attenuates both renal injury and hypertension in female NZBW/F1 mice (Venegas-Pont *et al*., 2010). We found reduced mRNA levels of TNF-α in renal cortex from SLE mice treated with LC40, which might account to reduce BP, in addition to the systemic vascular function improvement previously described.

Our results showed that NADPH oxidase activity is increased in renal cortex from SLE mice, consistent with previous published data (Venegas-Pont *et al*., 2010; Mathis *et al*., 2012). SLE mice treated with etanercept not only reduced renal injury but also abrogated the oxidative stress in the kidney (Venegas-Pont *et al*., 2010), showing that NADPH oxidase-mediated ROS production is linked to the TNF-α pathway. In addition, although the treatment with antioxidant (tempol + apocynin) did not alter SLE disease activity, renal injury (urinary albumin) was reduced in the treated SLE mice (Mathis *et al*., 2012). Our findings also revealed that renal cortex mRNA levels of TLR-4 were higher in NZBW/F1 mice. Up-regulation of TLR-4 expression in kidneys from LN patients plays a critical role in the pathogenesis of renal disorders in SLE (Elloumi *et al*., 2017). The activation of TLR-4 by bacterial products such as LPS, results in

increased NADPH oxidase dependent O_2^- production and inflammation (Liang *et al*., 2013). Moreover, TLR-4 deficiency results in ameliorated renal damage in lupus-prone B6lpr/lpr mice (Lartigue *et al*., 2009), whereas, overexpression of TLR-4 leads to autoimmune glomerulonephritis (Liu *et al*., 2006). LC40 administration reduced plasma LPS levels with the subsequent reduction in the mRNA levels of TLR-4 and, consequently, improving renal oxidative stress in SLE mice.

4. Toll-like receptor 7-driven lupus autoimmunity induces hypertension and vascular alterations in mice.

We demonstrate, for the first time, that TLR-7 activation by epicutaneous application of IMQ results in a gradual increase in arterial BP, which is likely associated with autoimmune disease progression as evidenced by elevated plasma levels of anti-dsDNA autoantibodies, splenomegaly and hepatomegaly, and severe expansion of splenic immune cells with enhancement of lymphocyte polarization towards a proinflammatory phenotype. Moreover, our present results show a marked hypertrophic effect on target organs for high BP, such as heart and kidney. Additionally, and as a novel finding, the activation of TLR-7 by IMQ also induces vascular remodelling in resistance arteries and endothelial dysfunction in aortas from wild-type mice. These vascular alterations seem to be related to a loss of NO bioavailability and to an increase in ROS production, as a result of enhanced NADPH oxidase activity and an enhanced vascular inflammation.

Recently, TLR-7 activation by topical application of IMQ has shown to induce severe glomerulonephritis and kidney injury associated with elevated autoantibodies generation (Yokogawa *et al*., 2014; Ren *et al*., 2016; Liu *et al*., 2018). In our experiment, we found increased plasma levels of anti-dsDNA autoantibodies in IMQ-treated mice, which are correlated with albuminuria and morphological alterations in kidney cortex from these mice, which were significant after 4 weeks of IMQ treatment. Interestingly, our results showed a severe expansion of splenic immune cells in association with lymphocyte polarization to a proinflammatory phenotype. Of note, we

observed an imbalance between Th cell subtypes (Th1 and Th17) and Treg in spleen from IMQ-treated mice, with a predominance of the former. These results are consistent with previous evidences showing that TLR-7 activation by IMQ is associated with autoimmune disease progression because of a lymphoproliferative disorder as a result of abnormalities in B-cell activation and enhanced Th1-type immune responses, at least partially attributable to a defect in immunosuppressive Treg function (Gong *et al*., 2014; Liu *et al*., 2018).

Furthermore, a defective clearance of apoptotic cells is also associated with a progressive lupus-like autoimmune disease and an increased production of autoantibodies (Nagata *et al*., 2010; Sakamoto *et al*., 2016). Notably, an impaired ability to engulf apoptotic cells has been demonstrated in both C1q-deficient humans and mice, which was related to a higher risk to develop SLE (Bottoand Walport, 2002; Crispín *et al*., 2013). Here, we found a reduced expression of hepatic opsonins only in IMQ-treated mice compared with control mice. This result suggests that the activation of TLR7 causes a deficiency in the clearance of apoptotic cells which, together with the increased percentage of splenic B cells and plasma levels of IL-21, might contribute to the exacerbation of the anti-dsDNA autoantibodies found in IMQ-treated mice, being these results consistent with those previously described (Spolski *et al*., 2014; Sakamoto *et al*., 2016).

Previous studies have shown that autoimmune disease progression and the resultant increase in systemic inflammation and kidney damage are important underlying factors involved in the development of hypertension and vascular dysfunction associated with SLE (Taylor and Ryan, 2016; Giannelou and Mavragani, 2017; Ocampo-Piraquive *et al*., 2018,). In fact, it has been shown that preventing autoimmunity with immunosuppressive therapy attenuates lupus disease progression and protects against the development of hypertension (Venegas-Pont *et al*., 2010; Taylor and Ryan, 2017). Our results demonstrate for the first time a progressive increase in blood pressure induced by TLR-7 activation in IMQ-treated mice, without changes in HR. Moreover, hypertensive IMQ-treated mice developed cardiac and renal hypertrophy. However, currently available data do not allow establishing a direct

relationship between glomerulonephritis and increased blood pressure in both murine models and patients with SLE (Rudofsky *et al*., 1984; Sabio*et al*., 2016; Taylor and Ryan, 2016). In our study, we found that the increase in BP begins after the development of proteinuria, suggesting that early kidney injury may contribute to the evolution of hypertension during lupus disease progression induced by TLR-7 activation.

Numerous studies suggest that the presence of vascular remodelling in resistance arteries and endothelial dysfunction are crucial in the pathogenesis of SLE hypertension in humans and animal models (Ryan and McLemore, 2007; Gómez-Guzmán *et al*., 2014; Tselios *et al*., 2016; Mak *et al*., 2017;). In the present study, we found that TLR-7 activation induced a significant M/L ratio increase as a result of a reduced LD and an increased MT in superior mesenteric arteries from IMQ-treated mice, observed only at 8 weeks of treatment.

Recently, Liu *et al*. (2018) have also found endothelial dysfunction triggered by IMQ treatment in wild-type mice (Liu *et al*., 2018). Importantly, we also demonstrate that IMQ-treated mice display significant impaired endothelium-dependent vasorelaxation compared to control mice. Endothelial dysfunction is characterized by an impaired NO availability and a concomitant increase in the generation of ROS (Touyz and Briones, 2011). It is well known that NO secretion is required for normal endothelium-dependent vasodilatation, and a deficiency of eNOS function in endothelial cells have been reported to happen in both murine models and humans with SLE (El-Magadmi *et al*., 2004; Romero *et al*., 2017). We found that endothelium-dependent relaxations induced by Ach were abolished by eNOS inhibition with L-NAME, suggesting a defect in NO pathway in IMQ-treated mice. However, no significant changes in vasodilator response to the NO donor nitroprusside were found in all experimental groups, suggesting that sensitivity to the NO-cGMP pathway in vascular smooth muscle cells was unaltered.

It is well established that vascular inflammation and inflammatory cells infiltration are contributing factors to the pathogenesis of vascular dysfunction in SLE,

largely driven by immune dysregulation (Sun *et al*., 2013; Tektonidou. *et al*., 2017). Previous studies have shown that TLR-7 activation causes an increase in circulating proinflammatory cytokines in both wild-type and TLR-9-deficient mice. These cytokines are potentially involved in the pathogenesis of lupus and its deleterious effects in the vasculature (Yokogawa *et al*., 2014; Liu *et al*., 2018). Accordingly, we also found increased plasma levels of the proinflammatory cytokines IFN-α, IFN-γ, IL-21, TNF-α, IL-6 and IL-17 in IMQ-treated mice, which were correlated with changes in lymphoid cell populations found in the spleen of these mice. High concentrations of proinflammatory cytokines downregulate eNOS and induce oxidative stress (Kofler *et al*., 2005; Small *et al*., 2018). Interestingly, we found a progressive decrease in eNOS mRNA levels and protein expression in aorta from IMQ-treated mice. Although our study is limited due to the lack of measurements of direct NO release and eNOS activity, our results suggest that changes in eNOS expression might contribute, at least partially, to the loss of NO production. In fact, a recent study has described that IFN-α negatively regulates the expression of eNOS and NO production in endothelial cells (Buie *et al*., 2017).

Oxidative stress is an important contributor to vascular remodelling and endothelial dysfunction associated with SLE, acting as mediator of the link between autoimmune responses and vascular inflammation (Tselios *et al*., 2016; Small. *et al*., 2018). Our results show an increased production of ROS in both aorta and mesenteric arteries from IMQ-treated mice. This ROS production is correlated with significant NADPH oxidase activity as a result of the overexpression of its catalytic subunits NOX2, p22phox and p47phox. Our results clearly demonstrated that this exacerbated NADPH oxidase-driven ROS production seems to be a key event in the development of vascular structural alterations and endothelial dysfunction induced by TRL7 activation. This was supported by i) the incubation with the NADPH oxidase inhibitor apocynin increased the aortic endothelium-dependent relaxation to Ach in IMQ-treated mice up to a level similar to that found in the control group, and ii) chronic antioxidant treatment prevented vascular remodeling and endothelial dysfunction in IMQ-treated mice. Furthermore, NADPH oxidase-derived ROS may be a key component in the

upregulation of TLRs in the vasculature (Chen and Stinnett, 2008). Accordingly, our results show a marked increase in vascular TLR-7 mRNA expression in aortas from IMQ-treated mice, while vascular TLR-9 mRNA expression was unaffected.

In addition, TLR-7 activation by IMQ stimulates the release of proinflammatory cytokines and chemoattractant proteins, which have an impact on the development of premature atherosclerosis in SLE (De Meyer *et al*., 2012). According to these previous results, we observe a marked increase in the mRNA expression of VCAM-1 and proinflammatory cytokines IFN-α, IFN-γ, IL-6, IL1β and IL-17 in homogenates of aortic and mesenteric arteries from IMQ-treated mice, whereas the mRNA expression of IL-10 and TFG-β is reduced. These cytokines regulate vascular ROS levels, vascular structure and tone and BP. In fact, low splenic Treg and low vascular IL-10 level were associated with angiotensin II-induced endothelial dysfunction and hypertension in mice (Kassan *et al*., 2011; Matrougui *et al*., 2011), similarly to that found in IMQ-treated mice. IL-17 plays a key role in vascular dysfunction induced by TLR-7 activation since nIL-17 injection decreased aortic NADPH oxidase activity, improved endothelial dysfunction and reduced SBP in IMQ-treated mice. Postnatal smooth muscle cells-specific deletion of TGF-β type II receptor is reported to cause the rapid thickening of the thoracic aorta (Li *et al*., 2014). Thus, reduced TFG-β mRNA levels found in mesenteric arteries from IMQ-treated mice might be also involved in the structural modification induced by TLR-7 activation. Therefore, the detrimental vascular effects of TLR-7 activation by IMQ might be the result of the increase in plasma cytokines and direct effects on the vasculature through increasing oxidative stress and vascular inflammation via an imbalance between proinflammatory and inhibitory cytokines.

5. Probiotics prevent hypertension in a murine model of SLE induced by TLR-7 activation

Our results demonstrate for the first time that the chronic treatment with the probiotics LC40 or BFM prevented hypertension and endothelial dysfunction in a mouse lupus model induced by TLR-7 activation. These findings identify a novel

alternative for vascular disorders in SLE patients based in gut microbiota manipulation through the administration of probiotics. These protective effects are the following: (a) a markedly attenuated lupus disease progression as evidenced by B cells accumulation, and lower plasma anti-dsDNA antibodies; (b) a restoration of the Th17/Treg balance in MLNs; (c) a significantly reduced SBP; (d) an endothelial function restoration associated to lower vascular Th1 and Th17 infiltration and vascular oxidative stress; and (e) an improvement in colonic integrity.

Our previous work showed that the oral administration of probiotics ameliorates BP in tacrolimus induced hypertension (Toral *et al*., 2018) and NZBW/F1 mice as results in this thesis, and the treatment based on the combination of probiotics was able to reduce the BP in spontaneously hypertensive rats (Gomez-Guzman *et al*., 2015). These data indicated that the effect of probiotics on BP should be closely related to the composition of intestinal flora. In our experiment, LC40 or BFM administered to IMQ mice prevented the raise of BP, suggesting that changes in gut microbiota might influence the mechanisms involved in the development of hypertension induced after TLR-7 activation.

The major change in gut microbiota found in IMQ-treated mice as compared with their healthy counterparts is an induced intestinal dysbiosis characterized by both a tendency to reduce the F/B ratio and a significant lower α-diversity, measured by numbers of species. Our results are in agreement with the microbiota alterations found in other animal models and even the inducible model through administration of agonist of TLR-7, IMQ as shown by other authors (Zegarra-Ruiz *et al*., 2019). The microbiota is characterized by an expansion of the families *Coriobacteriaceae* and *Rikenallecea*, and the reduction of *Clostridaceae*. At the genus level, it is remarkable the change in *Prevotella* and *Desulfovibrio* which were found elevated in the SLE model, and the decrease in the abundance of *Turicibacter*, *Bifidobacterium*, *Coprobacillus* and *Anaerostipes*. Finally, other authors found an increase in *Lactobacillus reuteri*, in faeces from IMQ-treated mice, which was also found translocated in MLN, spleen and liver, linking its translocation to the evolution of SLE. However, we were not able to find significant changes among groups in the abundance of *L. reuteri* (not shown),

suggesting an absence of involvement of this microorganism in the development of autoimmunity. This important difference could be related to the differences between mouse strains used by Zegarra-Ruiz *et a*l. (C57Bl/6 mice) and in the present experiment (BALB/c mice). In our experimental conditions, PCA of the bacterial taxa in faecal samples showed perfect clustering among groups (Ctrl and IMQ). The clusters corresponding to LC40 and BFM were more similar to IMQ. SCFAs-producing bacteria were also analysed, the level of acetate-producing bacteria was found elevated but neither of the probiotics restored it, ruling out a possible role of SCFAs in the protective effects of these probiotics. BFM and LC40 were found set in the gut microbiota of animals treated respectively, and could be responsible for the release of bacterial products, other than SCFAs, involved in blood pressure control.

Besides of these changes, in gut microbiota from patients and animal models of SLE takes place an alteration in the epithelium intestinal barrier characterized by impairment in junction proteins like occludin, ZO-1 and claudin and an increase in intestinal permeability, measured through fluorescein isothiocyanate (commonly referred to as FITC)-dextran (Mu *et al*., 2017). In fact, our data showed that the intestinal epithelium is compromised in IMQ mice characterized by a decreased expression of tight junction proteins, which could facilitate the translocation of LPS to the systemic circulation. In addition, the relative abundance of LPS-containing Gram-negative bacteria (*Proteobacteria*) tended to be higher in the IMQ group as compared with control mice, which could contribute to the increased plasma LPS levels found in this group. Interestingly, LC40 or BFM treatments can restore mucosal barrier integrity by increasing the expression of occluding, and mucin proteins that function primarily to protect the intestinal epithelium (Mack *et al*., 1999). In contrast with previous data in lpr mice mice treated with *Lactobacillus* (Mu *et al*., 2017), we found that both probiotics could not significantly reduce the LPS plasma levels. This data could be related to the absence of change in the relative abundance of LPS-containing Gram-negative bacteria induced by both probiotics. Together, these results suggest that probiotics can restore the intestinal mucosal barrier function that is compromised in lupus mice.

Current evidence suggests that immune system activation plays a central role in the pathogenesis of SLE immune cells, which can affect vascular reactivity, renal function, and blood pressure regulation (Ryan, 2013). In fact, the administration of a mouse anti-CD20 antibody (the equivalent of rituximab in humans) to deplete B cells markedly attenuates autoantibody production and prevents the development of hypertension in female NZBW/F1 mice (Mathis *et al*., 2014). TLR-7 activation increased type I IFN secretion in the blood increasing autoimmunity (Crow, 2014). We also found higher plasma IFN-α levels in the IMQ group, as compared with control, which were unaltered by both probiotic treatments, indicating that changes in anti-dsDNA antibodies induced by these probiotics were independent of the TLR-7-type I IFN pathway. However, we found a higher number of B cells in spleen in IMQ mice than in the control group, which was counteracted after LC40 and BFM treatment in lupus mice, leading to reduced plasma anti-dsDNA antibody levels. Additionally, an imbalance between anti-inflammatory Treg and inflammatory Th17 cells is widely recognized as being causative in the establishment of both human SLE and murine lupus (Mathis *et al*., 2014). These data are in agreement with the previous results in this Thesis. They suggested the ability of IMQ to promote T cell proliferation towards the expansion of Th17 cells in spleens, together with a reduction in Treg cell numbers, provides an additional mechanism that may contribute to the hypertension induced by IMQ, in addition to its direct deleterious effects on blood vessels. Furthermore, we found that IMQ reduced Treg and increased Th17 cells in mesenteric lymph nodes. Finally, preventing T-cell polarization by LC40 or BFM administration improved endothelial dysfunction induced by IMQ. *In vitro*, the addition of indole-3-lactic acid to culture media reduced Th17 polarization of T lymphocytes. This indole compound was mainly produced by *Lactobacillus* spp. (Wilck*et at*., 2017), which could inhibit inflammation and decrease BP. Moreover, BFM was unable to generate Th17 cells from naïve T lymphocytes in *in vitro* conditions (López *et al*., 2011), but reduced Th17 contents in MLNs from spontaneously hypertensive rats (Robles-Vera *et a*l., 2020), suggesting a possible role in BP control in IMQ-treated mice.

It is becoming more and more evident that hypertension is often associated with impaired endothelial function. We have demonstrated that chronic probiotic administration prevented the altered responses to Ach observed in aortas from control IMQ mice. Interestingly, the improvement in acetylcholine relaxation induced by LC40 and BFM in IMQ was suppressed by L-NAME, indicating a protective role in NO bioactivity. In the present study, the relaxant response to the activator of soluble guanylate cyclase SNP was similar in the aorta from all of the experimental groups, indicating that alterations in the cGMP pathway do not appear to contribute to endothelial dysfunction in lupus mice. These data are also consistent with our previous studies that showed an impaired aortic endothelium-dependent relaxation response to acetylcholine in NZBW/F1 mice (Gómez-Guzmán *et al*., 2014; Romero *et al*., 2017) and in the TLR-7 dependent mouse model, both also observed in this Doctoral Thesis.

A key mechanism of endothelial dysfunction involves the vascular production of ROS, particularly O_2^-, which reacts rapidly with NO and inactivates it (Tschudi *et al*., 1996). In our study, aortas from IMQ-treated mice showed higher ROS levels and, again both probiotics abolished this increase. The activity of the NADPH oxidase, considered the major source of O_2^- in the vascular wall, was markedly increased in IMQ mice. NADPH oxidase-driven ROS production is a key event in endothelial dysfunction in SLE because incubation with the selective NADPH oxidase inhibitor VAS2870 increased the aortic endothelium-dependent relaxation to acetylcholine in IMQ to similar levels found in control mice. All the results suggest that the reduction of O_2^- levels in the vascular wall, and the subsequent prevention of NO inactivation, constitute a key mechanism involved in the probiotics protective effects on endothelial function in SLE disease. Increased ROS production has also been involved in the raise of blood pressure in NZBW/F1 mice (Gómez-Guzmán *et al*., 2014) and the TLR7-model, as evidenced in the previous experiment, since chronic treatment with a mixture of antioxidants reduced BP.

TLR-7 activation induced by IMQ enhances vascular inflammation and inflammatory cells infiltration, which leads to vascular dysfunction in SLE, largely driven by immune dysregulation (Sun *et al*., 2013; Tektonidou *et al*., 2017). In agreement with

this, our data have shown that the mRNA expression of VCAM-1 and the proinflammatory cytokine IFN-γ were higher in aortae from the IMQ-treated vs the control mice. Moreover, LC40 or BFM administration, which reduced ROS levels, also prevented the raise in the mRNA levels of IFN-γ and VCAM-1 induced by IMQ. Interestingly, BP was reduced in mice receiving the LC40 or BFM treatment as compared with the IMQ group. Interestingly, increased vascular inflammation and oxidative stress, mediated in part by IL-17, as key factors contributing to hypertension in this TLR-7-driven lupus autoimmunity model. We found increased Th17 infiltration in aorta from IMQ mice, which was abolished by both probiotics, possibly related to the change in T cells polarization induced by LC40 and BFM in MLNs. Th17 is known to increase the NADPH oxidase activity through the production of IL-17a (Makhezer *et al*., 2019). Moreover, LC40 also increased Treg accumulation in the aorta. It is well stablished that IL-10 released by Treg improves endothelial dysfunction through inhibition of the vascular NADPH oxidase activity improving vascular oxidative stress (Kassan *et al*., 2011), which contributes to reduce BP in IMQ-treated mice. These data support the hypothesis stipulating that the modification in gut microbiota, which in turn reduced immune activation, can play an essential role in the antihypertensive effects of LC40 or BFM in IMQ-treated mice.

CONCLUSIONS

CONCLUSIONS

I) Vancomycin-sensitive gut bacteria are involved in SLE hypertension through the regulation of Th17 differentiation in gut lymph organs. Moreover, gut microbiota transfers the hypertensive phenotype to mice without genetic background of SLE. These results open new possibilities to the prevention of cardiovascular complications associated with SLE by the modulation of the gut microbiota through the administration of probiotics.

II) The LC40 treatment in SLE mice improves endothelium-dependent relaxation, reduces SBP and has a protective effect against LN conditions. These protective effects seem to be associated, at least in part, with a decrease in vascular and renal oxidative stress and proinflammatory elements.These results open new possibilities to the prevention of cardiovascular and renal complications associated with SLE by the modulation of the gut microbiota through the administration of probiotics.

III) TLR-7 activation by chronic topical application of IMQ induces a progressive increase in BP and vascular structural and functional changes in wild-type mice. In addition, our results highlight the increased vascular oxidative stress, mediated at least in part by IL-17, as key molecular mechanisms contributing to cardiovascular complications in this TLR7-driven lupus autoimmunity model. Therefore, our findings have highlighted the potential importance of TLR-7 signalling in SLE hypertension and vascular dysfunction, future studies should focus on TLR-7 as a therapeutic target.

IV) The probiotics LC40 and BFM prevented the development of hypertension and endothelial dysfunction in IMQ mice through a reduction in the vascular oxidative stress. These protective effects may be attributable to a reduction of SLE activity and vascular inflammation, possibly as a result of a decreased Th17 and increased Treg cells polarization in mesenteric lymph nodes, restoring Th17/Treg balance in vascular tissues.

BIBLIOGRAPHY

BIBLIOGRAPHY

- Abbate M, Zoja C, Remuzzi G. How does proteinuria cause progressive renal damage?. J Am Soc Nephrol. 2006;17(11):2974-2984.

- Alperovich G, Rama I, Lloberas N, et al. New immunosuppresor strategies in the treatment of murine lupus nephritis. Lupus. 2007;16(1):18-24.

- Alunno A, Bartoloni E, Bistoni O, et al. Balance between regulatory T and Th17 cells in systemic lupus erythematosus: the old and the new. Clin Dev Immunol. 2012;2012:823085.

- Alves JD, Grima B. Oxidative stress in systemic lupus erythematosus and antiphospholipid syndrome: a gateway to atherosclerosis. Curr Rheumatol Rep. 2003;5(5):383-390.

- Antharam VC, Li EC, Ishmael A, et al. Intestinal dysbiosis and depletion of butyrogenic bacteria in Clostridium difficile infection and nosocomial diarrhea. J Clin Microbiol. 2013;51(9):2884-2892.

- Armbrust T, Nordmann B, Kreissig M, Ramadori G. C1Q synthesis by tissue mononuclear phagocytes from normal and from damaged rat liver: up-regulation by dexamethasone, down-regulation by interferon gamma, and lipopolysaccharide. Hepatology. 1997;26(1):98-106.

- Arpaia N, Campbell C, Fan X, et al. Metabolites produced by commensal bacteria promote peripheral regulatory T-cell generation. Nature. 2013;504(7480):451-455.

- Asanuma Y, Oeser A, Shintani AK, et al. Premature coronary-artery atherosclerosis in systemic lupus erythematosus. N Engl J Med. 2003;349(25):2407-2415.

- Azzouz D, Omarbekova A, Heguy A, et al. Lupus nephritis is linked to disease-activity associated expansions and immunity to a gut commensal. Ann Rheum Dis. 2019;78(7):947-956.

- Barnado A, Oeser A, Zhang Y, et al. Association of estimated sodium and potassium intake with blood pressure in patients with systemic lupus erythematosus. Lupus. 2016;25(13):1463-1469.

- Bates JM, Akerlund J, Mittge E, Guillemin K. Intestinal alkaline phosphatase detoxifies lipopolysaccharide and prevents inflammation in zebrafish in response to the gut microbiota. Cell Host Microbe. 2007;2(6):371-382.

- Ben-Menachem E. Review article: systemic lupus erythematosus: a review for anesthesiologists. Anesth Analg. 2010;111(3):665-676.

-Bolland S, Yim YS, Tus K, Wakeland EK, Ravetch JV. Genetic modifiers of systemic lupus erythematosus in FcgammaRIIB(-/-) mice. J Exp Med. 2002;195(9):1167-1174.

- Botto M, Walport MJ. C1q, autoimmunity and apoptosis. Immunobiology. 2002;205(4-5):395-406.

- Briones AM, Touyz RM. Moderate exercise decreases inflammation and oxidative stress in hypertension: but what are the mechanisms?. Hypertension. 2009;54(6):1206-1208.

- Bruce IN, Gladman DD, Ibañez D, Urowitz MB. Single photon emission computed tomography dual isotope myocardial perfusion imaging in women with systemic lupus erythematosus. II. Predictive factors for perfusion abnormalities. J Rheumatol. 2003;30(2):288-291.

- Buie JJ, Renaud LL, Muise-Helmericks R, Oates JC. IFN-α Negatively Regulates the Expression of Endothelial Nitric Oxide Synthase and Nitric Oxide Production: Implications for Systemic Lupus Erythematosus. J Immunol. 2017;199(6):1979-1988.

- Caporaso JG, Lauber CL, Walters WA, et al. Global patterns of 16S rRNA diversity at a depth of millions of sequences per sample. Proc Natl Acad Sci U S A. 2011;108 Suppl 1(Suppl 1):4516-4522.

- Cavallo T, Granholm NA. Bacterial lipopolysaccharide transforms mesangial into proliferative lupus nephritis without interfering with processing of pathogenic immune complexes in NZB/W mice. Am J Pathol. 1990;137(4):971-978.

- Cervera R, Khamashta MA, Font J, et al. Morbidity and mortality in systemic lupus erythematosus during a 10-year period: a comparison of early and late manifestations in a cohort of 1,000 patients. Medicine (Baltimore). 2003;82(5):299-308.

- Chae CU, Lee RT, Rifai N, Ridker PM. Blood pressure and inflammation in apparently healthy men. Hypertension. 2001;38(3):399-403.

- Chan VS, Tsang HH, Tam RC, Lu L, Lau CS. B-cell-targeted therapies in systemic lupus erythematosus. Cell Mol Immunol. 2013;10(2):133-142.

- Chen JX, Stinnett A. Critical role of the NADPH oxidase subunit p47phox on vascular TLR expression and neointimal lesion formation in high-fat diet-induced obesity. Lab Invest. 2008;88(12):1316-1328.

- Chen XQ, Yu YC, Deng HH, et al. Plasma IL-17A is increased in new-onset SLE patients and associated with disease activity. J Clin Immunol. 2010;30(2):221-225.

- Chia S, Qadan M, Newton R, Ludlam CA, Fox KA, Newby DE. Intra-arterial tumor necrosis factor-alpha impairs endothelium-dependent vasodilatation and stimulates local tissue plasminogen activator release in humans. Arterioscler Thromb Vasc Biol. 2003;23(4):695-701.

- Christensen SR, Shlomchik MJ. Regulation of lupus-related autoantibody production and clinical disease by Toll-like receptors. Semin Immunol. 2007;19(1):11-23.

- Cieślik P, Hrycek A, Kłuciński P. Vasculopathy and vasculitis in systemic lupus erythematosus. Pol Arch Med Wewn. 2008;118(1-2):57-63.

- Cotillard A, Kennedy SP, Kong LC, et al. Dietary intervention impact on gut microbial gene richness [published correction appears in Nature. 2013 Oct 24;502(7472)580]. Nature. 2013;500(7464):585-588.

- Crispín JC, Hedrich CM, Tsokos GC. Gene-function studies in systemic lupus erythematosus. Nat Rev Rheumatol. 2013;9(8):476-484.

- Crow MK. Type I interferon in the pathogenesis of lupus. J Immunol. 2014;192(12):5459-5468.

- Crow MK, Olferiev M, Kirou KA. Targeting of type I interferon in systemic autoimmune diseases. Transl Res. 2015;165(2):296-305.

- Dar O, Salaman MR, Seifert MH, Isenberg DA. B lymphocyte activation in systemic lupus erythematosus: spontaneous production of IgG antibodies to DNA and environmental antigens in cultures of blood mononuclear cells. Clin Exp Immunol. 1988;73(3):430-435.

- De Groof A, Hémon P, Mignen O, et al. Dysregulated Lymphoid Cell Populations in Mouse Models of Systemic Lupus Erythematosus. Clin Rev Allergy Immunol. 2017;53(2):181-197.

- de la Visitación N, Robles-Vera I, Toral M, Duarte J. Protective Effects of Probiotic Consumption in Cardiovascular Disease in Systemic Lupus Erythematosus. Nutrients. 2019;11(11):2676.

- De Meyer I, Martinet W, Schrijvers DM, Timmermans JP, Bult H, De Meyer GR. Toll-like receptor 7 stimulation by imiquimod induces macrophage autophagy and inflammation in atherosclerotic plaques. Basic Res Cardiol. 2012;107(3):269.

- Deane JA, Pisitkun P, Barrett RS, et al. Control of toll-like receptor 7 expression is essential to restrict autoimmunity and dendritic cell proliferation. Immunity. 2007;27(5):801-810.

- Dhillion P, Wallace K, Herse F, et al. IL-17-mediated oxidative stress is an important stimulator of AT1-AA and hypertension during pregnancy. Am J Physiol Regul Integr Comp Physiol. 2012;303(4):R353-R358.

- Dixon FJ, Andrews BS, Eisenberg RA, McConahey PJ, Theofilopoulos AN, Wilson CB. Etiology and pathogenesis of a spontaneous lupus-like syndrome in mice. Arthritis Rheum. 1978;21(5 Suppl):S64-S67.

- Du Y, Sanam S, Kate K, Mohan C. Animal models of lupus and lupus nephritis. Curr Pharm Des. 2015;21(18):2320-2349.

- Edgar RC, Flyvbjerg H. Error filtering, pair assembly and error correction for next-generation sequencing reads. Bioinformatics. 2015;31(21):3476-3482.

- Ehlers M, Fukuyama H, McGaha TL, Aderem A, Ravetch JV. TLR9/MyD88 signaling is required for class switching to pathogenic IgG2a and 2b autoantibodies in SLE. J Exp Med. 2006;203(3):553-561.

- Eisenberg RA, Via CS. T cells, murine chronic graft-versus-host disease and autoimmunity. J Autoimmun. 2012;39(3):240-247.

- Elinav E, Henao-Mejia J, Flavell RA. Integrative inflammasome activity in the regulation of intestinal mucosal immune responses. Mucosal Immunol. 2013;6(1):4-13.

- Elloumi N, Fakhfakh R, Ayadi L, et al. The Increased Expression of Toll-Like Receptor 4 in Renal and Skin Lesions in Lupus Erythematosus. J Histochem Cytochem. 2017;65(7):389-398.

- El-Magadmi M, Bodill H, Ahmad Y, et al. Systemic lupus erythematosus: an independent risk factor for endothelial dysfunction in women. Circulation. 2004;110(4):399-404.

- Esdaile JM, Abrahamowicz M, Grodzicky T, et al. Traditional Framingham risk factors fail to fully account for accelerated atherosclerosis in systemic lupus erythematosus. Arthritis Rheum. 2001;44(10):2331-2337.

- Frostegård J. Systemic lupus erythematosus and cardiovascular disease. Lupus. 2008;17(5):364-367.

- Fujisaka S, Ussar S, Clish C, et al. Antibiotic effects on gut microbiota and metabolism are host dependent. J Clin Invest.

- García-Redondo AB, Aguado A, Briones AM, Salaices M. NADPH oxidases and vascular remodeling in cardiovascular diseases. Pharmacol Res. 2016;114:110-120.

- Geddes K, Philpott DJ. A new role for intestinal alkaline phosphatase in gut barrier maintenance. Gastroenterology. 2008;135(1):8-12.

- Gentile CL, Weir TL. The gut microbiota at the intersection of diet and human health. Science. 2018;362(6416):776-780.

- Giannelou M, Mavragani CP. Cardiovascular disease in systemic lupus erythematosus: A comprehensive update. J Autoimmun. 2017;82:1-12.

- Giannelou M, Mavragani CP. Cardiovascular disease in systemic lupus erythematosus: A comprehensive update. J Autoimmun. 2017;82:1-12.

- Gómez-Guzmán M, Jiménez R, Romero M, et al. Chronic hydroxychloroquine improves endothelial dysfunction and protects kidney in a mouse model of systemic lupus erythematosus. Hypertension. 2014;64(2):330-337.

- Gong L, Wang Y, Zhou L, et al. Activation of toll-like receptor-7 exacerbates lupus nephritis by modulating regulatory T cells. Am J Nephrol. 2014;40(4):325-344.

- Granholm NA, Cavallo T. Long-lasting effects of bacterial lipopolysaccharide promote progression of lupus nephritis in NZB/W mice. Lupus. 1994;3(6):507-514.

- Greiling TM, Dehner C, Chen X, et al. Commensal orthologs of the human autoantigen Ro60 as triggers of autoimmunity in lupus. Sci Transl Med. 2018;10(434):eaan2306.

- Guzik TJ, Hoch NE, Brown KA, et al. Role of the T cell in the genesis of angiotensin II induced hypertension and vascular dysfunction. J Exp Med. 2007;204(10):2449-2460.

- Guzik TJ, Korbut R, Adamek-Guzik T. Nitric oxide and superoxide in inflammation and immune regulation. J Physiol Pharmacol. 2003;54(4):469-487.

- Hahn BH. Systemic lupus erythematosus and accelerated atherosclerosis. N Engl J Med. 2003;349(25):2379-2380.

- Hang S, Paik D, Yao L, et al. Bile acid metabolites control TH17 and Treg cell differentiation [published correction appears in Nature. 2020 Mar;579(7798):E7]. Nature. 2019;576(7785):143-148.

- Harrison OJ, Srinivasan N, Pott J, et al. Epithelial-derived IL-18 regulates Th17 cell differentiation and Foxp3^{+} Treg cell function in the intestine. Mucosal Immunol. 2015;8(6):1226-1236.

- He Z, Kong X, Shao T, Zhang Y, Wen C. Alterations of the Gut Microbiota Associated With Promoting Efficacy of Prednisone by Bromofuranone in MRL/lpr Mice. Front Microbiol. 2019;10:978.

- He Z, Shao T, Li H, Xie Z, Wen C. Alterations of the gut microbiome in Chinese patients with systemic lupus erythematosus. Gut Pathog. 2016;8:64.

- Hemminki K, Li X, Sundquist J, Sundquist K. Familial associations of rheumatoid arthritis with autoimmune diseases and related conditions. Arthritis Rheum. 2009;60(3):661-668.

- Hevia A, Milani C, López P, et al. Intestinal dysbiosis associated with systemic lupus erythematosus. mBio. 2014;5(5):e01548-14.

- Hill C, Guarner F, Reid G, et al. Expert consensus document. The International Scientific Association for Probiotics and Prebiotics consensus statement on the scope and appropriate use of the term probiotic. Nat Rev Gastroenterol Hepatol. 2014;11(8):506-514.

- Hsieh CY, Osaka T, Moriyama E, Date Y, Kikuchi J, Tsuneda S. Strengthening of the intestinal epithelial tight junction by Bifidobacterium bifidum. Physiol Rep. 2015;3(3):e12327.

- Hsu TC, Huang CY, Liu CH, Hsu KC, Chen YH, Tzang BS. Lactobacillus paracasei GMNL-32, Lactobacillus reuteri GMNL-89 and L. reuteri GMNL-263 ameliorate hepatic injuries in lupus-prone mice. Br J Nutr. 2017;117(8):1066-1074.

- Hu WS, Rajendran P, Tzang BS, et al. Lactobacillus paracasei GMNL-32 exerts a therapeutic effect on cardiac abnormalities in NZB/W F1 mice. PLoS One. 2017;12(9):e0185098.

- Huang Y, Yan L, Rong S, Haller H, Kirch T. TNF-α induces endothelial dysfunction via PKC-ζ-dependent NADPH oxidase activation. J Huazhong Univ Sci Technolog Med Sci. 2012;32(5):642-647.

- Jacob CO, van der Meide PH, McDevitt HO. In vivo treatment of (NZB X NZW)F1 lupus-like nephritis with monoclonal antibody to gamma interferon. J Exp Med. 1987;166(3):798-803.

- Johnson BM, Gaudreau MC, Al-Gadban MM, Gudi R, Vasu C. Impact of dietary deviation on disease progression and gut microbiome composition in lupus-prone SNF1 mice. Clin Exp Immunol. 2015;181(2):323-337.

- Kaliannan K, Wang B, Li XY, Kim KJ, Kang JX. A host-microbiome interaction mediates the opposing effects of omega-6 and omega-3 fatty acids on metabolic endotoxemia. Sci Rep. 2015;5:11276.

- Kassan M, Galan M, Partyka M, Trebak M, Matrougui K. Interleukin-10 released by CD4(+)CD25(+) natural regulatory T cells improves microvascular endothelial function through inhibition of NADPH oxidase activity in hypertensive mice. Arterioscler Thromb Vasc Biol. 2011;31(11):2534-2542.

- Kasselman LJ, Vernice NA, DeLeon J, Reiss AB. The gut microbiome and elevated cardiovascular risk in obesity and autoimmunity. Atherosclerosis. 2018;271:203-213.

- Katz-Agranov N, Zandman-Goddard G. The microbiome and systemic lupus erythematosus. Immunol Res. 2017;65(2):432-437.

- Kelley VR, Wüthrich RP. Cytokines in the pathogenesis of systemic lupus erythematosus. Semin Nephrol. 1999;19(1):57-66.

- Kim F, Tysseling KA, Rice J, et al. Free fatty acid impairment of nitric oxide production in endothelial cells is mediated by IKKbeta. Arterioscler Thromb Vasc Biol. 2005;25(5):989-994.

- Kimura A, Kishimoto T. IL-6: regulator of Treg/Th17 balance. Eur J Immunol. 2010;40(7):1830-1835.

- Kleinbongard P, Heusch G, Schulz R. TNFalpha in atherosclerosis, myocardial ischemia/reperfusion and heart failure. Pharmacol Ther. 2010;127(3):295-314.

- Knight JS, Kaplan MJ. Lupus neutrophils: 'NET' gain in understanding lupus pathogenesis. Curr Opin Rheumatol. 2012;24(5):441-450.

- Kofler S, Nickel T, Weis M. Role of cytokines in cardiovascular diseases: a focus on endothelial responses to inflammation. Clin Sci (Lond). 2005;108(3):205-213.

- Krebs CF, Schmidt T, Riedel JH, Panzer U. T helper type 17 cells in immune-mediated glomerular disease. Nat Rev Nephrol. 2017;13(10):647-659.

- Kundu S, Ghosh P, Datta S, Ghosh A, Chattopadhyay S, Chatterjee M. Oxidative stress as a potential biomarker for determining disease activity in patients with rheumatoid arthritis. Free Radic Res. 2012;46(12):1482-1489.

- Kuryliszyn-Moskal A, Klimiuk PA, Ciolkiewicz M, Sierakowski S. Clinical significance of selected endothelial activation markers in patients with systemic lupus erythematosus. J Rheumatol. 2008;35(7):1307-1313.

- Lartigue A, Colliou N, Calbo S, et al. Critical role of TLR2 and TLR4 in autoantibody production and glomerulonephritis in lpr mutation-induced mouse lupus. J Immunol. 2009;183(10):6207-6216.

- Lauwerys BR, Renauld JC, Houssiau FA. Inhibition of in vitro immunoglobulin production by IL-12 in murine chronic graft-vs.-host disease: synergism with IL-18. Eur J Immunol. 1998;28(6):2017-2024.

- Li B, Selmi C, Tang R, Gershwin ME, Ma X. The microbiome and autoimmunity: a paradigm from the gut-liver axis. Cell Mol Immunol. 2018;15(6):595-609.

- Li J, Zhao F, Wang Y, et al. Gut microbiota dysbiosis contributes to the development of hypertension. Microbiome. 2017;5(1):14.

- Li W, Li Q, Jiao Y, et al. Tgfbr2 disruption in postnatal smooth muscle impairs aortic wall homeostasis. J Clin Invest. 2014;124(2):755-767.

- Li Y, Wang HF, Li X, et al. Disordered intestinal microbes are associated with the activity of Systemic Lupus Erythematosus. Clin Sci (Lond). 2019;133(7):821-838.

- Liang CF, Liu JT, Wang Y, Xu A, Vanhoutte PM. Toll-like receptor 4 mutation protects obese mice against endothelial dysfunction by decreasing NADPH oxidase isoforms 1 and 4. Arterioscler Thromb Vasc Biol. 2013;33(4):777-784.

- Lind L, Granstam SO, Millgård J. Endothelium-dependent vasodilation in hypertension: a review. Blood Press. 2000;9(1):4-15.

- Liu B, Yang Y, Dai J, et al. TLR4 up-regulation at protein or gene level is pathogenic for lupus-like autoimmune disease. J Immunol. 2006;177(10):6880-6888.

- Liu Y, Seto NL, Carmona-Rivera C, Kaplan MJ. Accelerated model of lupus autoimmunity and vasculopathy driven by toll-like receptor 7/9 imbalance. Lupus Sci Med. 2018;5(1):e000259.

- Liu Z, Davidson A. Taming lupus-a new understanding of pathogenesis is leading to clinical advances. Nat Med. 2012;18(6):871-882.

- Liu Z, Liu HY, Zhou H, et al. Moderate-Intensity Exercise Affects Gut Microbiome Composition and Influences Cardiac Function in Myocardial Infarction Mice. Front Microbiol. 2017;8:1687.

- López P, Rodríguez-Carrio J, Caminal-Montero L, Mozo L, Suárez A. A pathogenic IFNα, BLyS and IL-17 axis in Systemic Lupus Erythematosus patients. Sci Rep. 2016;6:20651.

- Luo XM, Edwards MR, Mu Q, et al. Gut Microbiota in Human Systemic Lupus Erythematosus and a Mouse Model of Lupus. Appl Environ Microbiol. 2018;84(4):e02288-17.

- Ma K, Li J, Fang Y, Lu L. Roles of B Cell-Intrinsic TLR Signals in Systemic Lupus Erythematosus. Int J Mol Sci. 2015;16(6):13084-13105.

- Ma Y, Xu X, Li M, Cai J, Wei Q, Niu H. Gut microbiota promote the inflammatory response in the pathogenesis of systemic lupus erythematosus. Mol Med. 2019;25(1):35.

- Mack DR, Michail S, Wei S, McDougall L, Hollingsworth MA. Probiotics inhibit enteropathogenic E. coli adherence in vitro by inducing intestinal mucin gene expression. Am J Physiol. 1999;276(4):G941-G950.

- MacKay CE, Shaifta Y, Snetkov VV, Francois AA, Ward JPT, Knock GA. ROS-dependent activation of RhoA/Rho-kinase in pulmonary artery: Role of Src-family kinases and ARHGEF1. Free Radic Biol Med. 2017;110:316-331.

- Madhur MS, Lob HE, McCann LA, et al. Interleukin 17 promotes angiotensin II-induced hypertension and vascular dysfunction. Hypertension. 2010;55(2):500-507.

- Mak A, Kow NY, Schwarz H, Gong L, Tay SH, Ling LH. Endothelial dysfunction in systemic lupus erythematosus - a case-control study and an updated meta-analysis and meta-regression. Sci Rep. 2017;7(1):7320.

- Makhezer N, Ben Khemis M, Liu D, et al. NOX1-derived ROS drive the expression of Lipocalin-2 in colonic epithelial cells in inflammatory conditions. Mucosal Immunol. 2019;12(1):117-131.

- Manfredo Vieira S, Hiltensperger M, Kumar V, et al. Translocation of a gut pathobiont drives autoimmunity in mice and humans [published correction appears in Science. 2018 May 4;360(6388):]. Science. 2018;359(6380):1156-1161.

- Mardani F, Mahmoudi M, Esmaeili SA, Khorasani S, Tabasi N, Rastin M. In vivo study: Th1-Th17 reduction in pristane-induced systemic lupus erythematosus mice after treatment with tolerogenic Lactobacillus probiotics. J Cell Physiol. 2018;234(1):642-649.

- Martens EC, Lowe EC, Chiang H, et al. Recognition and degradation of plant cell wall polysaccharides by two human gut symbionts. PLoS Biol. 2011;9(12):e1001221.

- Mathis KW, Venegas-Pont M, Masterson CW, Stewart NJ, Wasson KL, Ryan MJ. Oxidative stress promotes hypertension and albuminuria during the autoimmune disease systemic lupus erythematosus. Hypertension. 2012;59(3):673-679.

- Mathis KW, Wallace K, Flynn ER, Maric-Bilkan C, LaMarca B, Ryan MJ. Preventing autoimmunity protects against the development of hypertension and renal injury. Hypertension. 2014;64(4):792-800.

- Matrougui K, Abd Elmageed Z, Kassan M, et al. Natural regulatory T cells control coronary arteriolar endothelial dysfunction in hypertensive mice [published correction appears in Am J Pathol. 2011 Mar;178(3):1406.

- Morel L, Croker BP, Blenman KR, et al. Genetic reconstitution of systemic lupus erythematosus immunopathology with polycongenic murine strains. Proc Natl Acad Sci U S A. 2000;97(12):6670-6675.

- Morel L, Croker BP, Blenman KR, et al. Genetic reconstitution of systemic lupus erythematosus - Zakaria, Abd Elmageed [corrected to Abd Elmageed, Zakaria]]. Am J Pathol. 2011;178(1):434-441.

- Mu Q, Tavella VJ, Kirby JL, et al. Antibiotics ameliorate lupus-like symptoms in mice. Sci Rep. 2017;7(1):13675.

- Mu Q, Zhang H, Liao X, et al. Control of lupus nephritis by changes of gut microbiota. Microbiome. 2017;5(1):73.

- Nadeau JH. Maps of linkage and synteny homologies between mouse and man. Trends Genet. 1989;5(3):82-86.

- Nagata S, Hanayama R, Kawane K. Autoimmunity and the clearance of dead cells. Cell. 2010;140(5):619-630.

- Narshi CB, Giles IP, Rahman A. The endothelium: an interface between autoimmunity and atherosclerosis in systemic lupus erythematosus?. Lupus. 2011;20(1):5-13.

- Negi VS, Devaraju P, Gulati R. Angiotensin-converting enzyme (ACE) gene insertion/deletion polymorphism is not a risk factor for hypertension in SLE nephritis. Clin Rheumatol. 2015;34(9):1545-1549.

- Neumann P, Gertzberg N, Johnson A. TNF-alpha induces a decrease in eNOS promoter activity. Am J Physiol Lung Cell Mol Physiol. 2004;286(2):L452-L459.

- Nguyen H, Chiasson VL, Chatterjee P, Kopriva SE, Young KJ, Mitchell BM. Interleukin-17 causes Rho-kinase-mediated endothelial dysfunction and hypertension. Cardiovasc Res. 2013;97(4):696-704.

- Nickerson KM, Cullen JL, Kashgarian M, Shlomchik MJ. Exacerbated autoimmunity in

the absence of TLR9 in MRL.Fas(lpr) mice depends on Ifnar1. J Immunol. 2013;190(8):3889-3894.

- Nosalski R, Guzik TJ. Perivascular adipose tissue inflammation in vascular disease. Br J Pharmacol. 2017;174(20):3496-3513.

- Nzeusseu Toukap A, Galant C, Theate I, et al. Identification of distinct gene expression profiles in the synovium of patients with systemic lupus erythematosus. Arthritis Rheum. 2007;56(5):1579-1588.

- Ocampo-Piraquive V, Nieto-Aristizábal I, Cañas CA, Tobón GJ. Mortality in systemic lupus erythematosus: causes, predictors and interventions. Expert Rev Clin Immunol. 2018;14(12):1043-1053.

- Pieterse E, Rother N, Garsen M, et al. Neutrophil Extracellular Traps Drive Endothelial-to-Mesenchymal Transition. Arterioscler Thromb Vasc Biol. 2017;37(7):1371-1379.

- Plantinga LC, Patzer RE, Drenkard C, et al. Association of time to kidney transplantation with graft failure among U.S. patients with end-stage renal disease due to lupus nephritis. Arthritis Care Res (Hoboken). 2015;67(4):571-581.

- Pluznick JL, Protzko RJ, Gevorgyan H, et al. Olfactory receptor responding to gut microbiota-derived signals plays a role in renin secretion and blood pressure regulation. Proc Natl Acad Sci U S A. 2013;110(11):4410-4415.

- Qi Y, Aranda JM, Rodriguez V, Raizada MK, Pepine CJ. Impact of antibiotics on arterial blood pressure in a patient with resistant hypertension - A case report. Int J Cardiol. 2015;201:157-158.- Rajagopalan S, Somers EC, Brook RD, et al. Endothelial cell apoptosis in systemic lupus erythematosus: a common pathway for abnormal vascular function and thrombosis propensity. Blood. 2004;103(10):3677-3683.

- Rees F, Doherty M, Grainge MJ, Lanyon P, Zhang W. The worldwide incidence and prevalence of systemic lupus erythematosus: a systematic review of epidemiological studies. Rheumatology (Oxford). 2017;56(11):1945-1961.

- Ren D, Liu F, Dong G, et al. Activation of TLR7 increases CCND3 expression via the downregulation of miR-15b in B cells of systemic lupus erythematosus. Cell Mol Immunol. 2016;13(6):764-775.

- Ridlon JM, Kang DJ, Hylemon PB. Bile salt biotransformations by human intestinal bacteria. J Lipid Res. 2006;47(2):241-259.

- Rigat B, Hubert C, Alhenc-Gelas F, Cambien F, Corvol P, Soubrier F. An insertion/deletion polymorphism in the angiotensin I-converting enzyme gene accounting for half the variance of serum enzyme levels. J Clin Invest. 1990;86(4):1343-1346.

- Robles-Vera I, Toral M, de la Visitación N, et al. Probiotics Prevent Dysbiosis and the Rise in Blood Pressure in Genetic Hypertension: Role of Short-Chain Fatty Acids. Mol Nutr Food Res. 2020;64(6):e1900616.

- Robles-Vera I, Toral M, de la Visitación N, et al. Changes to the gut microbiota induced by losartan contributes to its antihypertensive effects. Br J Pharmacol. 2020;177(9):2006-2023.

- Rodríguez-Carrio J, Salazar N, Margolles A, et al. Free Fatty Acids Profiles Are Related to Gut Microbiota Signatures and Short-Chain Fatty Acids. Front Immunol. 2017;8:823.

- Romero M, Toral M, Robles-Vera I, et al. Activation of Peroxisome Proliferator Activator Receptor β/δ Improves Endothelial Dysfunction and Protects Kidney in Murine Lupus. Hypertension. 2017;69(4):641-650.

- Rudofsky UH, Dilwith RL, Roths JB, Lawrence DA, Kelley VE, Magro AM. Differences in the occurrence of hypertension among (NZB X NZW)F1, MRL-lpr, and BXSB mice with lupus nephritis. Am J Pathol. 1984;116(1):107-114.

- Rudofsky UH, Lawrence DA. New Zealand mixed mice: a genetic systemic lupus erythematosus model for assessing environmental effects. Environ Health Perspect. 1999;107 Suppl 5(Suppl 5):713-721.

- Ryan MJ. The pathophysiology of hypertension in systemic lupus erythematosus. Am J Physiol Regul Integr Comp Physiol. 2009;296(4):R1258-R1267.

- Ryan MJ. An update on immune system activation in the pathogenesis of hypertension. Hypertension. 2013;62(2):226-230.

- Ryan MJ, McLemore GR Jr. Hypertension and impaired vascular function in a female mouse model of systemic lupus erythematosus. Am J Physiol Regul Integr Comp Physiol. 2007;292(2):R736-R742.

- Sabio JM, Vargas-Hitos JA, Martínez-Bordonado J, et al. Cumulated organ damage is associated with arterial stiffness in women with systemic lupus erythematosus irrespective of renal function. Clin Exp Rheumatol. 2016;34(1):53-57.

- Sakamoto K, Fukushima Y, Ito K, et al. Osteopontin in Spontaneous Germinal Centers Inhibits Apoptotic Cell Engulfment and Promotes Anti-Nuclear Antibody Production in Lupus-Prone Mice. J Immunol. 2016;197(6):2177-2186.

- Sanz I, Lee FE. B cells as therapeutic targets in SLE. Nat Rev Rheumatol. 2010;6(6):326-337.

- Satoh M, Kumar A, Kanwar YS, Reeves WH. Anti-nuclear antibody production and immune-complex glomerulonephritis in BALB/c mice treated with pristane. Proc Natl Acad Sci U S A. 1995;92(24):10934-10938.

- Schiffer C, Lalanne AI, Cassard L, et al. A strain of Lactobacillus casei inhibits the effector phase of immune inflammation. J Immunol. 2011;187(5):2646-2655.

- Schiffrin EL. Vascular stiffening and arterial compliance. Implications for systolic blood pressure. Am J Hypertens. 2004;17(12 Pt 2):39S-48S

- Schmidt T, Paust HJ, Krebs CF, et al. Function of the Th17/interleukin-17A immune response in murine lupus nephritis. Arthritis Rheumatol. 2015;67(2):475-487.

- Segata N, Izard J, Waldron L, et al. Metagenomic biomarker discovery and explanation. Genome Biol. 2011;12(6):R60.

- Small HY, Migliarino S, Czesnikiewicz-Guzik M, Guzik TJ. Hypertension: Focus on autoimmunity and oxidative stress. Free Radic Biol Med. 2018;125:104-115.

- Singh N, Gurav A, Sivaprakasam S, et al. Activation of Gpr109a, receptor for niacin and the commensal metabolite butyrate, suppresses colonic inflammation and carcinogenesis. Immunity. 2014;40(1):128-139.

- Somers EC, Zhao W, Lewis EE, et al. Type I interferons are associated with subclinical markers of cardiovascular disease in a cohort of systemic lupus erythematosus patients. PLoS One. 2012;7(5):e37000.

- Spolski R, Leonard WJ. Interleukin-21: a double-edged sword with therapeutic potential. Nat Rev Drug Discov. 2014;13(5):379-395.

- Sun W, Jiao Y, Cui B, Gao X, Xia Y, Zhao Y. Immune complexes activate human endothelium involving the cell-signaling HMGB1-RAGE axis in the pathogenesis of lupus vasculitis. Lab Invest. 2013;93(6):626-638.

- Sun W, Jiao Y, Cui B, Gao X, Xia Y, Zhao Y. Immune complexes activate human endothelium involving the cell-signaling HMGB1-RAGE axis in the pathogenesis of lupus vasculitis. Lab Invest. 2013;93(6):626-638.

- Swaak AJ, Huysen V, Nossent JC, Smeenk RJ. Antinuclear antibody profiles in relation to specific disease manifestations of systemic lupus erythematosus. Clin Rheumatol. 1990;9(1 Suppl 1):82-94.

- Szabó C, Ischiropoulos H, Radi R. Peroxynitrite: biochemistry, pathophysiology and development of therapeutics. Nat Rev Drug Discov. 2007;6(8):662-680.

- Szulińska M, Łoniewski I, Skrypnik K, et al. Multispecies Probiotic Supplementation Favorably Affects Vascular Function and Reduces Arterial Stiffness in Obese Postmenopausal Women-A 12-Week Placebo-Controlled and Randomized Clinical Study. Nutrients. 2018;10(11):1672.

- Szulińska M, Łoniewski I, van Hemert S, Sobieska M, Bogdański P. Dose-Dependent Effects of Multispecies Probiotic Supplementation on the Lipopolysaccharide (LPS) Level and Cardiometabolic Profile in Obese Postmenopausal Women: A 12-Week Randomized Clinical Trial. Nutrients. 2018;10(6):773.

- Talaat RM, Mohamed SF, Bassyouni IH, Raouf AA. Th1/Th2/Th17/Treg cytokine imbalance in systemic lupus erythematosus (SLE) patients: Correlation with disease activity. Cytokine. 2015;72(2):146-153.

- Taylor EB, Ryan MJ. Understanding mechanisms of hypertension in systemic lupus erythematosus [published online ahead of print, 2016 Mar 15]. Ther Adv Cardiovasc Dis. 2016;11(1):20-32.

- Taylor EB, Ryan MJ. Immunosuppression With Mycophenolate Mofetil Attenuates Hypertension in an Experimental Model of Autoimmune Disease. J Am Heart Assoc. 2017;6(3):e005394.

- Tektonidou MG, Kravvariti E, Konstantonis G, Tentolouris N, Sfikakis PP, Protogerou A. Subclinical atherosclerosis in Systemic Lupus Erythematosus: Comparable risk with Diabetes Mellitus and Rheumatoid Arthritis. Autoimmun Rev. 2017;16(3):308-312.

- Toral M, Gómez-Guzmán M, Jiménez R, et al. The probiotic Lactobacillus coryniformis CECT5711 reduces the vascular pro-oxidant and pro-inflammatory status in obese mice. Clin Sci (Lond). 2014;127(1):33-45.

- Toral M, Jiménez R, Romero M, et al. Role of endoplasmic reticulum stress in the protective effects of PPARβ/δ activation on endothelial dysfunction induced by plasma from patients with lupus. Arthritis Res Ther. 2017;19(1):268.

- Toral M, Robles-Vera I, de la Visitación N, et al. Role of the immune system in vascular function and blood pressure control induced by faecal microbiota transplantation in rats. Acta Physiol (Oxf). 2019;227(1):e13285.

- Toral M, Romero M, Rodríguez-Nogales A, et al. Lactobacillus fermentum Improves Tacrolimus-Induced Hypertension by Restoring Vascular Redox State and Improving eNOS Coupling [published online ahead of print, 2018 May 30]. Mol Nutr Food Res. 2018;e1800033.

- Touyz RM, Briones AM. Reactive oxygen species and vascular biology: implications in human hypertension. Hypertens Res. 2011;34(1):5-14.

- Tschudi MR, Barton M, Bersinger NA, et al. Effect of age on kinetics of nitric oxide release in rat aorta and pulmonary artery. J Clin Invest. 1996;98(4):899-905.

- Tselios K, Gladman DD, Urowitz MB. Systemic lupus erythematosus and pulmonary arterial hypertension: links, risks, and management strategies. Open Access Rheumatol. 2016;9:1-9.

- Tucker LB, Menon S, Schaller JG, Isenberg DA. Adult- and childhood-onset systemic lupus erythematosus: a comparison of

onset, clinical features, serology, and outcome. Br J Rheumatol. 1995;34(9):866-872.

- Tzang BS, Liu CH, Hsu KC, Chen YH, Huang CY, Hsu TC. Effects of oral Lactobacillus administration on antioxidant activities and CD4+CD25+forkhead box P3 (FoxP3)+ T cells in NZB/W F1 mice. Br J Nutr. 2017;118(5):333-342.

- Van den Abbeele P, Belzer C, Goossens M, et al. Butyrate-producing Clostridium cluster XIVa species specifically colonize mucins in an in vitro gut model. ISME J. 2013;7(5):949-961.

- Venegas-Pont M, Manigrasso MB, Grifoni SC, et al. Tumor necrosis factor-alpha antagonist etanercept decreases blood pressure and protects the kidney in a mouse model of systemic lupus erythematosus. Hypertension. 2010;56(4):643-649.

- Wang P, Ba ZF, Chaudry IH. Administration of tumor necrosis factor-alpha in vivo depresses endothelium-dependent relaxation. Am J Physiol. 1994;266(6 Pt 2):H2535-H2541.

- Wang Q, Garrity GM, Tiedje JM, Cole JR. Naive Bayesian classifier for rapid assignment of rRNA sequences into the new bacterial taxonomy. Appl Environ Microbiol. 2007;73(16):5261-5267.

- Wenzel K, Haase H, Wallukat G, et al. Potential relevance of alpha(1)-adrenergic receptor autoantibodies in refractory hypertension. PLoS One. 2008;3(11):e3742.

- Wilck N, Matus MG, Kearney SM, et al. Salt-responsive gut commensal modulates T_H17 axis and disease. Nature. 2017;551(7682):585-589.

- Wofsy D, Chiang NY, Greenspan JS, Ermak TH. Treatment of murine lupus with monoclonal antibody to L3T4. I. Effects on the distribution and function of lymphocyte subsets and on the histopathology of autoimmune disease. J Autoimmun. 1988;1(5):415-431.

- Wu J, Saleh MA, Kirabo A, et al. Immune activation caused by vascular oxidation promotes fibrosis and hypertension [published correction appears in J Clin Invest. 2016 Apr 1;126(4):1607]. J Clin Invest. 2016;126(1):50-67.

- Wüthrich RP. RAS meets SLE. Nephrol Dial Transplant. 2009;24(9):2634-2636.

- Yacoub Wasef SZ. Gender differences in systemic lupus erythematosus. Gend Med. 2004;1(1):12-17.

- Yan X, Jin J, Su X, et al. Intestinal Flora Modulates Blood Pressure by Regulating the Synthesis of Intestinal-Derived Corticosterone in High Salt-Induced Hypertension. Circ Res. 2020;126(7):839-853.

- Yang T, Santisteban MM, Rodriguez V, et al. Gut dysbiosis is linked to hypertension. Hypertension. 2015;65(6):1331-1340.

- Yokogawa M, Takaishi M, Nakajima K, et al. Epicutaneous application of toll-like receptor 7 agonists leads to systemic autoimmunity in wild-type mice: a new model of systemic Lupus erythematosus. Arthritis Rheumatol. 2014;66(3):694-706.

- Yu CF, Peng WM, Schlee M, et al. SOCS1 and SOCS3 Target IRF7 Degradation To Suppress TLR7-Mediated Type I IFN Production of Human Plasmacytoid Dendritic Cells. J Immunol. 2018;200(12):4024-4035.

- Yung S, Ng CY, Au KY, et al. Binding of anti-dsDNA antibodies to proximal tubular epithelial cells contributes to renal tubulointerstitial inflammation. Clin Sci (Lond). 2017;131(1):49-67.

- Zamani B, Golkar HR, Farshbaf S, et al. Clinical and metabolic response to probiotic supplementation in patients with rheumatoid arthritis: a randomized, double-blind, placebo-controlled trial. Int J Rheum Dis. 2016;19(9):869-879.

- Zegarra-Ruiz DF, El Beidaq A, Iñiguez AJ, et al. A Diet-Sensitive Commensal Lactobacillus Strain Mediates TLR7-Dependent Systemic Autoimmunity. Cell Host Microbe. 2019;25(1):113-127.e6.

- Zeng Q, Li D, He Y, et al. Discrepant gut microbiota markers for the classification of obesity-related metabolic abnormalities. Sci Rep. 2019;9(1):13424.

- Zhang H, Liao X, Sparks JB, Luo XM. Dynamics of gut microbiota in autoimmune lupus. Appl Environ Microbiol. 2014;80(24):7551-7560.

- Zhang M, Yu G, Chan B, et al. Interleukin-21 receptor blockade inhibits secondary humoral responses and halts the progression of preestablished disease in the (NZB × NZW)F1 systemic lupus erythematosus model. Arthritis Rheumatol. 2015;67(10):2723-2731.

- Zhao Z, Weinstein E, Tuzova M, et al. Cross-reactivity of human lupus anti-DNA antibodies with alpha-actinin and nephritogenic potential. Arthritis Rheum. 2005;52(2):522-530.

- Zhou HW, Li DF, Tam NF, et al. BIPES, a cost-effective high-throughput method for assessing microbial diversity. ISME J. 2011;5(4):741-749.

- Zuo L, Yuan KT, Yu L, Meng QH, Chung PC, Yang DH. Bifidobacterium infantis attenuates colitis by regulating T cell subset responses. World J Gastroenterol. 2014;20(48):18316-18329.